

Magnesium single crystal for biodegradable implant applications

V. Shanov^{1,2}, P. Salunke¹, G. Zhang¹, M. Joshi¹, V. Chaswal¹, Z. Dong³, S. Woo⁴, K. Farraro⁴, C. Sfeir⁵, A. Brown⁵, S. Yarmolenko⁶, M. Pink⁷.

¹ Dept. of Biomedical, Chemical & Environmental Eng., College of Engineering & Applied Science, University of Cincinnati, USA. ² Dept. of Mechanical & Materials Eng., College of Engineering & Applied Science, University of Cincinnati, USA. ³ Dept. of Internal Medicine, College of Medicine, University of Cincinnati, USA. ⁴ Dept. of Bioengineering, University of Pittsburgh, USA. ⁵ Dept. of Periodontics & Preventive Dentistry, Oral Biology & Bioengineering, McGowan Institute for Regenerative Medicine, USA. ⁶ Center for Advanced Materials & Smart Structures, North Carolina A&T State University, USA. ⁷ Dept. of Chemistry, Indiana University, USA.

Magnesium is a promising material for orthopedic implants due to its biocompatibility and the ability to resorb in body [1]. Compared to polycrystalline Mg, single crystal is expected to reveal absence of grain boundaries which will result in high strength, non-catastrophic failures, high purity and increased corrosion resistance. All this motivated us to grow high quality Mg single crystals and study their properties, including in vitro and in vivo behavior. Magnesium single crystals were grown with a purity of 99.998% using modified Bridgman-Stockbarger method. Polycrystalline Mg of 99.95% purity (Alfa Aesar) was used as a starting material. A graphite crucible was employed to contain Mg melt in ultrahigh purity Ar. The crucible was heated and cooled under a controlled temperature gradient using a 2 zone vertical crystal grower model 7015 made by First Nano. Mechanical and corrosion properties have been studied in vitro using single crystal samples cut from bulk crystals by electrical discharge machining (EDM) [2,3]. Fig. 1 displays the Bridgman system for growing of Mg single crystal and images of the crystals.

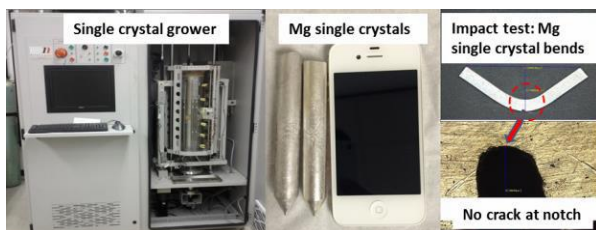


Fig. 1: Pictures of the Bridgman single crystal grower with Mg single crystals 100mm long and 15mm in diameter along with tested impact sample

The single crystallinity of (0001) Mg crystals was confirmed by Laue XRD, pole diffraction figures, X-Ray tomography, electron backscatter diffraction, metallography, and synchrotron characterization using the Advanced Photon Source at the Argonne National Labs. The high

purity of the grown crystals was determined using Energy Dispersive Spectroscopy (EDS) and Inductively Coupled Plasma Mass Spectrometry. Magnesium single crystals revealed mechanical properties close to those of the natural bone with an ultimate tensile strength of 60-70 MPa and a remarkable tendency for higher ductility (50-60%) compared to polycrystalline Mg, which is in the range of 10%. The overall toughness and energy absorption in Mg single crystal through twinning is much higher than in polycrystalline Mg which can help to reduce the risk of catastrophic failures in medical implants. Thanks to the absence of grain boundaries and the applied proprietary nanometre thin coating [3] the obtained corrosion of Mg single crystal was controlled and significantly suppressed in vitro and in vivo. Advanced machining was employed to fabricate disks, orthopedic screws, plates and ring-shaped devices for Anterior Cruciate Ligament (ACL) repair for in vivo studies. The obtained devices were tested in 3 animal models such as mouse, rabbit and goat. Implanted in a rabbit ulna fracture model, single crystal Mg plates & screws showed promising Mg resorption and bone overgrowth around the device. ACL rings implanted in goats successfully repaired the damaged ligament and have fully degraded in 12 weeks. No abnormal inflammatory response was observed. The conducted experiments confirmed that Mg single crystal is a promising material for biodegradable implant applications.

ACKNOWLEDGEMENTS: NSF ERC for Revolutionizing Biomaterials, EEC-EEC-0812348.

Customising absorbable magnesium alloys

J. D. Cao¹, M. Cihova¹, R. Schäublin¹, P. J. Uggowitzer¹, J. F. Löffler¹

¹ [Laboratory of Metal Physics and Technology](#), Department of Materials, [ETH Zurich](#), 8093 Zurich, Switzerland

INTRODUCTION: Unlike traditional metallic biomaterials, new absorbable alloys based on magnesium are designed to degrade inside the human body over time [1, 2]. The ideal alloy shall thus possess the following attributes: (1) controllable/predictable degradation rate/process, (2) low H₂ evolution, (3) intrinsically biocompatible, and (4) sufficient mechanical strength and ductility. Significant research has focused on studying the degradation mechanisms of magnesium alloys and increasing their corrosion resistance. In the present work, we demonstrate that aspects of an absorbable magnesium alloy can be customized based on the intended application.

METHODS: Magnesium alloy ZX10 (1.0 wt.% Zn, 0.3 wt.% Ca and Mg for the balance) was selected in this study for it concurrently contains two types of intermetallic phases, Mg₂Ca and a ternary intermetallic. The synthesis method has been reported elsewhere [3]. The extruded samples (Ø10 mm, T_{extrusion} = 300 °C) were subsequently heat treated at temperatures ranging from 275 to 375 °C and the resulting microstructures and degradation characteristics were studied.

Microstructural analysis was carried out using optical and electron microscopes. Grain size was determined using the linear intercept method on optical micrographs. Intermetallic phases were analysed by energy dispersive X-ray spectroscopy (EDX) maps collected using a 200 kV transmission electron microscope (TEM).

The degradation characteristics of the ZX10 alloys were determined using electrochemical measurements. A three-electrode flat-cell was used, which contained 300 mL of electrolyte (0.1 M NaCl in milli-Q water, pH 6.0). The unit was under the control of a potentiostat (AUTOLAB PGSTAT302).

RESULTS: Microstructural analysis showed measurable grain growth when heat treated at temperatures ranging from 275 to 375 °C. The type of intermetallic phase present was also affected.

Electrochemical tests showed the responses from heat treated ZX10 samples to be significantly different compared to the as-extruded sample.

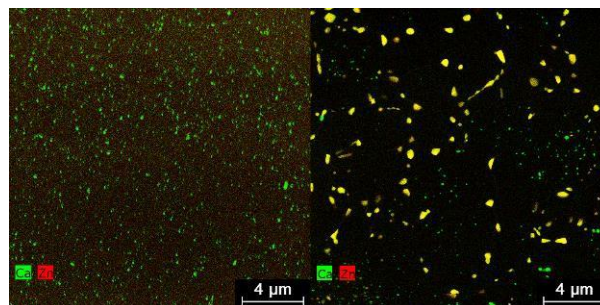


Fig. 1: TEM EDX maps of ZX10 in the following conditions: (left) as-extruded, (right) heat treated at 275°C/90h.

DISCUSSION & CONCLUSIONS: Following heat treatments the microstructure of ZX10 exhibited a range of grain sizes, and contained either Mg₂Ca or a ternary intermetallic phase, or both. Fig. 1 (left) shows a representative TEM EDX map of an as-extruded sample. Since the EDX map only displays Ca (green) and Zn (red), observation of only green precipitates means only Mg₂Ca precipitates were present. Upon heat treatment at 275°C/90h, Fig. 1 (right), yellow coloured precipitates appeared, which is a combination of Ca and Zn (mixing green and red), indicative of a ternary intermetallic phase.

The free corrosion potential also changed according to the type of dominant intermetallic phases present in the microstructure. The presence of the ternary intermetallic phase resulted in a significantly nobler potential to that of the as-extruded alloy, which contained only Mg₂Ca phase.

ZX10 alloys can thus be heat treated to yield different types of intermetallic phases. By careful selection of the heat treatment temperature and time, and understanding their effects on the resulting microstructure and its degradation characteristics, we have demonstrated that this absorbable magnesium alloy can be customised depending on the intended application.

Grain-boundary strengthening of MgZnCa lean alloys

M. Cihova, G. Biffi, P. J. Uggowitzer, J. F. Löffler

Laboratory of Metal Physics and Technology, Department of Materials, ETH Zurich, 8093 Zurich, Switzerland

INTRODUCTION: MgZnCa lean alloys were recently introduced as a bioabsorbable implant material with biologically acceptable elemental composition [1]. These alloys show satisfying biocorrosion and promising mechanical properties. For their applicability as load-bearing implant materials, high strength and simultaneous high ductility are essential. Because for the given small amount of alloying elements (<0.6 at.%), strengthening mechanisms such as precipitation and solid-solution hardening can only play a minor role, the mechanical performance of these Mg-based lean alloys relies on grain boundary-strengthening. In this study we highlight the importance of a fine-grained microstructure in MgZnCa lean alloys by investigating the impact of grain size (here, 1.6 – 10.7 μm) on the tensile behaviour of ZX10 (MgZn1Ca0.3, in wt.%).

METHODS: ZX10 alloys were directly extruded to 3 mm rods and subsequently heat-treated to generate an extended range of grain sizes. For data analysis, as-extruded ZX10 rods of 10 mm diameter were also considered, for which different grain sizes resulted from a variation of the thermomechanical processing parameters [2]. The processing conditions are summarized in Table 1 along with the average grain size obtained, determined via optical microscopy using the linear intercept method.

Table 1: Processing conditions and average grain size D .

Sample condition	As-extruded				Heat-treated		
$T_{\text{annealing}}$ [°C]	/	/	/	/	30	35	375
$T_{\text{extrusion}}$ [°C]	300 ⁽²⁾	325 ⁽²⁾	37	400 ⁽²⁾	37	37	375
D [μm]	1.6	3.0	4.2	6.8	5.0	8.8	10.7

Tensile tests were conducted using an electromechanical universal testing machine (Schenck Trebel, RSA100) with a hydraulic load cell of 100 kN and a strain rate of 10^{-3} s^{-1} . Tensile specimens ($n = 2-3$) were machined from the as-extruded and heat-treated rods with $d_0 = 2$ mm and gauge length = 10 mm.

RESULTS & DISCUSSION: A significant change in the materials behaviour under tension was detected as a function of microstructure. The

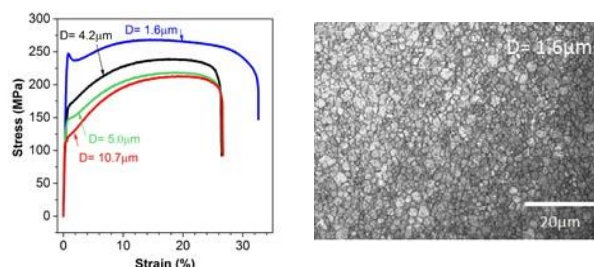


Fig. 1. Left: Stress-strain curves of ZX10 for different grain sizes D ; right: optical micrograph of fine-grained ZX10

most distinct impact of grain coarsening was a significant loss in tensile yield strength, TYS (see Fig.1, left). The dependence of yield strength on grain size can be described by the well-known Hall-Petch relation, $TYS = \sigma_0 + k_y D^{-1/2}$, where k_y is the Hall-Petch coefficient and σ_0 is the friction stress for dislocation movement. Least-square fitting of the TYS data resulted in $k_y = 253 \text{ MPa} \cdot \mu\text{m}^{1/2}$ and $\sigma_0 = 39 \text{ MPa}$ (ref. for pure Mg: $k_y = 220-250 \text{ MPa} \cdot \mu\text{m}^{1/2}$, $\sigma_0 = 11-18 \text{ MPa}$ [3, 4]). The greatly improved mechanical performance of ZX10 compared to pure Mg is achieved by finely distributed second-phase (IMP) particles, which restrict grain growth. They also impede full recrystallization, which would result in detrimental loss of ductility. These two counteracting mechanisms require a careful adjustment of thermomechanical process parameters.

CONCLUSIONS: The results reveal the significance of grain refinement for MgZnCa lean alloys and thus highlight the importance of further decreasing the grain size down to 1 μm , for which according to Hall-Petch, a TYS of > 290MPa is predicted for ZX10. Two counteracting mechanisms, i.e. (1) beneficial grain-growth restriction and (2) detrimental recrystallization constriction, are to be carefully considered in thermomechanical process optimization in order to achieve the desired simultaneous high strength and high ductility required for load-bearing applications.

New developments in Equal Channel Angular Pressing (ECAP) of Mg alloys

M Krystian¹, K Bryła², J Horkey¹, B Mingler¹

¹ [AIT Austrian Institute of Technology GmbH](#), Health & Environment Department, Biomedical Systems, Wr. Neustadt, AT. ² [Institute of Technology](#), The Pedagogical University of Cracow, Kraków, PL

INTRODUCTION: Mg-based alloys must meet many requirements in order to be promising materials for bioresorbable medical implants. Beside of high biocompatibility and low degradation rate, good mechanical properties, particularly high strength, are important. The former two properties can be achieved by microalloying, however, along with a reduction of solid-solution and precipitation hardening and thus a corresponding decrease of strength [1]. Fortunately, the strength can be enhanced due to grain-boundary hardening in ultrafine grained (UFG) materials as produced by severe extremely high plastic deformation during Equal Channel Angular Pressing (ECAP) [2].

METHODS: Two Mg-based alloys, as cast and rolled Mg-RE-Zn (EZ33) [3] and a lean, extruded Mg-Zn-Ca (ZX00) alloy were processed with two different ECAP dies having a channel intersection angle of 90° and 120°, respectively. In addition, a recently developed double-ECAP tool was employed at AIT. It was specially designed for Mg alloys and consists of three channels with two different intersection angles. Up to 4 passes using route Bc (90° rotation of the samples in the same direction after every pass) were applied. The temperature of the ECAP process was gradually decreased starting at 350/300°C down to 240/220°C for EZ33 and ZX00, respectively.

Mechanical properties of the materials were characterised by hardness measurements as well as by tensile and compression tests. Microstructural examination included optical, as well as scanning and transmission electron microscopy.

RESULTS: Figure 1 shows the remarkable increase in yield strength of as-cast EZ33 from 87 MPa to 325 MPa after ECAP (+270%) while retaining ductility. This is in best accordance with the raise in the compressive proof strength at 0.2% strain (86 MPa as cast vs. 345 MPa after ECAP).

In the case of the ZX00 alloy a doubling of compressive strength (from 180 MPa for as-extruded material to 360 MPa after ECAP) as well as an increase in ultimate tensile strength by 70% (from 225 MPa to 390 MPa) were observed.

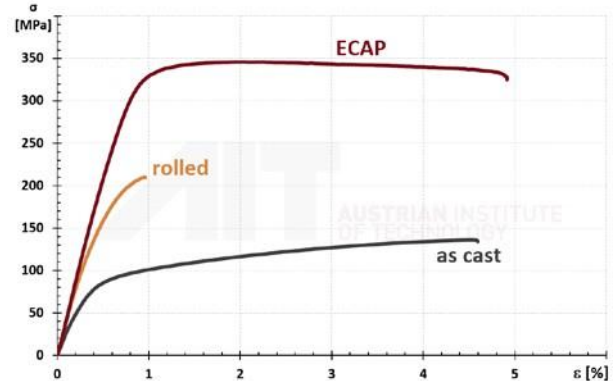


Fig. 1: Stress–strain curves for EZ33 in three different conditions.

DISCUSSION & CONCLUSIONS: The mechanical properties of Mg alloys can be strongly enhanced by appropriate ECAP processing resulting in exceptionally high hardness and strength. Compared to the conventional ECAP tools, processing Mg alloys with the new, double-ECAP tool raises the strength saturation limit. Furthermore, using the new ECAP tool the number of passes required can be reduced and more effective grain refinement is obtained. However, the parameters of the ECAP process have to be adjusted for each Mg alloy individually.

ACKNOWLEDGEMENTS: The authors appreciate the support of the K-project 'OptiBioMat', FFG, COMET program and the project 'HighPerformBioMat', FFG, Research Studios Austria.

Influence of primary forming on microstructure and corrosion of Mg-Ca-Zn

NA Zumdick¹, D Zander¹

¹ Chair of Corrosion and Corrosion Protection, RWTH Aachen University, Germany.

INTRODUCTION: Magnesium-calcium-zinc alloys are one of the most discussed alloys for biomedical application due to the potentially biocompatible alloying elements and the promising mechanical properties and corrosion behavior [1]. These properties are strongly influenced by the microstructure, which in turn is a result of the primary, and of course, secondary forming. The thermal conditions are one of the most critical aspects that affect the microstructure [2]. In the present study the manipulation of the microstructure was systematically conducted via the variation of alloying elements under a constant ratio and by implementing different cooling rates.

METHODS: Two low alloyed Mg-x·Ca-y·Zn alloys (x, y < 4 wt.%) with equal Zn/Ca-ratio (at.) were produced from pure raw materials and cast into two connected cylinder shaped sand molds and one die mold to obtain various defined cooling rates during one casting batch. The samples for microstructural and corrosion investigations were extracted and metallographically prepared to a polished surface. The microstructure and corroded samples was investigated using optical light and electron microscopy, x-ray diffraction and computational image analysis. The hydrogen evolution measurements, each condition performed in triplicate, were conducted in Hanks' balanced salt solution [3] without glucose.

RESULTS: The microstructures of both alloys revealed a very homogeneous microstructure with no visible porosity. In accordance to previous investigations, a minimum of two secondary phases were found to be precipitated on the grain boundaries and interdendritic interstices, as presented in Fig. 1. Three phases (α -Mg, Mg₂Ca and Mg₆Ca₂Zn₃) were identified in previous investigations of the ternary alloy system [1]. Additionally, an increasing alloying content was found to lead to an increase in secondary phases. In addition, similar grain sizes were observed when microstructures of the same alloy with different cooling rates were compared. For both alloys, the sand cast microstructure modification obtained by higher cooling rates (HCR) shows lower corrosion rates (LCR) than the microstructure that originated from lower cooling rates.

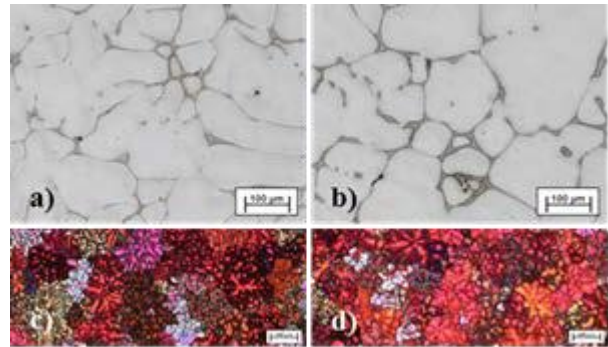


Fig. 1: Optical micrographs of the polished and color-etched microstructures of a), c) lower-alloyed alloy and b), d) higher-alloyed alloy, manufactured via sand casting with low cooling rates

DISCUSSION & CONCLUSIONS: Correlating the microstructural phenomena to the corrosion behavior, the following conclusions can be drawn. A higher amount of secondary phases does not necessarily produce higher corrosion rates. The grain size does not appear to affect the corrosion rates for equal alloy contents. The distribution and morphology of secondary phases appear to be the predominant effect for influencing the corrosion behavior. Thus, corrosion tailored alloy design may not only consider the amount of alloying elements but should also always include the consideration of the effect via differing cooling rates. As a variety of cooling rates may be present when complex components are manufactured, general rules for the quantification of microstructural phenomena, such as distribution and morphology of secondary phases in addition to grain sizes, need to be established. Finally, this study shows that microstructural manipulation by choosing dependent alloying contents and cooling rates is a powerful tool for corrosion tailored design.

Microstructure and properties of WE43 manufactured via SLM

NA Zumdick¹, L Jauer², LC Kersting^{1,3}, W Meiners², TN Kutz¹, D Zander¹

¹ Chair of Corrosion and Corrosion Protection, RWTH Aachen University, Germany. ² Fraunhofer Institute for Laser Technology ILT, Germany. ³ Chair for Laser Technology, RWTH Aachen University, Germany.

INTRODUCTION: Recently, the proof of concept for the generation of magnesium WE43 scaffold-like structures by using Selective Laser Melting (SLM) was confirmed [1]. These structures displayed interconnected macroscopic porosity and minimal microstructural porosity (<99.5%). Process characteristics of SLM are high local cooling rates leading to rapid solidification which highly influences the microstructure of the built component. The present study focusses on the investigation of the microstructure together with the resulting mechanical properties and degradation behavior to achieve a holistic image of the as-SLMed WE43 as a potential candidate for a biodegradable implant material.

METHODS: For microstructure and corrosion property investigations, samples of 12 x 12 x 12 mm³ were generated by using a laboratory SLM setup with previously described conditions and raw material [1]. Tensile specimen (type B 4 x 20 acc. to DIN 50125) were manufactured from SLMed bars and tested according to DIN EN ISO 6892-1. Hydrogen evolution measurements were conducted in Hanks' balanced salt solution in accordance to testing procedures in [2]. Microstructural analysis was conducted via SEM with EDX.

RESULTS: The microstructure, presented in Fig. 1 a), is characterized by a homogeneous distribution of second phases with minimal porosity. The SEM image in Fig. 1 b) further reveals at least one second phase, flake-shaped in appearance. EDX measurements indicate that this phase consists of high O and Y contents. Only minor Zr, Nd and Gd contents could be detected. Grain sizes of approx. 1 µm were observed. During hydrogen evolution measurements, accelerating degradation behavior with corrosion rates of 0.006 to 0.007 mg/(cm²·min) after 5 hours immersion was observed due to impurities in the test specimens.

Stress-strain curves, which were obtained by tensile measurements, show excellent reproducibility, as presented in Fig. 2. The resulting mean elastic modulus was 46 GPa. The

mean ultimate tensile strength was 308 MPa with a respective mean elongation of 12 %.

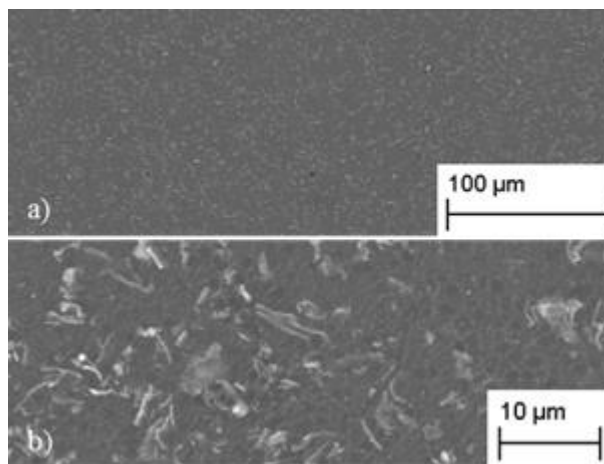


Fig. 1: Scanning electron microscope images of polished as-SLMed WE43 microstructural cross-sections.

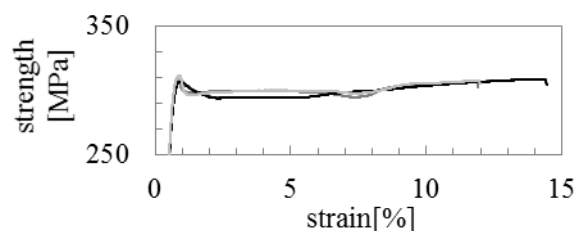


Fig. 2: Stress strain curves of as-SLMed WE43.

DISCUSSION & CONCLUSIONS: The SLM specimens exhibit a homogeneous extraordinarily fine microstructure consisting of grains approx. 1 µm in size and flake-shaped yttrium and oxygen containing second phases. The ultrafine grain microstructure appears to positively influence the mechanical properties which lie in the upper range of the common values [3].

Development of a novel biodegradable metallic stent based on micro-galvanic corrosion: Strength and ductility assessment

R Mongrain^{1,2}, J Frattolin¹, S Yue¹, OF Bertrand³

¹Department of Mechanical Engineering, McGill, ²Montreal Heart Institute, Montreal, Canada, ³Interventional Cardiology, Hôpital Laval, Laval University, Quebec, Canada

INTRODUCTION: Strut fracture (SF) has been associated with adverse pathological findings. The severity of SF is correlated with implant duration [1]. This suggests a fatigue phenomenon related with the dynamic loading of the stent. A possible solution is biodegradability for which the stent would disappear before the fatigue issues appear. A new approach is presented to generate a biodegradable stent using dissimilar metal powders mixed and deposited using a spray technique. The resulting intermixed compound exhibit micro-galvanic properties allowing for degradation. The ideal stent material should have a high density (for radio-opacity), a high elastic modulus (to minimize recoil), low yield stress (to facilitate expansion), high tensile strength (for radial strength and thinner struts), high ductility (to withstand deformation during expansion) [3].

METHODS: Cold gas-dynamic spraying (CGDS) propels fine metal powder particles at supersonic velocities (300-1500 m/s). The micro/nano-structured powder impacts with a substrate, the particles deform and adhere to form a coating. The particles remain relatively cold and retain their submicron to micron range dimensions. Therefore, unwanted effects of high temperatures, such as oxidation, grain growth and thermal stresses, are avoided [2]. Stainless steel 316L and pure iron particles (Sandvik Osprey, UK) are mixed in 20% to 80% by weight. Coatings are deposited on mild steel substrates (plates and rods). A pressure of 4 MPa and 700°C nitrogen is used as carrying gas with Kinetics® 4000 spray gun. The coated substrates are subsequently annealed at 1100 °C for 1 hour. Flat substrate separation of strips (10X4 mm, 85 mm thick) are shaped using electro-discharge machining (EDM). Rod substrates are centerless grinded, separated with EDM and laser cut to produce stents. A micro shear test was done forcing a cylindrical punch of 1.55 mm diameter through the strips at a rate of 0.001 s⁻¹.

RESULTS: Figures 1(a) shows the micro shear mechanical tests results for bulk 316L and bulk Fe and 20SS+80 Fe. Figure 1 (c) and (d) simply show

the prototype stent before and after a week corrosion in Hanks solution for illustration [4].

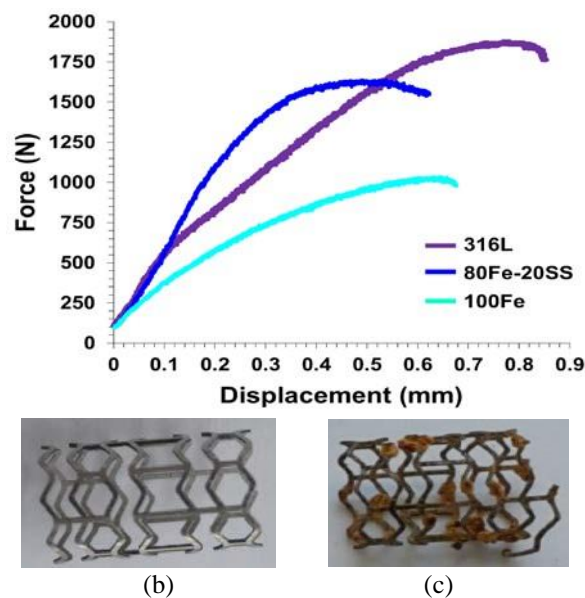


Fig. 1 (a) Micro punch tests for 100SS, 100Fe, 20SS+80Fe and (c, d) illustrations of a stent prototype before and after one week corrosion

Interestingly, the mechanical tests reveal that the 20SS+80 Fe amalgamate has essentially almost the same strength (and ductility) as of 100 % 316L. This would allow for high ratio of anodic material to degrade and thin struts.

DISCUSSION/CONCLUSION: Current biodegradable metals have limitations for designing thin struts for stents. Cold spray with dissimilar metals provides a new approach for making bioresorbable stents and allows for controllable rates and high strength for thin struts design.

ACKNOWLEDGEMENTS: The authors acknowledge funding by the Natural Sciences and Engineering Research Council of Canada.

Development of balloon-expandable EW31 alloy stent for pediatric airway problems

K Hanada¹, H Ueda², M Inoue², K. Matsuzaki¹

¹ [Advanced Manufacturing Research Institute, National Institute of Advanced Industrial Science and Technology \(AIST\), JAPAN.](#) ² [Product and Research Development Division, Fuji Light Metal Co., Ltd., JAPAN](#)

INTRODUCTION: Balloon-expandable metallic stent has been used to treat pediatric airway problems such as bronchomalacia congenital tracheal stenosis¹, and the development of such the stents with biodegradability are strongly desired in those treatments. In this study, we aim to develop balloon-expandable EW31 (Mg-3%RE-1%Y) alloy stent for the treatment of the pediatric airway problems, and the mechanical performance of the stent is investigated.

METHODS: Balloon-expandable EW31 alloy stent was fabricated through the processing shown in *Figure 1*. The prepared EW31 billet was extruded into a thin-walled tube ($\phi 3.2 \text{ mm} \times \phi 2.6 \text{ mm} \times L600 \text{ mm}$) at 748 K and was annealed at 673 K for 30 min. Then the extruded tube was repeatedly cold-drawn and annealed until the tube diameter and wall thickness reduced to the requested size. All the annealing was carried out at 673 K for 30 minutes. The obtained fine tube ($\phi 1.8 \text{ mm} \times \phi 1.5 \text{ mm} \times L500 \text{ mm}$, diameter error $< \pm 0.2 \%$, wall thickness error $< \pm 2.5 \%$) was processed into stent device shape by pulsed laser cutting and was finally surface-finished by electrochemical polishing.

The structural observation, balloon expansion test, and radial force test were made to examine the dimension size and surface morphology, and the mechanical properties of the fabricated EW31 alloy stent.

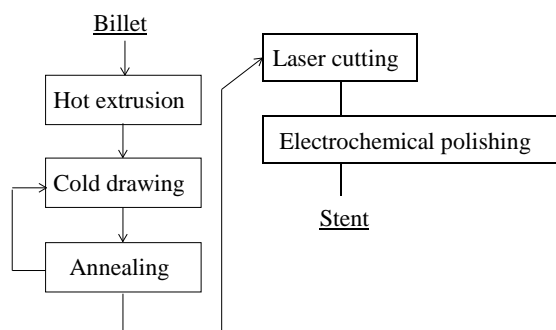


Fig. 1: Fabrication process of EW31 alloy stent.

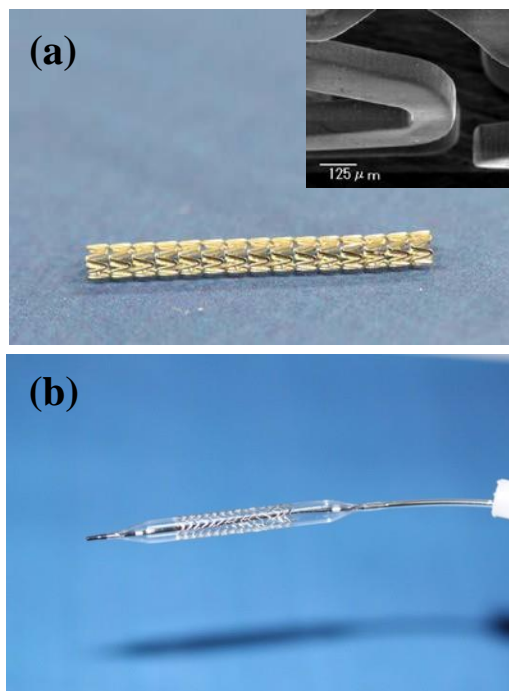


Fig. 2: EW31 alloy stent: a) as-fabricated, b) as-balloon expanded.

RESULTS: The fabricated EW31 alloy stent has smooth surface and round edge, without any burrs and stent strut fractures, as shown in *Figure 2(a)*. The strut dimension was about 130 μm in width and 130 μm in thickness, respectively. As shown in *Figure 2(b)*, the balloon expansion test and radial force tests show that the fabricated stent was safely expanded up to over-expansion size (about $\phi 3.6 \text{ mm}$ in outer diameter) without any strut fractures, and that this stent had enough radial force to open an intravascular lumen.

DISCUSSION & CONCLUSIONS:

The balloon-expandable EW31 alloy stent fabricated showed excellent mechanical performance, and this is expected to proceed the next stage with animals.

Degradation behaviour of biodegradable Mg staples used in stapler for gastrointestinal anastomosis

Jing Bai¹, Jian Cao², Ye Lu¹, Chenglin Chu¹, Feng Xue¹, Kewei Jiang², Xiaodong Yang², Yingjiang Ye²

¹ School of Materials Science and Engineering, Southeast University, Nanjing, China. ² Department of Gastroenterological Surgery, Peking University People's Hospital, China

INTRODUCTION: We developed biodegradable Mg staple used in stapler for gastrointestinal anastomosis[1] to replace current Ti staple which will be long-term left in the body and results in some adverse effects on patients[2][3]. However, non-uniform stress corrosion may occur resulting from the “ Γ ” and the “B” shape of staple during preparation and anastomosis (Fig. 1). Therefore, it is essential to investigate the degradation performance of Mg staple in vitro and vivo.

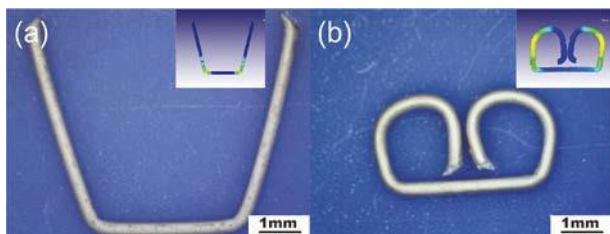


Fig. 1: (a) “ Γ ” shaped staple prepared from Mg wire and (b) “B” shape staple after anastomosis with stimulated stress distribution.

METHODS: The Φ 0.3mm AZ21 Mg alloy wires with surface coating were cut and processed into “B”-shape staples by stapler. To evaluate their in vitro degradation performance, the degradation behaviour of staples in SBF simulated body fluid with pH=7.4 were investigated. To evaluate their in vivo degradation performance, gastrointestinal anastomosis were performed for 24 beagles with equally divided into Mg staple and Ti staple group. Some standardized indicators after surgical were compared between two groups.

RESULTS: The staples can maintain the structure integrity after 14 days immersion in SBF solution. With prolonging immersion time, corrosion first occurs at the ends and the bending section of staples (Fig. 2).

In vivo degradation evaluation results show staples are kept as a whole from CT and surgical observations for a short-term (7 days) degradation in animals, and disappear after 90 days (Fig. 3). The experimental group and the control group had no significant difference in anastomotic time, body weight, postoperative complications, abdominal

cavity adhesion, diameter and blasting pressure of anastomotic stoma ($p > 0.05$).

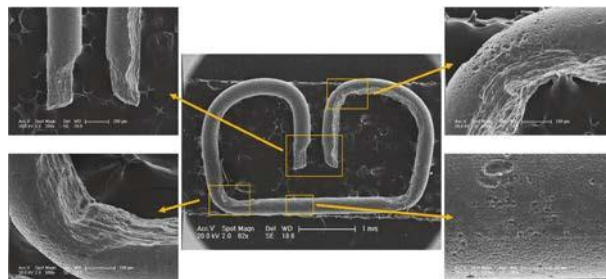


Fig. 2: corrosion morphology of staple after 10 days immersion in SBF with corrosion products and surface coating removed.

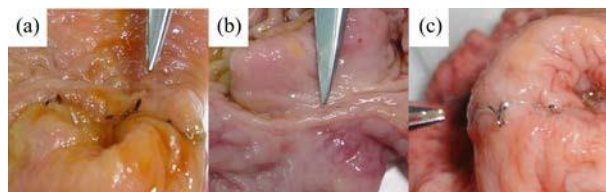


Fig. 3 in vivo degradation of staples: (a) short-term (7 days) Mg staple, (b) long-term (90 days) Mg staple, and (c) long-term (90 days) Ti staple.

DISCUSSION & CONCLUSIONS: Nonuniform corrosion of Mg staple can be attributed to the lack of protective coating at the ends of staple, and the stress corrosion associated with inner stress in bending section arising from the plastic deformation of “B”-shape staple.

Mg staples can maintain the structure integrity for more than 7 days in vitro and vivo, and are degraded completely in animals in 90 days in vivo, showing a good application prospect.

Sustained release of vancomycin from polymer coated micro-arc-oxidized (MAO) AZ31 alloy

A Roy^{1,3}, J Ohodnicki^{1,3}, B Lee^{1,3}, and PN Kumta^{1,2,3,4}

¹ [Department of Bioengineering](#), ² [Department of Chemical Engineering](#), ³ [Center of Complex Engineered Multifunctional Materials](#), ⁴ [Department of Mechanical Engineering and Materials Science](#), University of Pittsburgh, Pittsburgh, PA, 15261. pkumta@pitt.edu

INTRODUCTION: Metal implants are usually used in open bone fractures and related wound infections leading to delayed union, loss of limb or life. Despite availability of myriad clinical standards of care for treating bone infections, local treatment at implant surface is considered the best. Moreover, sustained prolonged antibiotics release is desired to prevent implant infection, allowing unimpeded vascularization and new bone formation. Magnesium (Mg) alloy bone implants have garnered much interest due to their degradability and bone regeneration abilities. To achieve infection free bone regeneration from degradable Mg implants, development of biocompatible coatings with sustained release of antibiotics is highly desirable. The present work reports the synthesis of degradable polymer coatings of vancomycin (VA) entrapped micro-arc-oxidized (MAO) AZ31, and sustained release of biologically active VA from these coating over four weeks.

METHODS: Commercial AZ31 (Alfa Aesar) substrates were used after polishing for MAO coatings and phosphate, silicate and fluoride was used as electrolyte. Coating was performed under a DC voltage of ~ 400 V and ~ 230 mA of current for 10 minutes. The MAO treated samples were washed with ethanol and dried in air. These MAO scaffolds were impregnated with the ethanol-water solution of VA and loading of VA was 2.0 mg per scaffold. Poly Lactic-co-Glycolic Acid (PLGA) and Polycaprolactone (PCL) in dichloroethane was used to dip coat the vancomycin containing MAO-AZ31 samples. *In vitro* release of VA was carried out in phosphate buffered saline (PBS) at 37°C and the concentration of VA released at each time point was determined by measuring the absorbance at 280 nm, from which the concentration was calculated using a standard calibration curve. The biological activity of the released VA was evaluated on staphylococcus aureus (*S. aureus*) by measuring the zone of inhibition using the disc diffusion method.

RESULTS: *In vitro* release kinetics of VA (Fig. 1a) showed a burst release for 5 % PCL and 10 % PLGA coated samples, whereas, PCL 10% and PLGA 30% exhibited sustained release over time. Due to sustained release from PCL 10% sample, the concentration of VA remained well above the minimum inhibitory concentration (MIC, Fig. 1b) and minimum bactericidal concentration (MBC, Fig. 1b). Moreover, the zone inhibition measured for all the coatings confirmed the biological activity of the released VA over time.

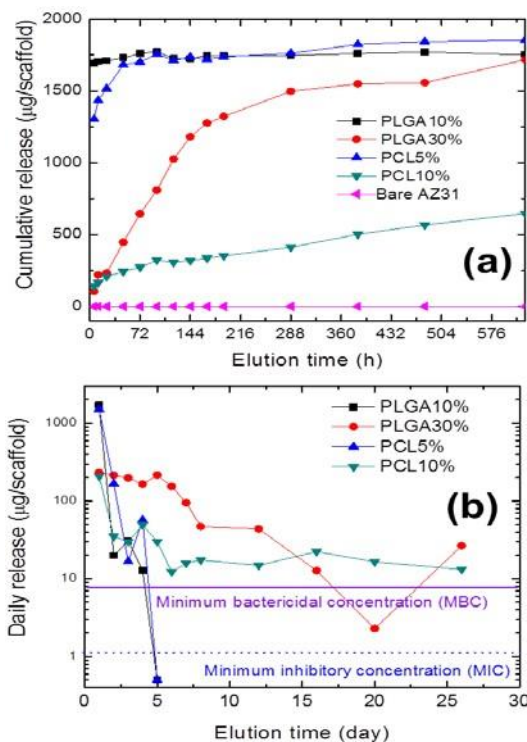


Fig. 1: Vancomycin release kinetics from various polymer coated samples, (a) cumulative release, and (b) daily release.

DISCUSSION & CONCLUSIONS: These results demonstrate that the VA incorporated MAO treated Mg alloys along with suitable polymer coatings could serve as a potential clinical option for treatment of infected bone defects.

ACKNOWLEDGEMENTS: Authors gratefully acknowledge the financial support of NSF-ERC, Grant # EEC-0812348.

Microstructure evolution and corrosion behaviour of the biodegradable EZK1110 alloy

A Steinacker¹, CL Mendis¹, M Mohedano¹, F Feyerabend¹, M Stekker², P Maier³,
 KU Kainer¹, N Hort¹

¹ Institute of Materials Research, Helmholtz-Zentrum Geesthacht, Geesthacht, Germany

² MeKo Laserstrahl-Materialbearbeitung, Sarstedt/Hannover, Germany

³ University of Applied Sciences Stralsund, Stralsund, Germany

INTRODUCTION: Magnesium alloys are widely studied for biological applications. The degradation behavior of every alloy needs to be investigated in detail before being considered for *in vivo* tests. The degradation behavior is not only influenced by the alloy composition but also by the microstructure of the material. Wrought processing, e.g. extrusion, and heat treatment can thus have a significant influence on the degradation behavior of the material. The microstructure evolution under T4 heat treatment and the attributed degradation behavior for an extruded Mg-RE alloy are investigated in this study.

METHODS: Heat treatment of the extruded rod was done at 500°C for 1 hour (W1) and 24 hours (W2). The microstructure is evaluated with a TESCAN Vega Scanning Electron Microscope (SEM) and FEI CM200 Transmission Electron Microscope (TEM). Gravimetric degradation tests are done on the as extruded and the heat treated conditions. The weight loss tests are conducted in Dulbecco's Modified Eagle Medium (DMEM)+10% fetal bovine serum (FBS) under cell culture conditions for 1 and 7 days.

RESULTS: Two intermetallic phases, bulk LPSO phase (MgDyZn based) and a ternary (MgDyNd) phase are observed in the extruded condition. TEM analysis shows a very fine distribution of LPSO phase within Mg matrix (Fig. 1). After W1 heat treatment the secondary phase fraction decreased, additionally the grain size increased from $4.3 \pm 2.6 \mu\text{m}$ to $42 \pm 26 \mu\text{m}$ and did not change significantly with longer heat treatment.

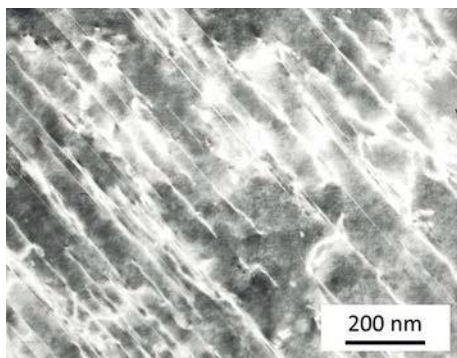


Fig. 1: LPSO phase in as extruded condition

The amount of LPSO phase increased with heat treatment. W2 contains coarser LPSO phase which is distributed throughout the matrix (Fig. 2).

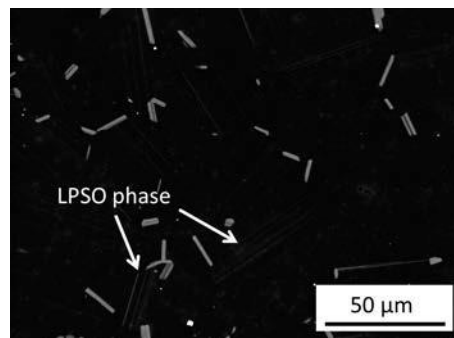


Figure 1: Microstructure of W2 sample

Short time heat treatment (W1) reveals a negative effect on the degradation behaviour of the alloy, whereas longer heat treatment time leads to a similar degradation performance compared to as-extruded alloy.

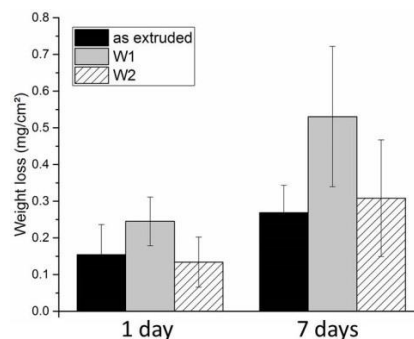


Figure 2: Weight loss in DMEM with FBS solution under cell culture conditions

DISCUSSION & CONCLUSIONS: Short time heat treatment leads to a change in the microstructure that decreases the corrosion resistance of the alloy in DMEM+FBS. With longer heat treatment a uniform distribution of LPSO phase is achieved which lowered the degradation. The alloying elements cause a complex microstructure which has an important influence on the degradation behaviour. Therefore microstructure needs to be optimised to achieve minimum degradation rates.

Fatigue performance of Resoloy® magnesium alloy wire

Adam J. Griebel¹, Jeremy E. Schaffer¹

¹ Research & Development, Fort Wayne Metals Research Products Corp., Fort Wayne, IN, USA

INTRODUCTION: One of the most common failure modes of medical devices today is fatigue¹. For devices made of absorbable metals, which are designed to undergo corrosion, the interactive effects of corrosion and fatigue are critical to device performance^{2,3}. Accurate *in vitro* corrosion fatigue testing of absorbable materials is exceedingly complex. However, prior to attempting to study the phenomena of corrosion fatigue, it is prudent to examine the effects of fatigue and corrosion independently. This study seeks to understand the fatigue performance of a high-strength Mg - rare earth alloy (Resoloy®^{*}) in fine wire form.

METHODS: Resoloy material was processed through cold wire-drawing techniques to a diameter of 127 μm with 70% cold work. Cold worked material was thermally treated at 350, 400, and 450°C, and tensile tested in each condition.

Rotary beam fatigue testing (Fig 1.) was conducted for each condition according to ASTM E2948-14. Specific parameters were: T = 22°C, air environment, f = 60 Hz, R = -1, N = 7, and runout = 10⁷ cycles. Strain levels began at 1% and were decreased until runout was achieved.

RESULTS: Tensile testing resulted in a wide range of properties (Fig. 2). Yield strength values ranged from 314 to 506 MPa at 0.2% offset, corresponding to yield strains of 0.86 to 1.5%.

The As Drawn, 350°C, and 400°C conditions all performed similarly, achieving 10⁷ cycles at 0.5% strain (Fig 3.) The 450°C condition achieved runout at 0.4%. Minimum cycles to failure are plotted for each level in Fig 3.

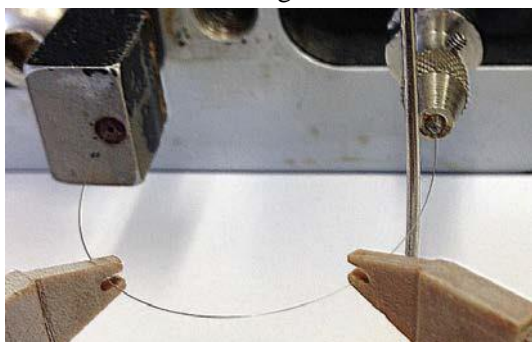


Fig. 1: Rotary Beam Fatigue testing apparatus. The wire is held at a predetermined strain by a rotating chuck, right, and a bushing, left.

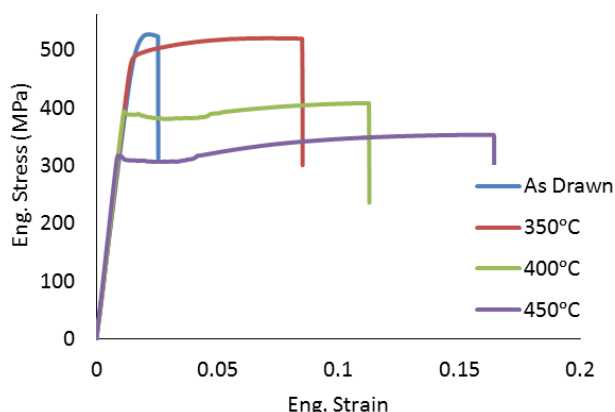


Fig. 2: Resoloy wire properties used in this study.

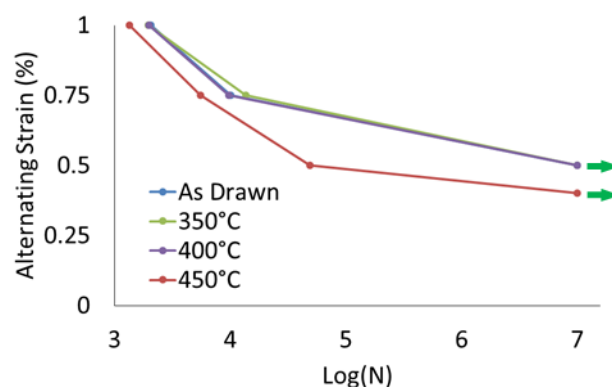


Fig. 3: Minimum results for each condition. All performed similarly with the exception of 450°C.

DISCUSSION & CONCLUSIONS: Absorbable medical devices requiring either high strength and elasticity or high plasticity may be well served by Resoloy wire, with properties being highly tuneable based on processing. The fatigue results presented herein are encouraging; 0.5% strain runout is on par with spring-temper superalloy wires⁴. Resoloy also compares favourably with a similar study conducted with WE43B, in which runouts ranging from 0.25-0.33% were achieved⁵. Continued testing will include additional strain levels, SEM fracture analysis, and introduction of corrosive media.

ACKNOWLEDGEMENTS: Drew Finan assisted with fatigue testing.

* Resoloy is a registered trademark of MeKo, Sarstedt, Germany.

In vitro and in vivo corrosion, cell response, and biocompatibility of high strength Mg-Ca-Zr, Mg-Y-Ca-Zr, and Mg-Y-Zn-Ca-Zr alloys for orthopaedic implant applications

DT Chou^{1,2,4}, D Hong^{1,2,4}, S Oksuz⁵, R Schweizer⁶, A Roy^{1,2,4}, B Lee¹, V Gorantla^{2,3}, [PN Kumta](#)^{1,2,4*}

¹Departments of Bioengineering, ²McGowan Institute for Regenerative Medicine, ³Department of Plastic Surgery, University of Pittsburgh, Pittsburgh, PA, US, ⁴NSF-ERC for Revolutionizing Metallic Biomaterials, ⁵Gulhane Military Medical Academy, Department of Plastic and Reconstructive Surgery, Istanbul, Turkey, ⁶Department of Plastic Surgery and Hand Surgery, University Hospital Zurich, Switzerland

INTRODUCTION: Degradable Mg alloys have emerged as a promising biomaterial for orthopaedic applications due to their unique degradation properties, positive bone remodeling behaviour, and good biocompatibility. Increasing strength and controlling corrosion are ongoing goals in Mg alloy research. In order to address these goals, novel Mg-Ca-Zr, Mg-Y-Ca-Zr, and Mg-Y-Zn-Ca-Zr based alloys were developed. The effects of varying concentrations of Y and other alloying elements as well as the introduction of a long period stacking order (LPSO) phase on *in vitro* cell response was evaluated. Finally, the Mg-Y-Zn-Ca-Zr alloy was implanted in a rat femoral fracture model to evaluate its effects on bone healing, its toxicity, and degradation.

METHODS: Mg-Ca-Zr (KX11), Mg-Y-Ca-Zr (WK11 and WK41), and Mg-Y-Zn-Ca-Zr (WZ42) based alloys were melted, cast, and extruded. MC3T3 pre-osteoblast cells and human mesenchymal stem cells (hMSCs) were cultured directly on alloys or in the presence of their degradation products. Viability of cells attached to the alloys was evaluated after 1 and 3 days using fluorescence imaging and SEM. Viability and proliferation of cells cultured with degradation products and with alloy element salts were assessed using the MTT and CyQUANT assays. Osteogenic differentiation as a result of the degrading alloys was also investigated by quantifying ALP activity. Pins of Mg-Y-Zn-Ca-Zr alloy were implanted into rat femurs to fix a full osteotomy. Rats were sacrificed after 2, 8, and 14 weeks to investigate degradation by volume loss using micro-CT, local tissue response and bone healing using Goldner's trichrome histological staining, and systemic toxicity by blood cell counts, serum biochemical tests, and liver and kidney histology and elemental analysis.

RESULTS: Cells attached to the surface of alloys after 3 days culture are shown in Fig. 1 demonstrating high cell attachment.

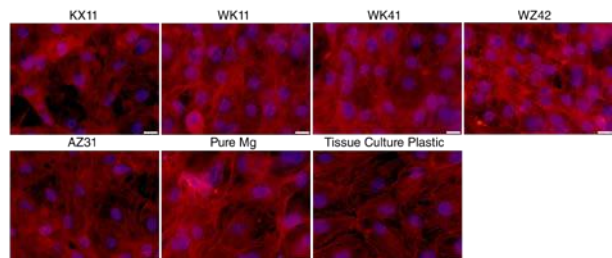


Fig. 1: Stained F-actin (red) and nuclei (blue) of MC3T3 cells on the surface of new Mg alloy surfaces (first row), AZ31, pure Mg, and culture plastic after 3 days. Scale bar = 20 μ m.

High cell viability and proliferation of MC3T3 and hMSCs were observed after culture in the presence of extract media collected from the degrading alloys. Addition of Y and Zr specifically were shown to improve cell proliferation. Low toxicity, gradual degradation, and normal bone healing was observed surrounding the Mg-Y-Zn-Ca-Zr pins implanted into rat femurs (Fig. 2).

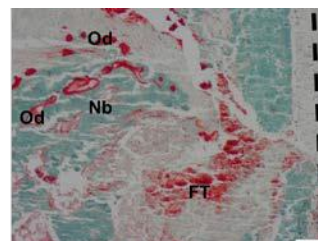


Fig. 2: Goldner's Trichrome stained section at the femoral defect site. Fibrin, muscle, and osteoids are represented in red; bone is represented in blue-green. The dashed line approximates the implant pin-bone interface. Scale bar = 200 μ m. Od, osteoids; FT, fibrous tissue; Nb, new bone.

DISCUSSION & CONCLUSIONS: The low *in vitro* and *in vivo* toxicity, controlled degradation, and non-detrimental effects to bone healing and local tissue response to the Mg-Ca-Zr, Mg-Y-Ca-Zr, and Mg-Y-Zn-Ca-Zr alloys explored in this study indicated their promise as orthopedic and craniofacial implant biomaterials.

ACKNOWLEDGEMENTS: NSF funded ERC-Revolutionizing Metallic Biomaterials (grant-EEC-0812348) and Pennsylvania State funding are gratefully acknowledged.

Preliminary research on biodegradation performances of MgZnCa amorphous ribbon for tissue regeneration membrane application

YP Zhang¹, YB Ren¹, HM Fu¹, L Tan¹, K Yang¹

¹ Institute of metal research, CAS, Shenyang, P.R. China. ² Shengjing Hospital of China Medical University, Shenyang, P.R. China

INTRODUCTION: Amorphous ribbon ($Mg_{70}Zn_{25}Ca_5$) is fabricated and its feasibility as tissue regeneration membrane application has been evaluated by microstructural, thermal, surface analysis, immersion and electrochemical tests in vitro. The degradation characteristics analyzed by immersion and electrochemical tests in Hank's solution reveal a slow and homogeneous biodegradable behavior. Surface analysis shows that a Zn-rich protective layer is detected and no visible pitting is found on the surface of amorphous ribbon. After degradation, the porous structure is observed for matrix.

METHODS: $Mg_{70}Zn_{25}Ca_5$ alloy ingots were prepared by melting the mixture of pure elements of Mg (99.99 wt.%), Zn (99.9 wt.%) and Ca (99.9 wt.%) with graphite crucibles in an induction furnace under the Ar gas atmosphere. The ingots were re-melted in quartz tubes under a high vacuum ($3.5E-3$) to produce the amorphous ribbons by melt spinning with the help of high purity Ar. All the samples were then successively ultrasonically cleaned in acetone, absolute ethanol and deionized water for further experiments.

RESULTS: $Mg_{70}Zn_{25}Ca_5$ ribbon was successfully fabricated with the dimension of 2.26mm in width and 36 μ m in thickness. The high-resolution TEM images together with electron diffraction pattern show that $Mg_{70}Zn_{25}Ca_5$ ribbon is a single amorphous phase with the isotropic disordered pattern. These data from XRD, DSC and TEM measurement together indicate the glassy nature of $Mg_{70}Zn_{25}Ca_5$ ribbon. Electrochemical testing indicates that amorphous ribbon is more noble with higher corrosion resistant and lower degradation rate than pure Mg. From the results of weight loss, the corrosion rate of $Mg_{70}Zn_{25}Ca_5$ ribbon is about 0.19 mm/year (in 2 weeks) and 0.22 mm/year (in 3 weeks) which show a slow and uniform corrosion.

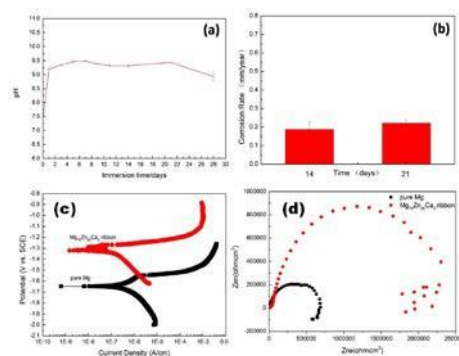


Fig. 1: The in vitro degradation and electrochemical tests of $Mg_{70}Zn_{25}Ca_5$, (a) pH monitoring, (b) weight loss, (c) polarization curve, (d) EIS spectrum

DISCUSSION & CONCLUSIONS: In this study, amorphous ribbon may be an appropriate choice for tissue regeneration membrane application based on the following conclusions:

1. Surface morphology analysis reveals homogeneous degradation for amorphous ribbon without pitting corrosion which could ensure the stability and security for biomaterials.
2. Electrochemical testing indicates that amorphous ribbon is more noble with higher corrosion resistant and lower degradation rate than pure Mg, and also the surface film with corrosion products functions more than the electric double layer.
3. The roughnesses of the ribbon surfaces are different: one is smooth and the other is rough according with the structure of tissue regeneration membrane.

ACKNOWLEDGEMENTS: This work was financially supported by National High Technology Research and Development Program of China (863 Program, No.2015AA033701).

Remote laser cutting of Mg alloy with a ps-pulsed laser

AG Demir¹, A Purnama^{1,2}, B Previtali²

¹*Department of Mechanical Engineering, Politecnico di Milano, Milan, Italy*

²*Lab. for Biomaterials and Bioengineering, Laval University, Quebec City, Canada*

INTRODUCTION: Laser microcutting is the most widely used method for stent manufacturing in the industry [1]. It is by now an established process for more common permanent stent materials, namely stainless steel and Co-Cr alloys [2]. Concerning Mg alloys, the process yields different limitations due to low melting point, high reactivity and viscosity in the molten phase [3]. New high power ultrafast lasers operating with ps pulse durations and green/UV wavelengths allow for ablation based machining with improved cutting quality. In particular, these lasers can be used in remote cutting. The process is preferred for cutting low thickness materials with high sensitivity to heat input, being potentially appealing for biodegradable stent materials such as Mg alloys. The ps pulse duration avoids heat interaction compared to longer ns pulses and continuous wave lasers. Green and UV wavelengths provide higher precision compared to near infrared lasers.

This work demonstrates the feasibility analysis of remote cutting of Mg alloy using a ps-pulsed laser operating with green and UV wavelengths.

METHODS: Fig.1 reports the functioning principles of conventional laser cutting with the use of a process gas and remote cutting. In microprocessing, remote cutting is employed with pulsed lasers and scanner heads. By scanning the laser beam over the surface, limited amount of material is removed at each scan pass. The material is cut by applying multiple scans on the cut area until a through kerf is obtained.

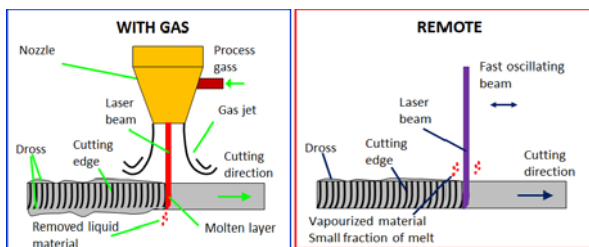


Fig. 1: Working principles of conventional and remote laser cutting.

The laser source used in this work produced pulse durations shorter than 15 ps and allowed to operate with fundamental emission wavelength at 1064 nm

as well as second and third harmonics at 532 nm and 355 nm (Coherent Lumera Hyper Rapid 50 HE). Remote cutting was applied on AZ31 Mg sheets with 250 μm thickness. In a preliminary analysis parameter combinations were analysed for quality comparisons.

RESULTS: Fig. 2 shows representative cuts obtained by laser remote cutting with the ps-pulsed laser and compared to a ns-pulsed laser operating at 1064 nm wavelength. It can be observed that the ps-pulsed laser provides much cleaner and regular kerf. The use of 355 nm wavelength with the ps-pulsed laser provided a cleaner kerf compared to 532 nm wavelength. The required power density for through cuts was found to be around 130 Ws/cm^3 for both of the wavelengths indicating similar levels of efficiency in material removal.

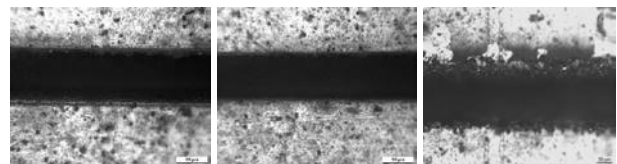


Fig. 2: Cut kerfs obtained with ps laser operating 532 nm (left) and 355 nm (middle) wavelength and ns pulsed laser at 1064 nm (right).

DISCUSSION & CONCLUSIONS: This work provides an extension for microcutting strategies on Mg alloys. The results demonstrate that ps-pulsed remote cutting can provide excellent cutting quality and reduce post-processing complexity. The laser microcutting quality can be further improved through the control of pulse profile and pulse train shaping.

ACKNOWLEDGEMENTS: The authors would like to acknowledge a NSERC PostDoctoral Fellowship awarded to Agung Purnama and Coherent GmbH for the use of the laser source.

Corrosion behaviour of newly developed biodegradable zinc alloys for medical applications

E Mostaed¹, M Sikora-Jasinska^{1,2}, S Loffredo¹, D Mantovani², M Vedani¹

¹ [Department of Mechanical Engineering, Politecnico di Milano, Milan, Italy](#) ² [Lab. for Biomaterials & Bioengineering, CRC-I, Dept. Min-Met-Materials Engineering & CHU de Québec Research Center, Laval University, Québec City, Canada.](#)

INTRODUCTION: Biodegradable metals are a class of materials which is expected to be used for medical applications where an implant has a non-permanent character. In the last ten years, Mg and Fe-based alloys were extensively investigated. However, both families present issues related to their degradation time: Mg alloys degrade too quickly, while Fe alloys have a very small corrosion rate [1]. Zinc, on the other hand, was shown to possess an ideal degradation rate [2]. In addition to this, it was observed that pure zinc possesses excellent arterial biocompatibility [3]. However, pure zinc has poor mechanical properties. Because of this, there is the need to develop Zn-based alloys with enhanced performances, while keeping the optimal corrosion rate of pure zinc.

METHODS: Twelve zinc alloys, namely Zn-XMg (X=0.15, 0.5, 1, 3), Zn-ZAl (Z=0.5, 1) and Zn-ZAl-XMg (X=0.15, 0.5, 1) were prepared by melting pure Zn (99.995 %), pure Al (99.995 %) and pure Mg (99.95 %) at 500 °C. The cast ingots were then homogenized for 48 hours at 350°C. Tube extrusion was carried out at 300°C for producing stent precursors. For evaluating the corrosion behaviour of the extruded alloys, both static immersion and potentiodynamic polarization tests were performed at 37°C using Hank's modified solution as corrosion medium. Pure Zn was used as reference.

RESULTS: The corrosion rates obtained from static immersion tests are reported in Figure 1. It can be seen that binary alloys show a degradation rate which is comparable to that of pure Zn, thus indicating good potential for the expected application. On the other hand, ternary alloys exhibit a significantly higher corrosion rate with respect to pure zinc and binary alloys. The corrosion mechanism of binary alloys may depend on the role of the simple second phases which form during casting and processing. On the other hand, more complex phases may form in ternary alloys: the different nature of these phases may cause very low potential sites, especially if Mg and

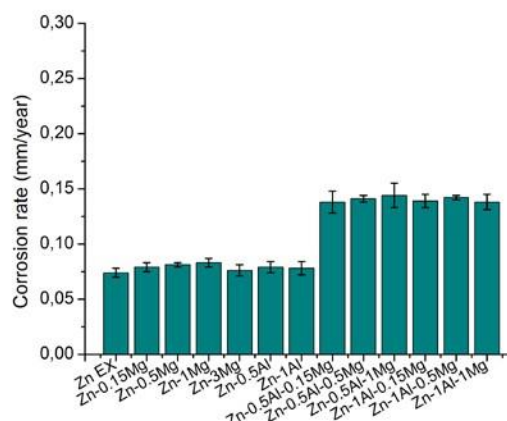


Fig. 1: Corrosion rates of Zn alloys obtained from static immersion tests

Al (known for being very low potential elements) are discovered to react together to form those second phases, giving rise to strong galvanic corrosion reactions when coupled to Zn matrix.

DISCUSSION & CONCLUSIONS: Twelve zinc alloys were synthesized and processed into tubes. Pure Zn and binary alloys possess a corrosion rate which is about half that of ternary alloys. This difference in behaviour may be ascribed to the formation of new second phases, which give strong galvanic corrosion. Further tests are in progress to characterize the corrosion behaviour of these alloys, in terms of analyses of corrosion products and of sample surface after corrosion.

Effect of initial powder preparation on mechanical and biodegradation properties of newly developed Fe-Mg₂Si composites for medical applications.

M Sikora-Jasinska^{1,2}, C Paternoster², E Mostaed¹, R Tolouei², R Casati¹, M Vedani¹, D Mantovani²

¹*Department of Mechanical Engineering, Politecnico di Milano, Milan, Italy*

²*Lab. Biomaterials & Bioengineering, (CRC-I), Dept. Min-Met-Materials Engineering & Research Center CHU de Québec, Laval University, Québec City, Canada*

INTRODUCTION: Biodegradable metals used for cardiovascular and other medical applications are expected to degrade completely upon fulfilling their mission, to support the damaged tissue during healing process without generating any toxic effects¹. Pure iron has shown promising potential especially for cardiovascular stent application. However, its degradation rate is too slow. One approach to solve the mentioned drawback is the use of Fe metal matrix composites, where the second phase is aimed at tuning the corrosion behavior. In this study, the influence of Mg₂Si particles incorporated into the microstructure to create Fe-Mg₂Si composites was investigated as a novel material for degradable biomedical applications. *In vitro* degradation of the samples was reported.

METHODS: Powder metallurgy was selected as a processing route, aimed at fabricating the composite. Micro-hardness and tensile tests were performed to characterize the mechanical properties of the new material. Modified Hanks' solution was used for *in vitro* corrosion test. Samples were immersed for two weeks in a controlled environment. Scanning electron microscopy (SEM), X-ray dispersive spectrometry (EDS), X-ray diffraction (XRD) and X-ray photoelectron spectroscopy (XPS) were used as characterization techniques. Corrosion rates were calculated by weight loss method accordingly to *ASTM G31* standard.

RESULTS: The reinforcing particles improved the performance of the Fe matrix in terms of mechanical strength, microhardness, but also accelerated the degradation rate. Surface morphologies after *in vitro* test varied depending on the initial powder preparation method, mixing and mechanical milling, as shown in Fig.1.

The degradation layer on the surface of pure Fe was found to be composed mainly of iron and oxygen, with traces of phosphorus and calcium. Iron showed moderate and uniform degradation (Fig. 1a). In composites, localized corrosion could be observed with corrosion products covering the surface of sample reinforced with coarse

particulate reinforcement (Fig.1b) whereas for fine particulate reinforced sample (Fig. 1c), corrosion products almost covered the whole surface, indicating a relatively uniform corrosion mode. The degradation of composite prepared from mechanically milled powders led to the formation of homogeneous FeCO₃ deposit on the surface (Fig. 1d).

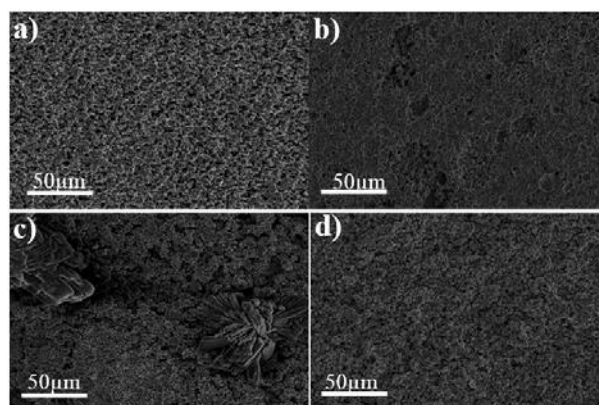


Fig. 1: Surface morphology after *in vitro* degradation tests (a) pure Fe (b) Fe-Mg₂Si with coarse reinforcement (c) Fe-Mg₂Si with fine reinforcement, (d) Fe-Mg₂Si prepared from mechanically milled powders.

DISCUSSION & CONCLUSIONS: Fe-Mg₂Si composite showed a higher corrosion rate compared to that of pure Fe. The preparation method of the starting powders played a significant role in the degradation/passivation process as well as degradation mechanism of the final composite. To sum up, Fe-based composites are promising candidates for degradable material for biomedical application with proper mechanical properties and faster degradation rate.

ACKNOWLEDGEMENTS: The authors would like to thank the MRI-Italy for partially funding this research.

Zn-based biodegradable alloys: recent achievements and novel alloy development

E Mostaed¹, M Sikora-Jasinska^{1,2}, A Mostaed³, S Loffredo¹, R Beanland³, D Mantovani², M Vedani¹

¹ [Department of Mechanical Engineering, Politecnico di Milano, Milan, Italy.](#) ² [Lab. for Biomaterials & Bioengineering \(CRC-I\), Dept. Min-Met-Materials Engineering, Laval University, Québec City, Canada.](#) ³ [Department of Physics, University of Warwick, Coventry, UK.](#)

INTRODUCTION: In the last decade, Mg and Fe based alloys, as two main classes of biodegradable metals have been extensively investigated. Mg degrades too fast and rarely homogenous, while degradation rate of Fe is too slow. Recently, Zn has been proposed as a potential material for biodegradable applications. Zn has an intermediate standard corrosion potential between Fe and Mg. Beside, Zn is an essential element for human, playing a key role in cell proliferation. Thus, Zn is believed to be a promising candidate for degradable stent application.

The present contribution is aimed at reviewing recent achievements on Zn and Zn alloys for biodegradable applications. In addition, strategies related to the development of new Zn-based alloys are discussed and experimental results related to a wide set of proposed materials are given.

METHODS: Zn-based binary alloys were prepared by melting pure Zn (99.995%), Mg (99.95%) and Al (99.995%) at 500 °C. Tube extrusion was performed at 300 °C aimed at producing small size tubes as precursors for biodegradable stents. Microstructural observation in terms of grain size distributions and grain orientation maps were obtained using Electron Backscattered Diffraction (EBSD) in a field emission gun scanning electron microscopy (FEG-SEM). Mechanical properties were characterized by tensile tests along the extrusion direction. An overview about in-vitro corrosion behavior is also given to support evaluation of the different alloys.

RESULTS: Microstructural observation showed a significant grain refinement after the extrusion. It was found that by increasing the Mg content, the tensile strength of the Zn-Mg alloys increased owing to the increasing volume fraction of the hard Mg₂Zn₁₁ intermetallic phase. Al seemed to be less effective in improving the mechanical properties of Zn-based alloys which is attributed to its higher solubility in Zn. EBSD study on the extruded Zn-Mg tubes showed nearly similar microstructure to their billet extruded counterparts, resulting in comparable mechanical behavior.

EBSD analysis in the adjacent to the laser cut Zn-Mg tubes revealed no occurrence of grain growth, confirming that after laser cutting the grain size of the final stent remains unchanged. Thus, the cut stent might have reasonably comparable mechanical properties to that of uncut material.

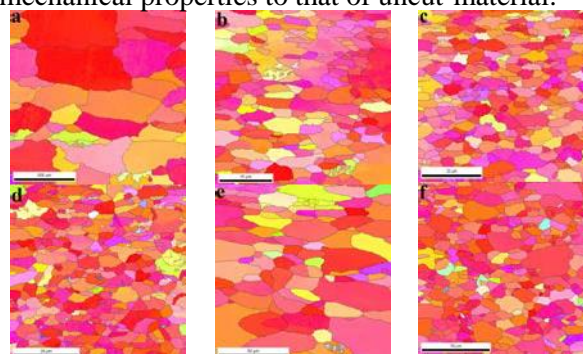


Fig. 1: Microstructure of the extruded samples: (a) Zn, (b) Zn-0.15Mg, (c) Zn-0.5Mg, (d) Zn-1Mg, (e) Zn-0.5Al and (f) Zn-1Al.

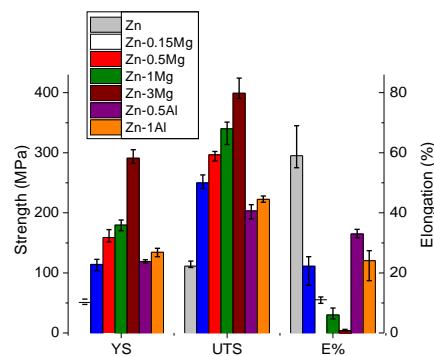


Fig. 2: Tensile properties of the extruded samples.

DISCUSSION & CONCLUSIONS: Zn-based alloys with different Al and Mg contents were proposed for biodegradable stent applications. Hot extrusion led to a considerable grain refinement in the all samples. With increasing Mg content, mechanical properties of the Zn-Mg alloys were improved due to the increasing volume fraction of the Mg₂Zn₁₁ phase. Among all the investigated alloys, Zn-0.5Mg owing to having combination of reasonable mechanical properties and a proper rate of loss of mechanical integrity provided a promising potential for stent application.

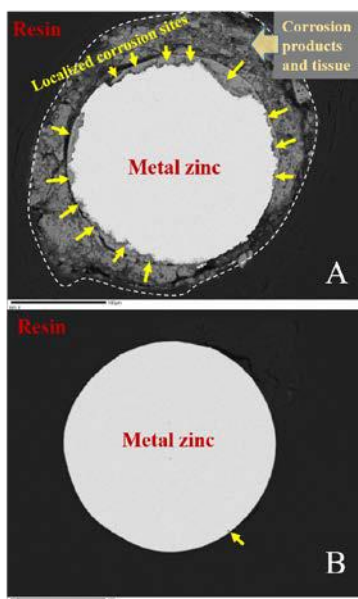
Importance of stable oxide film in endovascular biodegradable stents

JW Drelich¹, A Drelich¹, PK Bowen¹, L LaLonde², J Goldman²

¹ Department of Materials Science and Engineering, ² Department of Biomedical Engineering, Michigan Technological University, Houghton, MI 49931, USA

INTRODUCTION: Our report showed that zinc (Zn) wires exhibit an average penetration rate of 0.01 to 0.02 mm/year in the first 3 months of *in vivo* degradation, less than half the rate observed at 4.5 and 6 months [1]. The cause of the variable degradation rate of Zn is attributed to a thin passive surface oxide film. The oxide film functions as a temporary inhibitor of ion release in biodegradable stents. As a result, a better understanding of the surface oxide film on biodegradable metals could lead to the design of smarter, surface responsive biodegradable stents with improved biocompatibility and controlled degradation rates at different stages of implantation. In the present study, the surface finish of Zn was manipulated through different material processing conditions. High purity zinc wires with oxide films of varying surface characteristics such as thickness, structure and roughness were tested *in vivo* to understand their response to a biological environment [2].

METHODS: Zn wire of 99.99+% purity with a diameter of 0.25mm (Table 1 - C) from Goodfellow was used. Selected samples of wires were oxidized in air at 350°C for 1 and 2 hours (F1 and F2). Electropolishing of selected wires (E) was done in a mixture of ethanol (885mL), butanol (100mL), AlCl₃•6H₂O (109g), ZnCl₂ (250g), and water (120mL) for 2 min using a current density of 0.25 A/cm² and voltage of 10V. Samples were cleaned and sterilized before *in vivo* testing. 1.2-1.4 cm segments of wires were implanted into the wall of the abdominal aorta of a rat for 4 weeks - as described in Ref. [2]. Cross-sectional imaging and analysis are described in [1].



RESULTS: Table 1 summarizes biodegradation results for four (duplicate) samples studied. Figure 1 shows examples of two cross – sections at different locations of the same biodegraded zinc wire sample (electropolished): one is severely biocorroded and another shows nearly no signs of corrosion. A similar variability in cross sections was recorded for all samples, although a larger number of severely biocorroded sections were seen for oxidized wire samples.

Table 1. *In vivo* degradation results.

Sample	Oxide film thickness [μm]	4 week biodegradation	
		Cross area reduction [%]	Penetration rate [μm/y]
C	0.2-0.3	5.9 + 2.4	51 + 20
E	0.1-0.2	5.9 + 2.6	45 + 21
F1	0.2-0.6	8.1 + 3.7	70 + 33
F2	0.7-1.2	7.9 + 2.7	67 + 24

DISCUSSION & CONCLUSIONS: The degradation rate was mainly dependent on the quality and stability of the oxide film. Defects/cracks in the oxide film structure serve as local corrosion sites and their increased density accelerates corrosion rate. Therefore, the surface oxide film could be engineered to delay and decrease the stent degradation rate for the early stage of zinc material biodegradation. We further hypothesize that the activity of the surface oxide film depends upon an interplay between kinetics of ion release and rebuilding the passive film. Over time, as we hypothesize, an ion exchange process in the oxide film loosens the film's structure, exposing the bare metal to fluid and prompting an accelerated dissolution process.

ACKNOWLEDGMENT: U.S. NIH – NIBIB (Grant #5R21 EB 019118-02) and U.S. NIH – NHLBI (Grant #1R15HL129199-01).

Figure 1 (at left). Cross sections of electropolished zinc wire after 4 weeks in an arterial wall of rat. A) Highly corroded, and B) nearly intact.

A Prediction of degradation of Mg and Mg alloys, why it is not easy?

WD Mueller¹, T.Zimmermann¹

¹ *Charité Universitaetsmedizin Berlin, CC3, Biomaterial Res. Gr., Berlin, Germany*

INTRODUCTION:

The chemical properties of Mg, as an element of the second row of the periodic system, seem to be easy to explain. But since many years a lot of researchers try to find a way to predict exactly the degradation or corrosion behaviour of Mg, or Mg-alloys for biomedical application.

There are broad discrepancies in the corrosion rates (CR) between in-vitro to in-vivo experiments. Various techniques are applied trying to estimate the corrosion or degradation rate in various in-vitro environments.

At least only one experiment is giving a clear data set, the immersion of a piece of Mg as long as it is dissolving.

But that is not a solution because no information about the degradation process are given, which are very important for decision for further applications.

Electrochemical techniques have a great potential to obtain reliable CR data of Mg and Mg-alloys. The future task will be to develop standardized measurement protocols for these purposes using the advantages of electrochemical measurements, as measuring under nearly real conditions, assessment of interface processes, reduction of number of specimens, measurements with various resolutions and improvement of reproducibility. Techniques, as electrochemical impedance spectroscopy, cyclic voltammetry and potential measurements are feasible with any electrochemical set up. These techniques should be

combined, and the results should be compared with results from independent investigations, in order to improve and qualify the results of electrochemical measurements. One option may be the reduction of the measurement area, combined with an improvement of resolution. In order to prevent contact problems at clamps, the MCS setup or miniaturized sensors ought to be chosen. Both, Mini Cell System (MCS) and Ultra Micro Electrodes (UME) (Scanning Electrochemical Microscopy (SECM)) are able to render information about degradation process kinetics.

AIM: The aim of this presentation is a summary of techniques to determine of CR especially from the electrochemical measurement point of view, focussing on the problems appearing with a perspective based on first experiments of in situ observation of electrochemical measurements at Mg alloy surfaces.

Flow-induced corrosion of absorbable magnesium alloy: *in situ* and real-time electrochemical study

J Wang^{1,2}, J Sankar¹, N Huang², Y Yun¹

¹NSF Eng. Res. Center for Revolutionizing Metallic Biomaterials, North Carolina A&T State Univ., Greensboro, USA. ²School of Mat. Sc. and Eng., Southwest Jiaotong University, Chengdu, China.

INTRODUCTION: Absorbable metals have a dynamic corrosion profile depending on the environments [1,2]. The *in vivo* condition around an implant critically determines the implant's chemical dynamic processes. For example, the flow of blood plays a significant role in the initial stage of Mg-based stent degradation. In this work, a three-electrode cell was introduced into a fluid dynamic vascular bioreactor to monitor *in-situ* and real-time corrosion behavior of Mg alloy as a function of flow-induced shear stress (FISS).

METHODS: A Mg-based alloy with 5 wt.% zinc and 0.3 wt.% calcium was used. The vascular bioreactor, according to our latest work [2], was developed to imitate physiological conditions encountered in vessels. It consists of a test channel, electrolyte (Dulbecco's modified Eagle's medium with 10% fetal bovine serum and 1% penicillin-streptomycin), variable-flow pump, reservoir and incubator (37 °C, 5% CO₂, 95% RH). FISS was varied at 0, 0.3, 0.6, 1.2 and 2.3 Pa. A typical three-electrode cell was introduced into the vascular bioreactor (Fig.1). It consists of a Ag/AgCl/3 M KCl reference electrode (RE-6 (MW-2030)), a platinum wire counter electrode, and the MgZnCa specimen sealed by epoxy resin with an exposed area of 13.5 mm² as the working electrode. A potentiostat was used to perform electrochemical impedance spectroscopy (EIS), open circuit potential (OCP) and linear polarization measurement (LPM) studies in 30-min loop measurements for 24 h.

RESULTS & DISCUSSION: To better understand the effect of hydrodynamics on corrosion kinetics, corrosion types, corrosion rate and corrosion products, the multiple-supporting methods and profiles provided the quantitative and straightforward data of the comprehensive corrosion behavior, based on the electrochemical assessment and interface morphology characterization:

a. The FISS was found to accelerate electron transfer, leading to an increase in the comprehensive (uniform and localized) corrosion, especially for the initial stage.

b.

layer, but reduced the resistance of this layer at 0.31 and 0.62 Pa, due to an increase in filiform corrosion on the surface.

c. FISS increased the localized corrosion area and removed some loose corrosion products (almost all corrosion products peeled off at 0.62 Pa) owing to an increased mass transfer effect and mechanical force.

d. With the increase of FISS, the localized corrosion dominated more and more of the entire corrosion, compared with the uniform corrosion.

e. EIS-estimated and LPM-measured polarization resistances (R_{polar}) showed a great consistency. Both had a good correlation with average corrosion rate calculated by micro-CT. R_{polar} displayed a FISS dependence and also was associated with the acceleration of anodic dissolution.



Fig.1: Schematic of the vascular bioreactor with an electrochemical monitoring system. Equivalent electrical circuit used to fit the EIS data shown on the cross-section of the corroded sample at each FISS and time condition. Typical 3-D reconstructions using X-ray micro-CT of samples with the increase of FISS.

CONCLUSIONS: The work herein presented a model for the *in-situ* and real-time electrochemical monitoring of Mg alloy corrosion in a simulated vascular flow environment. This simple approach provided an accurate, instantaneous and capable long-term determination of Mg corrosion for the application of vascular stents.

ACKNOWLEDGEMENTS: USA NSF-0812348, China NSF-81330031.

FISS thickened the uniform corrosion product

Degradation morphology and pitting factor compared to degradation rate

P Maier¹, J Gonzalez², R Peters¹, F Feyerabend², T Ebel², N Hort²

¹University of Applied Sciences Stralsund, Stralsund, Germany. ²Institute of Materials Research, Helmholtz-Zentrum Geesthacht, Geesthacht, Germany

INTRODUCTION: Since degradation pits act as notches causing an increase of stress intensity a uniform degradation is needed for materials used as biodegradable implants. High degradation rates and local pitting are the main limitations. [1] Mg-RE alloys show an acceptable performance. For a Mg-Y-Nd-Dy-Gd wrought alloy good mechanical and degradation properties are found. [2]

METHODS: A hot-extruded WE32 alloy [2] in 3 different conditions (extruded, T4 and T6) is used to compare degradation rates (by weight loss after immersion: 7 days in Ringer-Acetate at 37°C) with degradation morphology characterised by shape/depth of degradation pits and degraded areas (by micrographs of cross-sectional area) after potentiodynamic polarization to 500 mV, see degraded sample in Fig. 1. The undegraded outer ring is used as the original surface. The mean degradation rate DR_m is calculated using the equation:

$$DR_m = \frac{8.76 \cdot 10^4 \cdot \Delta m}{A \cdot t \cdot \rho} \text{ (in mm/year)}$$

where Δm is the weight change in g, A is the surface area of the sample, t the immersion time in h and ρ is the density in g/cm³. The diameter of the cylinders used is 15 mm with a height of 10 mm. The pitting factor is the ratio of the deepest degradation pit p divided by the average penetration d (Fig. 2. [3, 4]), which was calculated from the degraded area after polarization of the cross-section of the degraded samples divided by diameter of the exposed surface, which is 11 mm.

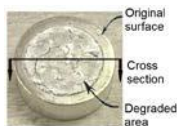


Fig. 1: Degraded sample after polarization test

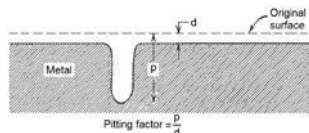


Fig. 2: Sketch of deepest pit in relation to average penetration calculating the pitting factor [4]

RESULTS: Tab. 1 shows the degradation rates of the immersion tests and the parameter calculated from the micrographic characterisation after polarization. T6 reduces the degradation rate significantly. The degraded areas of extruded, T4 and T6 are 1.35, 1.51 and 1.24 mm², respectively. Micrographs in Fig. 3 reveal the most homogenous degradation attack for the T6 condition.

Table 1. Characterisation of degradation of WE 32 in three conditions: extruded, extruded-T4 and extruded-T6, *immersion test, **potentiodynamic polarization

	DR_m^* (mm/year)	deepest pit / average** degradation (mm)	pitting factor**
extruded	14.6	0.36 / 0.124	2.95
T4	25.2	0.42 / 0.137	3.06
T6	5.3	0.30 / 0.113	2.65

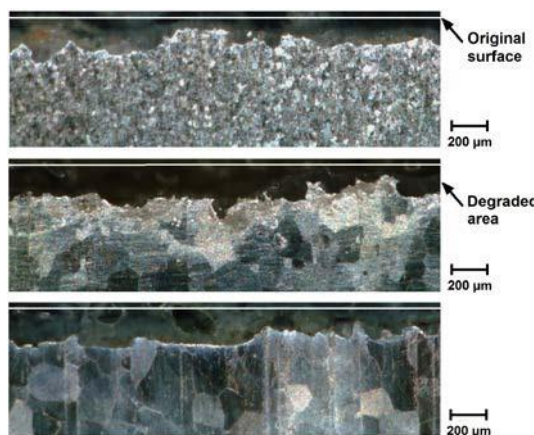


Fig. 3: Degradation morphology after polarization: a) extruded, b) extruded-T4 and c) extruded-T6 condition

DISCUSSION & CONCLUSIONS: Degradation rates revealed from immersion tests agree with the degraded area data taken from polarization: T4 condition degrades faster than the extruded and T6 condition. Also in agreement is the degradation morphology characterisation: most shallow pits, lowest average degradation (penetration) and the smallest pitting factor is found for T6. However, the pitting factors are very similar and compared to AZ31B in [5] with 20-50 and LAE442 in [1] with 4 rather small. The application of profilometry to measure the whole surface is in progress. The fine dispersed particles formed during precipitation hardening are responsible for the best degradation properties, agreeing with the mechanical properties [2]: T6 after extrusion shows the highest strength.

Influence of surface condition on the corrosion of XHP-Mg alloy wire

S Johnston¹, Z Shi^{1,2}, M Dargusch², A Atrens¹

¹The University of Queensland, Materials Engineering, School of Mechanical & Mining Engineering, Brisbane, Qld 4072, Australia. ²The University of Queensland, Centre for Advanced Materials Processing and Manufacturing (AMPAM), Brisbane, Qld 4072, Australia

INTRODUCTION: Wires form the basic building block for numerous biomaterial applications, including orthopaedic K-wires and sutures in wound closure. Magnesium (Mg) alloys were considered for wire based applications more than a century ago, but did not gain acceptance largely due to high corrosion rates¹, now known to have been caused by high levels of impurity elements². Ultra-High-Purity (XHP) Mg alloys have been developed with a novel distillation method³, and have shown superior corrosion resistance compared to conventional HP Mg, attributed to the reduction in impurity levels^{3,4}. Alloying XHP-Mg with relatively low concentrations of zinc (Zn) and calcium (Ca) has been shown to improve the mechanical properties, while maintaining good biocompatibility and corrosion resistance⁵. Cold drawn samples of XHP-Mg wires are believed to be good candidates for wire based biomaterials. The aim of this work was to study the corrosion of XHP-Mg alloys in various surface conditions in order to further improve the corrosion resistance of cold drawn XHP-Mg alloy wires for biomedical applications.

METHODS: The alloy used in this study was XHP-ZX00 (XHP-Mg alloyed with 0.45 wt% Zn and 0.45 wt% Ca). Six surface conditions were studied: as extruded (AE), as drawn (AD), annealed at 340°C for 5min (HT), mechanically cleaned with SiC grinding paper (MC), chemically polished with a phosphoric acid based cleaning solution (CP) and cleaned with acetic acid (AA). Samples were studied *in vitro* in CO₂-bicarbonate buffered Hanks' solution for 7 days at 37 °C and pH of 7.4. Each surface treatment was tested in triplicate. Corrosion rates were evaluated by mass loss, hydrogen evolution and radius reduction (an adapted corrosion evaluation method).

RESULTS: The corrosion rates evaluated from mass loss, hydrogen evolution and radius reduction for all surface conditions are presented in fig. 1. The CP samples fragmented during testing and experienced a significant change in length. This broke one of the conditions for the radius reduction method and as such, a corrosion rate was not evaluated for this condition with this method.

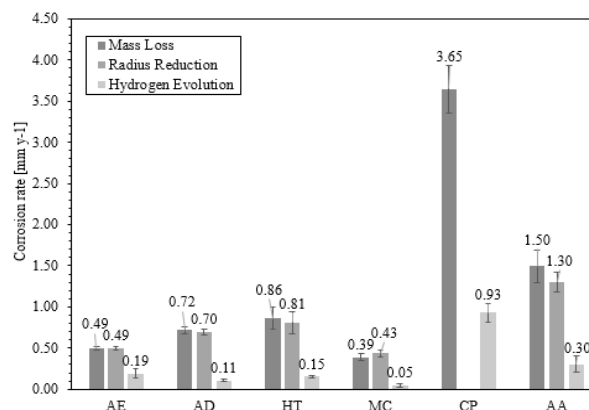


Fig. 1: Corrosion rates evaluated for XHP-ZX00 extruded and wire samples.

DISCUSSION & CONCLUSIONS: Fig. 1 indicates that surface condition was correlated with the corrosion resistance of the XHP-ZX00 samples. The untreated samples (AE, AD, HT) had relatively low corrosion rates. Both the chemical surface treatments (CP and AA) increased the corrosion rates of the wire samples. The mechanically cleaned samples had the lowest corrosion rate of all the samples tested, and was determined to be the best surface condition for XHP-Mg alloy wires. The low corrosion rates suggest that XHP-ZX00 is a good candidate for bio-corrosion applications.

There was good agreement between *Pm* and *Pr* for all of the samples that were evaluated with both methods. This suggests that radius reduction is an appropriate method for corrosion evaluation of samples with slow corrosion rates, simple geometries, high aspect ratios, and which do not experience significant length reduction.

Improvement of corrosion resistance and biocompatibility of WE43 magnesium alloy treated by titanium and oxygen dual plasma implantation

Z Lin^{1,2}, Y Zhao³, HM Wong^{1,2}, KMC Cheung¹, F Leung^{1,2}, PK Chu⁴, [KWK Yeung](#)^{1,2*}

¹Dept. of Orthopaedics and Traumatology, The University of Hong Kong, Pokfulam, Hong Kong, China.

²Shenzhen Key Laboratory for Innovative Technology in Orthopaedic Trauma, The University of Hong Kong Shenzhen Hospital, Futian District, Shenzhen, China. ³ Center for Human Tissues and Organs Degeneration, Shenzhen Institutes of Advanced Technology, Chinese Academy of Sciences, Shenzhen 518055, China. ⁴Dept. of Physics and Materials Science, City University of Hong Kong, Tat Chee Avenue, Kowloon, Hong Kong, China.

INTRODUCTION: Magnesium alloy is a potential candidate for degradable orthopaedic implantation due to its degradability. However, rapid corrosion and subsequent severe hydrogen release under *in vivo* conditions limit its clinical application. Therefore, various methods e.g. alloying, coating, and heat treatment have been applied to reinforce its corrosion property. In this study, we have developed titanium and oxygen dual plasma immersion ion implantation (PIII) [1] technique to improve the corrosion resistance and biocompatibility of WE43 alloy.

METHODS: The casted WE43 alloy was treated by titanium and oxygen dual implantation. For characterization of PIII-treated WE43 alloy, the atomic force microscope (AFM) and X-ray photoelectron spectroscopy (XPS) were conducted to investigate surface chemical states and morphology of the PIII-treated WE43 alloy. In order to systematically examine corrosion resistance of the untreated and PIII-treated alloys, immersion and electrochemical tests in the simulated body fluid (SBF) at 37°C were also carried out. The biocompatibility of PIII-treated WE43 alloy was evaluated by MTT, ALP assays and cell attachment analysis cultured with mouse osteoblastic cells.

RESULTS: The XPS and AFM results indicated that the surface of WE43 magnesium alloy appeared a dense TiO₂ protective film with the thickness of about 120nm created by titanium and oxygen dual implantation. The electrochemical tests in SBF showed that the PIII-treated WE43 alloy exhibited excellent performance of corrosion resistance. Its electrochemical impedance increased eighty times approximately, while corrosion density sharply dropped in the untreated group. Moreover, the TiO₂ protective film could still reduce corrosion and the subsequent Mg ion release effectively in comparison with the untreated alloy after three days of immersion in SBF. It was an evidence that the created dense

TiO₂ film could suppress rapid corrosion of WE43 magnesium alloys. The WE43 alloy treated by Ti & O dual implantation exhibited achieved higher cell viability and ALP activity. Furthermore, the morphology of cells flattened and more F-actins were observed on the surface of PIII-treated WE43 alloy while culturing with MC3T3-E1 pre-osteoblasts, indicating that the cyto-compatibility of WE43 alloys can be significantly improved by titanium and oxygen dual PIII treatment.

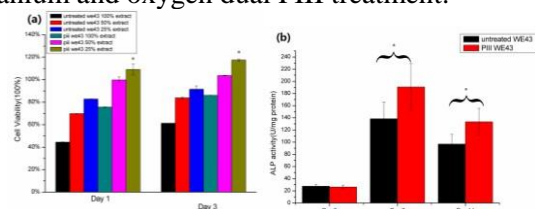


Fig. 1(a) The cell viability and (b) ALP assay of MC3T3-E1 pre-osteoblasts cultured with the extracts of PIII-treated WE43 alloy that immersed in DMEM for 24h) *denotes the significant difference between PIII-treated WE43 alloy and untreated WE43 alloy (p < 0.05)

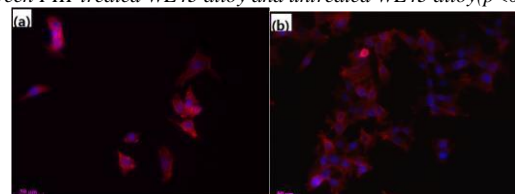


Fig.2 fluorescence image of MC3T3-E1 pre-osteoblasts cultured on the surface of (a) untreated we43 and (b) PIII treated WE43 alloys (incubation for 5h)

DISCUSSION & CONCLUSIONS: In summary, the corrosion resistance and cyto-biocompatibility of WE43 magnesium alloys can be significantly enhanced by Ti and O dual plasma ion immersion implantation. It is expected that the PIII-treated WE43 alloy may potentially apply for the management of large bone segmental defect after systematic *in vivo* pre-clinical analyses.

ACKNOWLEDGEMENTS: National Natural Science Foundation of China No. 31370957 and Hong Kong Research Grant Council General Research Fund (#718913).

Bioactive CaP-coated iron foam for potential bone scaffolds

Y Su^{1,2}, S Champagne¹, A Trenggono¹, R Tolouei¹, D Mantovani¹, H Hermawan¹

¹ *Dept. Mining Metallurgical and Materials Engineering & CHU de Québec Research Centre, Laval University, Québec City, Canada.* ² *The Key Lab of Automobile Materials, Ministry of Education, College of Materials Science and Engineering, Jilin University, Nanling Campus, Changchun, China.*

INTRODUCTION: Iron foam was proposed for biodegradable metal-based bone scaffolds due to its strength, degradability and acceptable toxicity under *in vitro* and *in vivo* settings [1, 2]. The foam structure greatly enhances iron's degradation rate, but an excessive degradation could be harmful to a wound healing, especially at the early stage of the process [3]. Coating has been applied to modulate the degradation rate of iron foam structure [4]. In this work, the degradation of pure iron foam was controlled by calcium phosphate (CaP) coating, in view of its potential for increasing surface bioactivity toward bone cell proliferation.

METHODS: Open-porous pure iron foam (99.9% purity, 800 μm pore size, 88% porosity) was used as substrate material. The substrate was pretreated in 2% HNO₃ solution to remove oxides then a layer of CaP coating was deposited via chemical conversion in a phosphating bath containing Ca(NO₃)₂·4H₂O + H₃PO₄ (15:85 v/v) at pH 2.8-3.0, 60°C for 5 min. Coating characterization was done by using SEM, EDS and XPS. Corrosion properties of coated and uncoated specimens were electrochemically evaluated. They were also subjected to compression test before and after 1 week of immersion test. Both tests were done in modified Hanks solution at 37°C.

RESULTS: Figs. 1a-d show typical surface morphologies of the CaP-coated and uncoated iron foams. The foam's struts are completely covered with random distributed flakes of high roughness CaP layer. EDS result (Fig. 1e) indicates that the Ca/P atom ratio is 1.1, slightly higher than that of dibasic calcium phosphate dihydrate (DCPD).

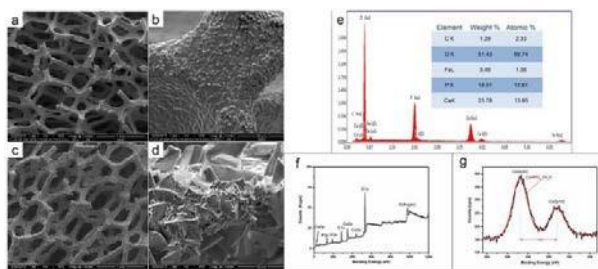


Fig. 1: Surface morphology of: (a,b) uncoated and (c,d) CaP-coated foams, (e) EDS and (f-g) XPS spectra.

Deconvolution of high-resolution XPS spectra of the Ca 2p peak (Fig. 1g) splits the peak into two peaks as a result of spin orbit splitting. Binding energy of the Ca 2p_{3/2} peak of the CaP coating can be fitted to DCPD (347.6 eV) confirming the EDS result. The coated specimens have: ~7X lower degradation rate, as calculated from potentiodynamic polarization (PDP) (Fig. 2b), and ~25X higher polarization resistance, as measured by electrochemical impedance spectroscopy (EIS) (Fig. 2c), compared to the uncoated ones. Table 1 shows that rigidity and compressive strength of the coated specimens decreased ~2X lesser than those of the uncoated ones, after immersion test.

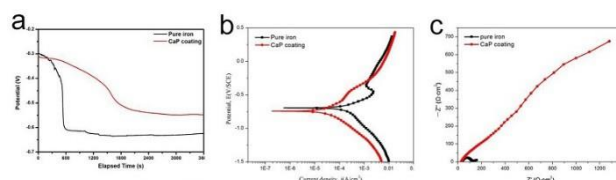


Fig. 2: Results of electrochemical test: (a) open circuit potential, (b) PDP and (c) EIS.

Table 1: Results of compression test before and after immersion.

Fe foam	Rigidity (MPa)		Strength (MPa)	
	Before	After	Before	After
Uncoated	20.28±3.59	7.00±1.34	0.41±0.03	0.27±0.09
Coated	16.02±1.07	12.57±2.74	0.51±0.09	0.40±0.04

DISCUSSION & CONCLUSIONS: CaP coating was deposited on the surface of 3D structure porous iron by a conversion coating process. The coated specimens have lower degradation rate compared to the uncoated ones due to the high resistivity of the CaP layer. This layer also protects the iron structure from an abrupt decrease of rigidity and compressive strength after immersed in modified Hanks solution.

ACKNOWLEDGEMENTS: NSERC Canada and the China Scholarship Council.

Iron-based biodegradable alloys degradation behaviour modulation by grain sizing and alloying

A Purnama^{1,2}, C Sunday Obayi^{1,3}, E Mouzou¹, R Tolouei¹, C Paternoster¹, H Hermawan¹,
D Mantovani¹

¹Lab. Biomaterials and Bioengineering, CRC-I, Dept. of Min-Met-Materials Eng., Laval University, Canada. ²Laboratory for Laser Application, Dept. of Mechanical Engineering, Politecnico di Milano, Italy. ³Dept. of Metallurgical & Materials Engineering, University of Nigeria, Nsukka, Nigeria.

Iron-based alloys have been reported previously as biodegradable metals for cardiovascular stent applications due to their biocompatibility and comparable mechanical properties to those of stainless steel [1]. Iron has been alloyed principally with manganese [2], with minor addition of other elements such as palladium [3], carbon [4], and silicon [5] to tailor its strength and degradation rate corresponding to 6-12 months temporary need. New fabrication techniques such as powder metallurgy [2], electroforming [6], and magnetron sputtering [7] were also tried for the same objectives. Despite all the approaches taken to enhance the degradation rate of iron-based alloys, there are limited studies focused on the factors that influence their degradation rate. It was previously reported that the change of grain size influenced the degradation behaviour of pure iron since superior number of grain provides higher density of matrix and grain boundary where corrosion reaction takes place [1,6]. Therefore, the objective of the current study is to investigate the effect of grain sizes towards the corrosion behaviour of pure iron. In order to do so, pure iron sheets (Armco soft ingot, purity >99.8%, Goodfellow, UK) with various grain sizes were produced by thermomechanical treatments comprising cold rolling (75-85% thickness reduction) and annealing (550°C-1000°C). The resulting sheets composed of pure iron sheets with grain size varied from 14 µm to 168 µm. In the effort of producing iron sheet with grain size smaller than 14 µm, electrodeposition of pure iron on titanium cathode was used resulting iron sheet (99.7% purity) with the average grain size of 6 µm following annealing at 550°C. The results showed that smaller grain size iron sheet produced by electrodeposition exhibited superior degradation rate (0.51 mmpy) compared to those of the iron sheets with modified grain size by thermo-mechanical treatments. Moreover, it showed superior mechanical properties (YS=270MPa, UTS=292MPa) compromising its elongation at break (E=18.4%) when compared to other iron sheets. Additionally, when manganese was added (35% wt.) to enhance

the degradation behaviour of pure iron by powder metallurgy, it gave average grain size of 50 µm with degradation rate close to that of electrodeposited iron. The results suggested that the grain size influences the degradation rate of pure iron. Specific window of grain size was observed, in which the degradation rate of pure iron decreased along with the reduction of the grain size (range 10-160 µm of grain size). Moreover, alloying was observed to excite the degradation rate of pure iron since in the range where degradation rate of pure iron was low. Suggestively, manganese as the alloying element contributes to the galvanic corrosion process that accelerates the degradation rate of pure iron. This study provides evidence in different approaches to modulate the degradation behaviour of iron-based alloys by changing the grain size and alloying technique.

ACKNOWLEDGEMENTS: Natural Science and Engineering Research Council of Canada.

The influence of phosphates, bicarbonates and chlorides ions on degradation behaviour of pure Fe in pseudo-physiological solutions

R Tolouei, C Paternoster, P Chevallier, S Turgeon, D Mantovani

Lab. for Biomaterials & Bioengineering, CRC-I, Dept Min-Met-Materials Eng & CHU de Québec, Research Center, Laval University, Quebec City, Canada

INTRODUCTION: Over the past decade, the design of a new class of metals for the development of biodegradable cardiovascular stents has emerged in world of biomedical research [1]. Previous studies have investigated biocompatibility and biodegradability of pure iron in simulated body fluids [2]. Biodegradation in human is a complex phenomenon which needs to be thoroughly investigated to mimic the in-vivo response more precisely. In fact, the synergy of chlorides, carbonates and phosphates present in body environment is a key factor affecting both in-vivo and in-vitro degradation of biodegradable materials, and especially iron and its alloys. Here we highlight the multi-facet behaviour of pure iron as a function of a selected number of solutions for immersion static corrosion tests. This approach could become a reliable and standard practice in the performance assessment of biodegradable metals.

METHODS: As-received commercial pure iron foils were cut, rolled and subsequently thermally homogenized. Samples were immersed for 14 days in 0.153 M NaCl (NCS), Dulbecco phosphate buffered saline (DPBS), Hanks' (CHBS) and modified Hanks' [3] (MHBS) solutions (pH=7.4) under controlled atmosphere. After the 14-day immersion test, the morphologies and microstructure of the test samples were observed and characterized by scanning electron microscopy (SEM) and stylus profilometry (DEKTAK) techniques. The chemical and phase composition of the degradation layers were evaluated by energy dispersive X-ray spectrometry (EDS) and X-ray diffractometry (XRD).

RESULTS: At the iron/solution interface, ions present in the form of Fe^{2+} , OH^- , Cl^- , $\text{HPO}_4^-/\text{H}_2\text{PO}_4^-$ and HCO_3^- . They favor the degradation of sample and/or formation of degradation product layer on the sample surface. SEM images of specimens immersed in DPBS shows precipitates of spherical shape (Figure 1). EDS clearly show the incorporation of phosphates into the surface. The sample surfaces immersed in Hanks' solutions, CHBS and MHBS, are rough and associated with relatively coarse transgranular degraded surfaces. CHBS solution with a higher amount of chloride

ions generated wider valleys (valley height= 2.4 μm) than those of the samples immersed in MHBS solution (valley height= 1.6 μm). Moreover, samples immersed in saline solution (NCS) revealed a porous iron oxide surface, confirmed by XRD.

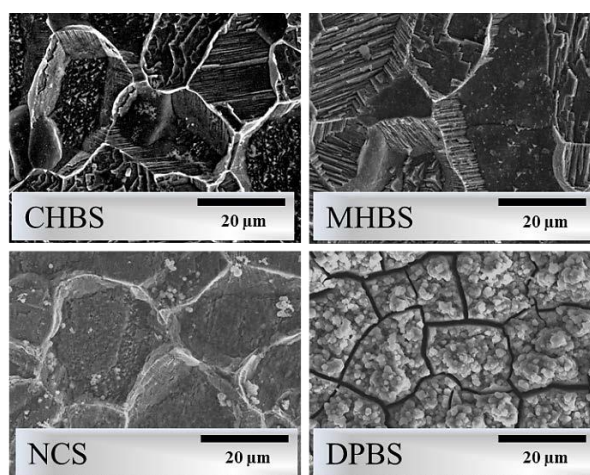


Fig. 1: SEM images of sample surfaces after the 14-day static immersion test.

DISCUSSION & CONCLUSIONS: These results revealed that the presence of different biological ions e.g. carbonates and phosphates had a considerable effect on pure iron degradation behavior. Mainly, because the degradation behavior of pure iron is solution-dependent, the overall result of the current work reveal the importance of conducting in-vitro static immersion test in multiple solutions simultaneously. It could also offer a more complete approach to filling the gap between in-vivo and in-vitro test results by assessing the single and combined effects of ions and complex molecules (proteins, glucose).

ACKNOWLEDGEMENTS: This work was partially supported by NSERC-Canada, CIHR-Canada, CFI-Canada, FRQ-NT-Quebec, and MRI-Quebec.

Towards standardization: Influence of CO₂ rich atmosphere on degradation behaviour of Fe-Mn-C alloy

E Mouzou¹, C Paterneoster¹, R Tolouei¹, P Chevallier¹, C A Biffi², A Tuissi², D Mantovani¹

¹Lab. Biomaterials and Bioengineering, CRC-I, Dept. Min-Met-Materials Eng. & CHU de Québec Research Center, Laval University, Québec City, Canada. ²National Research Council, Institute for Energetics and Interphases, CNR-IENI Corso Promessi Sposi, Lecco, Italy

INTRODUCTION: Biodegradable metals emerged as potential candidates for biomedical applications to replace permanent implants and avoid long-term threats [1]. For this purpose, biodegradable alloys should be biocompatible and their degradation rate should ideally match tissue-healing processes. In literature, various test-systems and solutions were used to evaluate the degradation behavior, which makes it difficult to compare the results, because the degradation behavior is affected not only by the chemical composition of the material, but also by the environmental conditions. In a CO₂ rich medium, like blood, different carbonates with various stabilities could form. For example, Fe ones are not stable [2] whereas Mn ones are considered more stable. This work aimed to investigate the influence of CO₂ atmosphere on the degradation behavior of a new austenitic Fe-Mn-C alloy.

METHODS: Fe-Mn-C samples were obtained by vacuum and melted under uncontaminated conditions at CNR-IENI (LC, Italy). The material was worked to 0.45 mm thick sheets that were thermally treated for 1 h at 800 °C in Ar + 5% H₂ atmosphere (TT) and tested. A modified Hanks' solution (MH) was used for static degradation test (ASTM G31). Two groups of five samples were aged up to 14 days, one under controlled atmosphere (CA, 37 °C; 5% CO₂) and another one in ambient atmosphere (AA, 37 °C; 0.04% CO₂). Scanning electron microscopy (SEM), electron dispersion spectroscopy (EDS), X-ray diffraction (XRD) and atomic absorption spectroscopy (AAS) were used to characterize surfaces and degradation products. Degradation rate was calculated based on the weight loss.

RESULTS: The degradation rate ratio between AA samples and CA ones was approximately two. MnCO₃ crystals mainly covered degraded surfaces of CA samples, while Fe oxides and hydro-oxides were found mainly in degradation product powders. For AA samples, Fe and Mn oxides and hydro-oxides were found both on the degraded surfaces and in the degradation product powders.

AAS investigations revealed that Fe ion concentration in exhausted solutions was higher than Mn one for both CA and AA samples. The results clearly evidenced that different CO₂ concentrations led to a different degradation patterns regarding this Fe-Mn-C alloy. Indeed the formation of stable carbonates (such as MnCO₃) adhering to the CA sample surface significantly affected its degradation rate.

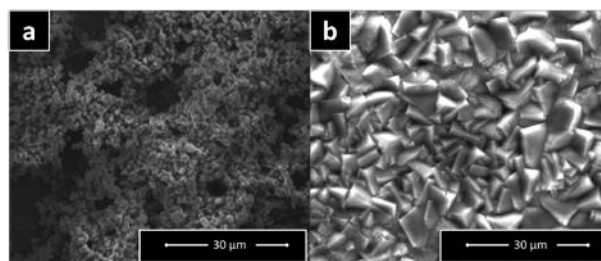


Fig. 1: SEM images of different Fe-Mn-C alloy surfaces after test in a) CA and b) AA conditions.

DISCUSSION & CONCLUSIONS: The degradation behaviour resulted to be strongly affected by material chemistry, the composition of the chemical solution and the test atmosphere. An accurate understanding of these parameters is needed both to compare the results obtained by different researchers, especially in an attempt to predict the correlation between in-vitro and in-vivo experiences.

ACKNOWLEDGEMENTS: The authors would like to acknowledge the kind help and guidance of S Turgeon from CHSFA de Québec. They would like to thank V. Dodier, D. Marcotte, N. Moisan, J. Frenette, M. Choquette and A. Ferland of Min-Met-Materials Eng. at Laval University. They would also acknowledge ACDI and PCBF for the scholarship provided to E. Mouzou. This work was partially supported by NSERC-Canada, CIHR-Canada, CFI-Canada, FRQ-NT-Quebec, and MRI-Quebec/Italy.

Biodegradation of a novel Zn-Li alloy in abdominal aorta of rat

S Zhao¹, R Guillory², PK Bowen¹, JM Seitz¹, HJ Maier³, J Goldman², J Drelich¹

¹ Department of Materials Science and Engineering, ² Department of Biomedical Engineering, Michigan Technological University, Houghton, Michigan 49931, USA. ³ Institut für Werkstoffkunde, Leibniz Universität Hannover, Garbsen, Germany

INTRODUCTION: The first implantation of pure Zn into the abdominal aorta of Sprague-Dawley rats exhibited an excellent corrosion rate [1] and optimal biocompatibility [2]. In this study, a novel Zn-Li alloy (with 0.20 wt% Li and <0.25 wt% additives including Cd, Fe, Pb, Al, Cu, Sn) was produced aiming to replicate the outstanding corrosion behaviour and at the same time improve mechanical properties and uniformity of *in vivo* degradation behaviour.

METHODS: Cast billets of Zn alloy were produced in a vacuum induction caster and then extruded into wires with a diameter of 0.25 mm. Wires of 10 mm length were deployed into the abdominal aorta of six Sprague-Dawley rats. Rats were euthanized and vessels containing the wire implants were harvested after 2, 4, and 6.5 months, with experiments ongoing. Environmental scanning microscopy (FEI Philips XL 40) was used for morphological and elemental mapping (EDS) analysis. Penetration rate was calculated based on the area reduction measurements with ImageJ software, see ref [1]. Cross sections of the explanted wires with aortas were ethanol fixed and then stained with hematoxylin and eosin (H&E), mounted in Permount solution and imaged using an Olympus BX51, DP70 brightfield microscope.

RESULTS: The ultimate tensile stress was measured at 320-340 MPa, with an elongation to failure of ~ 10% for the Zn-Li alloy (data not shown). Backscattered electron images (Fig.1) indicated a loss of the circular integrity at 2 and 4 months of *in vivo* degradation, which progressed further at 6.5 months. EDS maps showed the presence of Zn, Ca, P, O, C, indicating the formation of CaP, ZnO and ZnCO₃ [1]. Cross-sectional analysis showed that the average penetration rate for the 2-month sample was ~0.008 mm/yr, which increased to ~0.016 mm/yr at 4 months and ~0.019 mm/yr at 6.5 months, half the rate found for pure Zn over the same time [1].

H&E stained sections (Fig.2) showed that the wire was surrounded by a neointima at 2 months. The thickness of the neointima at the lumen side was relatively thin, at about 25 µm, increasing to 100 µm at 6.5 month. Lower cell density was observed at the luminal portion of the implant than the medial and adventitial side, confirming the possible suppressive effect from the zinc implant [2]. No evidence of particle embolization, thrombosis, excess inflammation, or fibrin deposition was observed so far, indicating acceptable biological performance as a vascular implant.

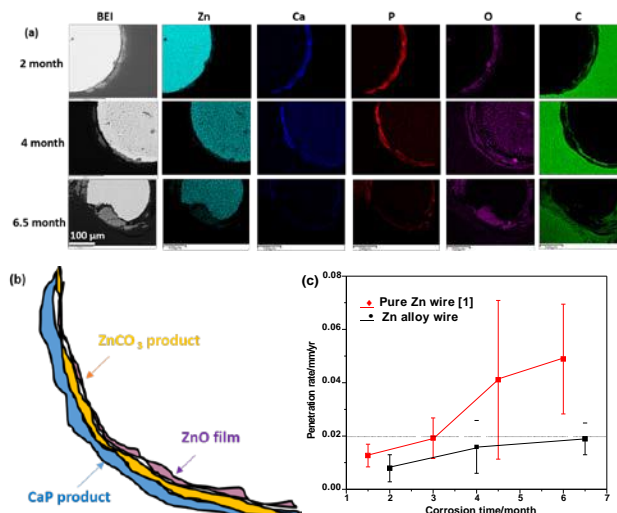


Fig.1. (a) Backscatter electron images and elemental maps (EDS) of Zn alloy wire sections after residing in rat arterial lumen for 6.5 months ($\times 260$ magnifications); (b) Schematic phase map for 6.5-month residence; (c) Penetration rates calculated from reduction of cross sectional areas.



Fig.2 H&E stained sections from excised Zn alloy wire sections after residing in arterial lumen for 2(a) and 6.5(b) months ($\times 10$ magnifications with scale bar of 500 µm).

DISCUSSION & CONCLUSIONS: The novel Zn alloy with <0.45 wt% additives (Cd, Fe, Pb, Al, Cu, Sn and Li) is a promising candidate as a biodegradable coronary stent material. Results indicate its moderate degradation rate of 0.019 mm/yr in 6.5 months, and biocompatibility in the endovascular environment.

ACKNOWLEDGMENT: U.S. NIH – NIBIB (Grant #5R21 EB 019118-02) and U.S. NIH – NHLBI (Grant #1R15HL129199-01).

Study of Mg coating fabrication on orthopaedic implants and its biological properties

K Yang¹, X Li², Z Liu¹, X Yu¹, L Tan¹, Z Guo²

¹*Institute of Metal Research, Chinese Academy of Sciences, Shenyang, China.* ²*Xijing Hospital, Fourth Military Medical University, Xi'an, China*

INTRODUCTION: Mg alloys are considered as a new generation medical metals due to their biodegradable characters and multiple biological functions [1], such as promoting osteogenesis and antibacterial performance resulting from high alkaline during degradation. In this study, a Mg coating was fabricated on Ti alloy, expecting to promote bone formation and osteointegration and reduce the infection for Ti implants.

METHODS: Pure Mg was deposited on both flat and porous Ti6Al4V substitutes by arc ion plating method. The phase composition and surface morphology were analyzed by XRD and SEM. The biodegradation behavior was studied by immersion test. The proliferation and differentiation of BMSCs were estimated using CCK-8 and alkaline phosphatase staining, respectively. A cylinder defect was made on lateral condyle of each femur of rabbits, and then porous Ti alloy samples with and without Mg coating were implanted. The bone formation ability was studied by micro-CT, fluorescence microscope and histological analyses.

RESULTS: The Mg coating on Ti alloy was uniform and smooth, and no defect was observed as shown in Fig.1. The coating consisted of uniform Mg grains of about 1 μ m. The thickness of the coating was about 5 μ m. EDS and XRD analyses showed single phase pure Mg was observed on the surface of Ti6Al4V substrate. The Mg ions release gradually increased to about 73 ppm after 7 days immersion, indicating a continuous release of Mg ions due to the degradation of Mg coating. Both proliferation and differentiation of bone cells for the Mg coated alloy extract were higher than those of control group at 4th and 7th day. As shown in Fig.2, ALP staining showed that the cell differentiation for Mg coated alloy extract was higher than control group at 4th and 7th day. The micro-CT scan shown in Fig.3 indicates that the bone volume to total volume (BV/TV) of Mg coated alloy in region of interest (ROI) was significantly higher than Ti6Al4V group 4 and 8 weeks after operation (P<0.05).

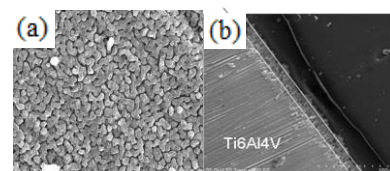


Fig. 1: Surface (a) and cross section (b) of Mg coating on flat Ti6Al4V substitute

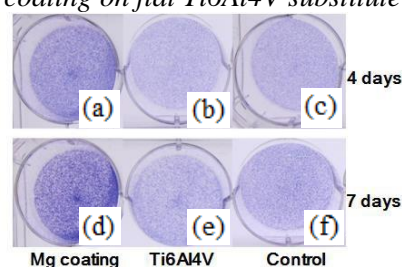


Fig.2 : ALP staining of Mg coating(a)(d), Ti6Al4V(b)(e) and control group(c)(f) after 4 and 7 days cultutures

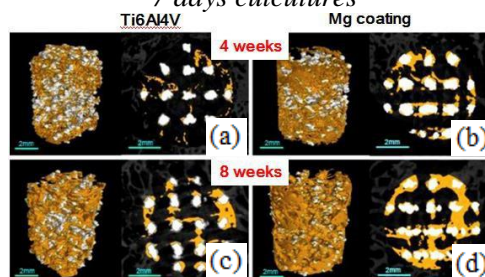


Fig.3: Micro-CT images of Ti6Al4V implants without coating (a)(c)and with Mg coating after 4 and 8 weeks implantation

DISCUSSION & CONCLUSIONS: A uniform Mg coating was successfully deposited on the surface of Ti6Al4V alloy. Compared to porous titanium alloy, the Mg coated porous Ti alloy showed a better biological activity on proliferation and differentiation of BMSCs. The Mg coated porous Ti alloy could significantly promote the new bone formation and had a positive effect of osteoconductivity and osteogenesis.

Corrosion protection and improved endothelial cytocompatibility of plasma polymerized allylamine coatings on biodegradable vascular stent

Y Yang¹, PK Qi¹, J Wang¹, N Huang¹

¹Key Lab. of Advanced Materials Technology, Ministry of Education, Southwest Jiaotong University, China.

INTRODUCTION: The past decades have witnessed the study of degradable biomaterials becoming one of the most revolutionary research topics in the field of biomaterials [1]. The corrosion resistant properties and the biocompatibility are still challenges in the face of application in clinic. Surface modification is one of the most effective ways not only to reduce and control the degradable behavior but also improve the biocompatibility of the biodegradable stents [2]. In this work, pulse plasma polymerized allylamine (PPAam) coatings are successfully deposited onto widely used biodegradable metals in prosthetic and cardiovascular implants, namely magnesium alloys (MgZnMn) and pure iron (Fe).

METHODS: The PPAam coating was fabricated at 6.0 Pa system pressure, 80 V negative bias voltage, 30 W RF power, and pulsed duty cycle was chosen to be 40% ($t_{on}=20$ ms, $t_{off}=30$ ms). The time of deposition was 4 h, then the samples were immediately thermal treated at 120 °C for 1 hour in the vacuum environment of 1.0×10^{-4} Pa.

RESULTS: The surface characteristics of PPAam modified samples indicated that this ultra-thin, pinhole-free polymer-like layers rich in amine functional groups covered the substrate completely. The anti-corrosion properties of PPAam coated MgZnMn and Fe were systematically evaluated by *in vitro* electrochemical experiments. A significant larger capacitive loop arcs in the Nyquist mode and the enhanced corrosion potentials/current confirmed the improved corrosion resistant properties of PPAam coated MgZnMn and Fe (Fig.1 A-D). To investigate the potential application of PPAam on biodegradable stents, endothelial cytocompatibility evaluation and balloon expansion tests were also carried out. The results revealed that the PPAam coating presented good endothelial cells adhesion and proliferation properties (Fig.1 E). And this protective coating could strongly adhere on substrate with neither cracks nor webbings after balloon expansion (Fig.1 F).

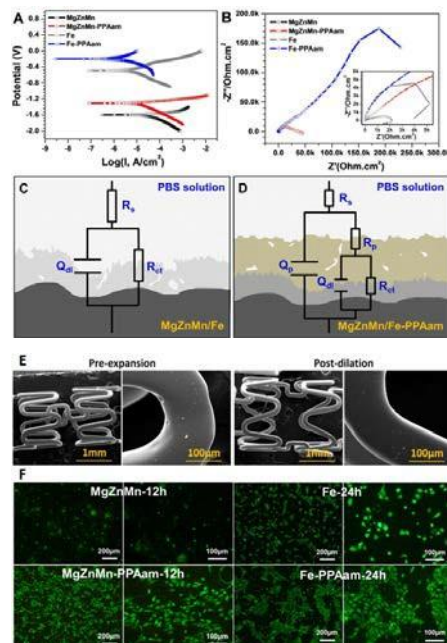


Fig. 1: Polarization curves (A), Nyquist impedance spectrum (B) and equivalent circuit diagram (C and D) of samples. Pre-expansion and Post-dilation images of stent coated with PPAam coating by SEM (E). Results of endothelial cell evaluation (E).

DISCUSSION & CONCLUSIONS: The PPAam modified substrates has significantly decreased the corrosion rate and the formation of biodegradable products. Compared to uncoated samples, MgZnMn-PPAam and Fe-PPAam exhibited higher cell viabilities with the enhancement of ECs attachment, spreading and proliferation properties. Our work suggested that PPAam technique might provide a promising potential platform in surface modification on biodegradable stents.

ACKNOWLEDGEMENTS: NSFC Project 81271701, 51173149 and 81330031, Excellent PhD Cultivation Project of SWJTU (2014).

Preliminary tests to biodegradable metals for ureteral stents

S Champagne¹, D Paramitha^{1,2}, S Chabaud², S Bolduc², H Hermawan¹

¹ [Dept. Mining Metallurgical and Materials Engineering](#) & [CHU de Québec Research Centre, Laval University.](#) ² [Faculty of Medicine](#) & [CHU de Québec Research Centre, Laval University, Québec City, Canada.](#)

INTRODUCTION: Ureteral stents are widely used in patients with urologic disorders when a relief of ureteral obstruction is needed [1]. An ideal ureteral stent maintains an excellent urine flow to optimize upper tract drainage, be resistant to infection and encrustation, and biodegradable [2]. At this point, biodegradable metals are viewed as potential materials for biodegradable ureteral stents. A preliminary study was done on the degradation and antibacterial properties of Mg-Y alloy in artificial urine (AU) and suggested the alloy's potentiality in urological applications [3]. In this work we tested iron (Fe), magnesium (Mg) and zinc (Zn) for their degradation in AU and their cytocompatibility toward urothelial cells.

METHODS: Specimens of high purity Fe (12x10x0.5 mm), Mg (Ø10x4 mm), Zn (12x10x4 mm), were tested for corrosion in AU solution prepared as per ASTM F2129, at pH 6.0 and 37°C using potentiodynamic polarization method as per ASTM G102. Similar specimens were incubated in AU in 8% CO₂ at 37°C for 1-72 h and the extract was filtered using 0.22 µm membrane. 100 µL extract was added into 100 µL media in each of 96-well plate seeded with 5x10⁴ normal human urothelial cells (NHUC)/well. After 1 day of incubation, the conditioned media was removed, the cells were washed twice with sterile 1x PBS. 10 µL WST-1 in 100 µL media were added to each well and incubated for 30 min. The optical density was measured at 440 nm using a microplate reader.

RESULTS: Fig. 1 shows polarization curves of the metals and their corresponding corrosion parameters derived by Tafel extrapolation.

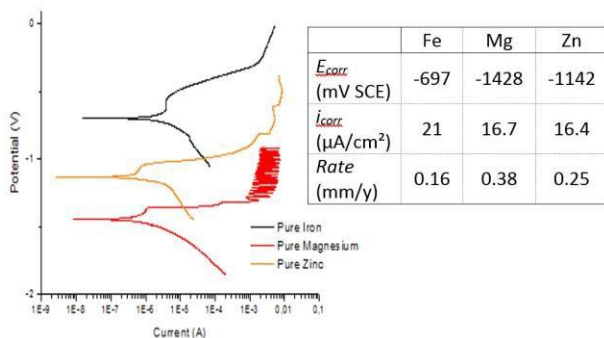


Fig. 1: Polarization curves and corrosion parameters.

Mg shows the highest degradation rate followed by Zn and Fe. Fig. 2 shows NHUC response (%viability vs control) toward the metal's extracts incubated at different time. Mg marks the highest viability followed by Zn, and Fe.

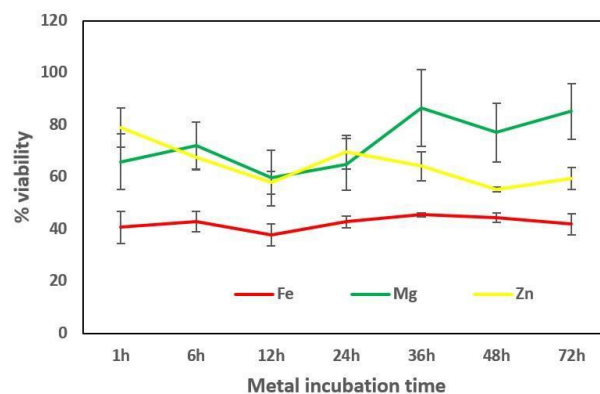


Fig. 2: Result of cell viability test.

DISCUSSION & CONCLUSIONS: Degradation behavior of Fe, Mg, Zn in AU is different than that in other simulated body fluids where generally Mg degrades much faster than 0.38 mm/y. The unique ion content in AU (i.e. NH₄⁺, SO₄²⁻) and pH below neutral may have an effect on passive layer formation as indicated by the polarization curve in anodic zone (Fig. 1). Further assessment by electrochemical impedance spectroscopy is on-going. Fe extract caused low viability of NHUC at all metal incubation time, while for Mg group the viability increased as incubation time prolonged (Fig. 2). The IC₅₀ for each metal is estimated at the metal's extract of 36 h incubation time for Fe and 12 h for Mg and Zn. Further analysis on ionic content in the extracts is on-going and the result will be useful to explain the findings in both viability and degradation. This is a preliminary study and more tests are needed to gain better understanding of degradation of biodegradable metals in AU and its effect toward NHUC.

ACKNOWLEDGEMENTS: CHU de Québec Research Center and the NSERC CREATE program for regenerative medicine (NCPRM).

Effects of zinc on the morphologies and properties of calcium phosphate coating on magnesium alloys

J Wang¹, L Chang¹, D Mei¹, L Wang¹, S Zhu¹, S Guan¹

¹ *School of Materials Science and Engineering, Zhengzhou University, Zhengzhou450001, China*

INTRODUCTION: As a degradable metal, magnesium alloy exhibit several advantages, including improving biocompatibility and enhancing bone formation in vivo [1]. The rapid degradation of magnesium, however, is a double-edged sword as it is necessary to control the corrosion rates to match the rates of bone healing. In response, calcium phosphate coating has been applied to improve the corrosion resistance. Zinc has an important effect on the preservation of bone mass by stimulating osteoblastic bone formation and inhibiting osteoclastic bone resorption [2]. However, there are few studies about Zn-modified calcium phosphate coating on magnesium substrates. In this study, we fabricated Zn-modified calcium phosphate coating on magnesium alloy successfully and explored the potential of this coating for use on degradable orthopaedic material.

METHODS: Mg-Zn-Ca alloy is cut into specimens of 25×10×4 mm³. Samples are polished and cleaned. Electrical parameters are the same as that referred in Ref. [3]. The surface morphology and elementary composition of the coatings are identified by scanning electron microscopy (SEM), which is equipped with energy dispersion spectroscopy (EDS) facility. The structural analysis of the coating is performed by X-ray diffractometer (XRD). In vitro corrosion resistance were evaluated by potentiodynamic polarization in simulated body fluid (SBF). The antibacterial properties were evaluated against *S. aureus* and *E. coli* by a plate-counting method. The cytotoxicity of coating was determined by MTT assay.

RESULTS: From Fig.1 (a) and (b), we can see Zn-modified calcium phosphate coating is composed of flake crystals with ratio of Ca+Zn to P being 1.27:1, which is different from the common calcium phosphate coating without Zinc showing needle-like microstructure with ratio of Ca to P being 1.20:1, as shown in Fig.1 (c) and (d). According to XRD results, the Zn-modified calcium phosphate coating mainly contains biodegradable nonstoichiometric parascholzite. Potentiodynamic polarization results suggest the novel coating has better corrosion resistance than

common coating without Zinc. Furthermore, results of antibacterial and cytotoxicity test show Zn-modified coating has better antibacterial property without cytotoxic effect.

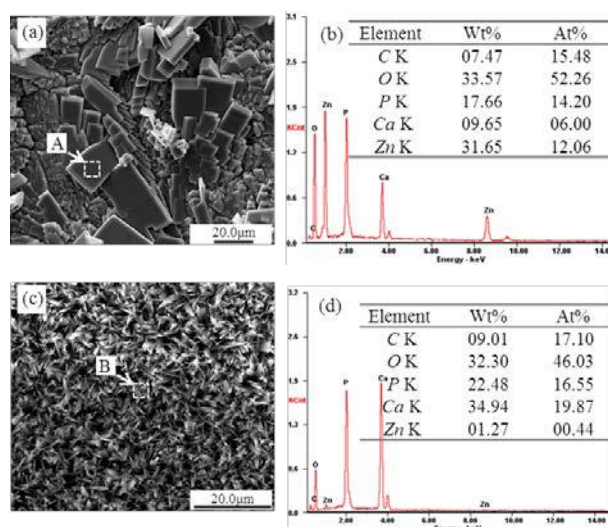


Fig. 1: The typical surface morphologies and EDS analysis of the calcium phosphate coating: (a) containing Zinc, (b) the chemical composition of area in A, (c) without Zinc (d) the chemical compositions of area in B.

DISCUSSION & CONCLUSIONS: In present study, Zn-modified calcium phosphate coating was fabricated on Mg-Zn-Ca alloy successfully. This novel coating shows better corrosion resistance and biocompatibility compared with common calcium phosphate coatings, which has promising applications on magnesium alloy as degradable orthopaedic material.

ACKNOWLEDGEMENTS: The authors are grateful for the financial support of the National Key Technology R&D Program of China (No. 2015AA033603; No. 2015AA020301), Major Science and Technology Project of Henan Province (No. 141100310900).

Corrosion behaviour of T4-treated Mg-5Sn-xZn alloys in simulated body fluid

CD Yim^{1,2}, SK Woo², HS Kim¹, BS You^{1,2}

¹ [Materials Commercialization Department](#), Korea Institute of Materials Science, Korea

² [Advanced Materials Engineering](#), University of Science and Technology, Korea

INTRODUCTION: The fast degradation rate and low strength of magnesium alloys should be enhanced for them to be widely used in human body. The addition of alloying element is one of the solutions. It has been reported [1-2] that Sn was effective to improve extrudability and tensile strength by formation of thermally stable Mg₂Sn phase and Sn dissolved in the matrix also contributed to high corrosion resistance. In this study, the effect of T4 treatment on the corrosion behavior of Mg-5Sn-xZn alloys in simulated body fluid was evaluated systematically.

METHODS: The specimens of Mg-5Sn-xZn alloys for immersion and potentiodynamic tests were prepared by an indirect extrusion and T4 treatment. The specimens were immersed into Hank's Balanced Salt Solution (HBSS) at 310±0.5K. The change of open circuit potential (OCP) was recorded during 3600s and then potentiodynamic polarization test was carried out. The external voltage was changed from -0.25V to 0.5V referred to OCP at the rate of 1mV/s during potentiodynamic test. The average corrosion rate was calculated from the weight loss before and after 10, 20, and 30 days immersion in HBSS.

RESULTS: The corrosion potentials and the cathodic current densities of Mg-5Sn-xZn alloys decreased after T4 treatment while the anodic current densities increased. The cathodic current density decreased with increasing Zn content. The average corrosion rate decreased after T4 treatment and with increasing Zn content. The change of corrosion behavior by T4 treatment was strongly dependent on the microstructural changes. The average grain size increased 6 times after T4 treatment, which resulted in the decrease of the corrosion potential and the cathodic current density. Mg₂Sn particles which were precipitated during extrusion were completely decomposed into the matrix by T4 treatment, which resulted in the decrease of the corrosion potential and the cathodic current density and the increase of the anodic current density as reported in [3]. According to thermodynamic calculation, Sn content dissolved in the matrix would increase after T4 treatment, which made the corrosion potential and the cathodic current density

decreased. It was reported [4] that the average corrosion rate of Mg alloys containing Zn in Kokubo solution decreased with increasing Zn content because the surface film containing Zn acted as an inhibitor of corrosion. Therefore, it is reasonable that Zn would be helpful to corrosion resistance by formation of more stable surface film.

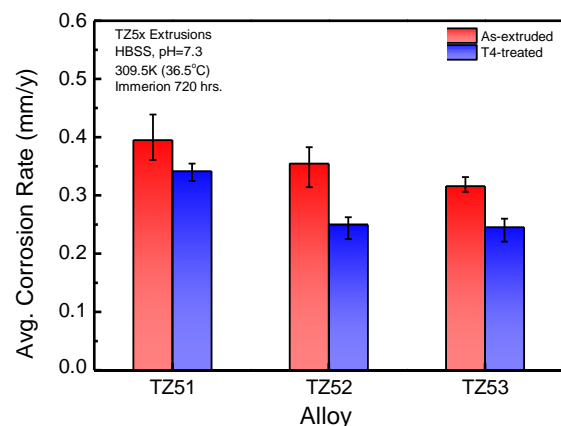


Fig. 1: Average corrosion rates of Mg-5Sn-xZn alloys during immersion in HBSS at 309.5K.

DISCUSSION & CONCLUSIONS: The corrosion behavior of Mg-5Sn-xZn alloys was strongly dependent on the microstructural changes by T4 treatment. The polarization behavior and corrosion rate were affected by average grain size of matrix phase, fraction of second phase particle, and solute content in the matrix phase. The properties of surface film also played an important role in determining the overall corrosion behavior.

ACKNOWLEDGEMENTS: This study was financially supported by internal project of Korea Institute of Materials Science (PNK4120).

In vitro and in vivo characterizations of zinc alloy coronary stent

J Zhou, H Gong, X Miao, Y Wang, X Yan, Y Zhang, G Guo, K Ning, G Qu

Xi'an Advanced Medical Technology, China. Drexel University, Philadelphia, USA

INTRODUCTION: Degradation speed of Zinc (Zn) alloy is in between of Mg alloy and iron, so Zn alloy as a novel biodegradable metal holds great potential in biodegradable implant applications. However, there is very little publication regarding the mechanical properties, In-vitro and In-vivo biodegradation behaviors of Zn alloy. In this study, Zn alloy and stents were tested In-vitro and In-vivo.

METHODS: To prepare Zn-0.5 wt% Mg alloy, pure Zn(99.99%) was melted in a resistance furnace and Mg chips(99.95%) were dipped in. A mechanical stir was used to homogenize the melt. A mixture of argon and SF₆ was used as protection gas to prevent Mg from oxidation and achieve accurate alloy composition. Samples were cut from extruded Zn alloy rods for cytotoxicity test and antibacterial test. Indirect cytotoxicity test was performed according to ISO 10993-5:2009.22 To prepare extract mediums, Zn alloy were cleaned, sterilized, and incubated in Dulbecco's modified Eagle's medium with 10% fetal bovine serum for 72 h under physiological conditions (5% CO₂, 20% O₂, 95% humidity, 37 °C). Fibroblast (L-929) cells were seeded in 96-well plate at 5000 cells per well density for overnight. The medium was replaced with 100 µl/well diluted extract in the next day. After 24 hours of incubation, cell viability was tested using MTT. Zn alloy stents were laser cut from drawn mini-tubes. Zn stents were implanted in New Zealand rabbit aorta abdominalis through left femoral artery using a balloon catheter (Φ 2.5mm×16mm).

RESULTS: Extract of Zn alloy showed cell toxicity to L929 while diluted extracts is biocompatible. It was found that Zn alloy has significant antibacterial effect. Implantation and expansion of Zn alloy stent was successful without any broken struts (Fig 2). Endothelialization was completed at the 28th day. Zinc alloy's mechanical properties has also be tested, and it is comparable with Mg alloy.

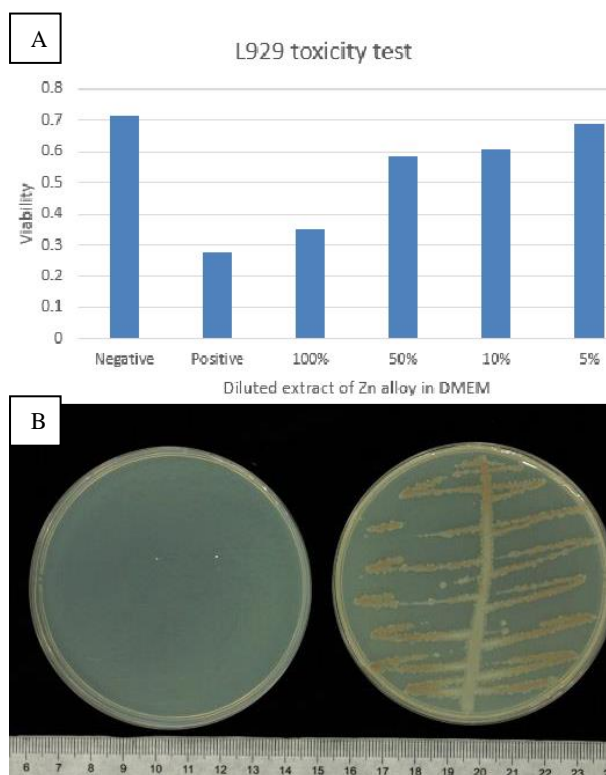


Fig. 1: A) Cytotoxicity test of Zn alloy, B) Antibacterial test of Zn alloy

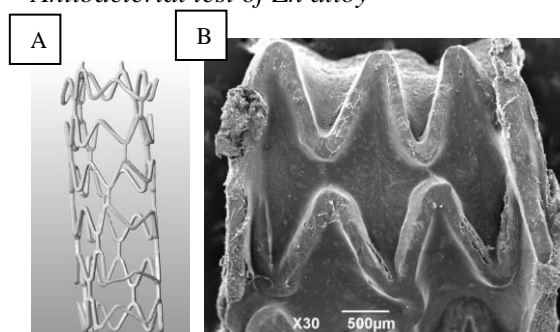


Fig. 2: A) One day and B) 28 days after implantation of Zn alloy stent

DISCUSSION & CONCLUSIONS: The main advantage of Zn over Mg alloy is its high corrosion resistance in body environment. From this study, it's believed that Zn alloy has good biocompatibility and mechanical strength; and also Zn alloy with desirable biodegradation behavior is a suitable candidate material for load-bearing biodegradable implant applications.

Dynamic corrosion behaviour of WE43 Mg alloy in a modified simulated body fluid solution

M Ascencio¹, M Pekguleryuz², S Omanovic¹

¹ Department of Chemical Engineering, McGill University, Montreal, Quebec, Canada

² Department of Mining and Materials Engineering, Montreal, Quebec, Canada

INTRODUCTION: The development of biodegradable Mg alloys is hampered by the lack of a complete understanding of the Mg alloy biodegradation mechanisms *in vivo* and by difficulties at emulating the physiological environment *in vitro*. Traditional static immersion tests are often accompanied by an increase in the electrolyte pH above the physiological value, the accumulation of corrosion products such as Mg²⁺ ions and the depletion of relevant electrolyte components such as Ca and P, possibly affecting the Mg alloy corrosion mechanisms and leading to inaccurate degradation behaviour results [1-2]. The degradation behaviour of Mg alloys has been shown to be different in static and dynamic tests [3]; however, little information has been provided regarding the corrosion mechanisms under dynamic conditions. Therefore, the objective of this work was to investigate the short-term corrosion behaviour and corrosion mechanisms of WE43 Mg alloy in a dynamic experimental set-up and compare the outcome with previous results obtained from traditional static immersion experiments and immersion experiments with daily electrolyte renewal.

METHODS: Test samples were prepared from cast WE43 Mg alloy. Modified simulated body fluid (m-SBF) with an initial pH of 7.4 was used as electrolyte. A test platform was designed to have an electrochemical cell (EC) with inward and outward electrolyte flow to yield a continuous electrolyte renewal at a rate of 745 ml day⁻¹. Immersion experiments were performed in triplicate, at room temperature and for a period time up to 5 days. Electrochemical impedance spectroscopy (EIS) was used to investigate the kinetics and mechanisms of the alloy corrosion. The alloy corroded surface was characterized by scanning electrode microscopy (SEM), energy-dispersive spectroscopy (EDS) and attenuated total reflectance Fourier transformed infrared spectroscopy (ATR-FTIR). The electrolyte concentration of Mg, Ca and P in the EC was monitored using inductively coupled plasma optical emission spectroscopy (ICP-OES).

RESULTS: EIS results showed an increasing impedance response with a quasi-constant shape on the Nyquist plot. Analysis of the EIS data by an equivalent electrical circuit (EEC) model revealed a gradual increase of the charge transfer resistance with time (Fig. 1, DCER). An increase in the electrolyte pH and concentration of Mg²⁺ was initially observed, followed by quasi-constant values after 24 h. SEM, EDS and ATR-FTIR results showed the presence of a carbonated apatite /Mg(OH)₂ mixed corrosion layer with a uniform cracked-mud surface morphology.

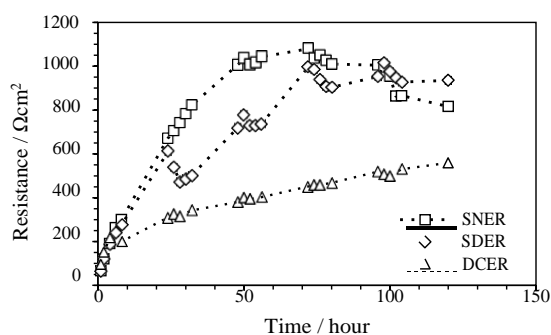


Fig. 1: Time-dependent charge transfer resistance behaviour of WE43 Mg alloy in m-SBF from static tests with no electrolyte renewal (SNER)[1] and daily electrolyte renewal (SDER)[2] and dynamic test with continuous electrolyte renewal (DCER).

DISCUSSION & CONCLUSIONS: Charge transfer resistance values obtained from static and dynamic immersion tests (Fig. 1) show that the DCER test leads to a slower increase in the corrosion layer barrier film coverage, delaying the occurrence of localized corrosion observed in static tests. The present results describe the corrosion behaviour of WE43 Mg alloy at conditions that better resemble physiological homeostasis and demonstrate the importance of the experimental set-up for the accurate determination of the Mg alloy corrosion behaviour.

The effect of CO₂ or O₂ on biocorrosion of Mg alloys

A. Yamamoto, A. Kikuta, Y. Kohyama

¹ *Biometals group, International Center for Materials Nanoarchitectonics, National Institute for Materials Research, Namiki 1-1, Tsukuba, Japan*

INTRODUCTION: Recently, biomedical application of magnesium (Mg) and its alloys are intensively studied for the realization of biodegradable devices. One of the important issues in this field is to control their degradation rate in the human body since it severely influences their mechanical integrity and biocompatibility. The degradation of Mg and its alloys depends on the surrounding tissue and microenvironments. Various factors can be influential; pH and chemical components of body fluids, amount of dissolved O₂ and CO₂, and so on. The pH of body fluid is maintained as 7.4 mainly by a carbonate buffer system including dissociation of dissolved CO₂ as carbonate ions. The concentration of CO₂ in the body is about 5%, which is higher than that in air (0.04%). However, that of O₂ is ~5%, which is less than 1/4 of that in air. In this study, we examined the effect of CO₂ and O₂ concentration on biocorrosion of Mg alloys by electrochemical methods.

METHODS: The materials used are extruded bars of pure Mg (pMg) and Mg-Al alloy. In vitro degradation behaviour of these samples was studied in Eagle's minimum essential medium (E-MEM) or that supplemented with 10% fetal bovine serum (E-MEM+10%FBS) under cell culture condition, i.e., 37°C and 5% CO₂ in humidified air. A standard three-electrode system was employed; Ag/AgCl (3M NaCl), a platinum mesh, and the Mg alloy sample as a working electrode. Electrochemical impedance spectroscopy (EIS) was performed under following conditions; at open circuit potential (OCP), 5mV, 0.01~10⁵ Hz after 2, 6, 12, and 24h of incubation. Potentiodynamic measurement was carried out after 24h of incubation at the scanning rate of 0.5mV/s and OCP-0.25V to -1.2V.

RESULTS & DISCUSSION: Fig.1 shows typical polarization curves of Mg-Al alloy samples with and without 5% CO₂, which clearly indicate the suppression effect of 5% CO₂ on Mg-Al alloy corrosion in cell culture condition. It may be attributed to the higher buffering ability of carbonate buffer system with 5% CO₂; the pHs of the media after the measurement were 7.6-7.8 with CO₂ but were 8.8-8.9 without. A similar trend is

also observed for pMg samples. Fig.2 shows typical EIS spectra of Mg-Al alloy under 5% CO₂ with 20% or 1% O₂. Smaller capacitive loops under the atmosphere of 1% O₂ suggest the acceleration effect of low O₂ environment on the corrosion of Mg-Al alloy.

These data indicate the importance of testing condition for biocorrosion evaluation of Mg alloys. Not only the chemical components of the testing solution¹ or the existence of living cells², but also the testing environment such as 5% CO₂ or ~5% O₂ is crucial for the estimation of the corrosion behaviour of Mg alloy for the biomedical application.

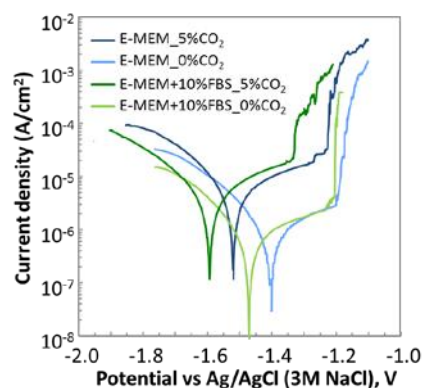


Fig. 1: Typical polarization curves of Mg-Al alloy in cell culture condition with/without 5% CO₂.

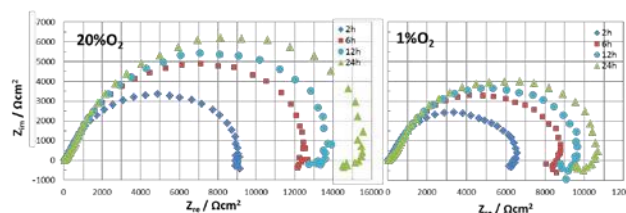


Fig. 2: Typical EIS spectra of Mg-Al alloy in cell culture condition with 1% or 20% O₂.

Visualisation of corrosion initiation of Mg and Mg alloys

T.Zimmermann¹, WD Mueller¹

¹ *Biomat Res. Gr., CC3 Charité niversitaetsmedizin Berlin, D*

INTRODUCTION: Mg and Mg-alloys are on the way as applied biomaterials but one of the not yet solved problems is the prediction and control of degradation in vitro.

Reasons therefore are: difficulties in measuring of the degradation as well via gas evolution or using electrochemical experiments.

Aim of this work is to look for a possibility to visualize corrosion phenomena at the surface of Mg and Mg-alloys in combination with electrochemical measurements.

METHODS: A set up based on the Keyence microscope combined with a miniaturized flow cell connected at the MCS was developed.

Surface polished Mg and Mg-alloy specimens were measured under microscopic control. Before starting the measurements all specimens were polished and etched so that the grains could be seen and counted. The polishing procedure was made up the point to get a clear picture of structure.

Electrochemical measurements were performed using the MCS, described earlier (1).

OCP measurements over 1h were followed by cyclic voltammetry with threshold potential of $\pm 500\text{mV}$ vs. OCP. And a scan rate of 10mV/s for at least 3 cycles. During the electrochemical measurements the surface was controlled optically by a magnification of 200x.

At all specimens the composition was analyse by EDX. The surface was polished to measure the grain size. Various samples of cp Mg, pure Mg and HP Mg as well as MgAg alloys and JDBM alloys were investigated.

RESULTS: Under OCP measurement conditions it was observed that gas bubbles appears shortly after contacting the surface with electrolyte but these bubbles disappear, but not by diffusion to the top of the cell no into the metal.

In case of voltammetric cycles some interesting phenomena would observe. The increase of gas bubbling is clear to see at two points of the polarization curves with different intensity.

Even a change of coloration of parts of the surface can be observed.

DISCUSSION & CONCLUSIONS:

The intention was to see where the gas evolution starts, how the potential is changing with time and what can be observed during a voltammetric cycle.

The first experiments based on polished Mg and Mg-alloy surfaces have shown that a visualisation of the corrosion processes at the surface is possible. Based on it the assessment of degradation can be improved but there are some more investigations are necessary. Especially the localisation of hydrogen evolution seems to be helpful and interesting concerning the parts where it is takes place, depend on the composition of the alloy and the grain structure.



Fig.1: measurement set-up for live control of measurements

Effects of stent manufacturing on degradation behaviour of Fe-based biodegradable metals

CS Obayi^{1,2}, PS Nnamchi¹, R Tolouei², D Mantovani²

¹ Dept Metallurgical & Materials Engineering, University of Nigeria, Nsukka, Nigeria. ² Lab. Biomaterials and Bioengineering, CRC-I, Dept Min-Met-Materials Eng & CHU de Québec Research Center, Laval University, Québec City, Canada.

INTRODUCTION: Biodegradable metallic stents (BMS) are the current proposed strategy for treating severe coronary artery disease. BMS have the same structural attributes and appropriate properties of high strength, ductility (20-30%) and biocompatibility as permanent metallic stents (PMS). Unlike PMS, BMS are designed to degrade in anatomical sites without generating toxicity in the human body [1]. From a clinical point of view, BMS are expected to have a degradation rate targetable as a function of the case. From an industrial point of view, for easiness and practical concerns, BMS are expected to be processed with the same manufacturing steps as PMS. The key processing steps in PMS manufacture are plastic deformation (tube drawing), laser cutting and annealing at 1050°C for 30 minutes to promote recrystallization of small-sized grains [2]. PMS fabrication process affects microstructure, notably grain size, texture and residual stress, which could implicate degradation rate, strength and ductility of BMS. This work investigated the effects of the key plastic deformation processes and annealing on the degradation rate of pure Fe.

METHODS: Pure Fe sheet (99.9%) was cold rolled to 50% (UD50%CR), 75% (UD75%CR) and 85% (UD85%CR) thickness reduction and annealed in a tube furnace in the temperature range of 550 °C – 1000 °C, under high purity argon atmosphere. The grain sizes were measured with optical microscope; crystallographic texture evolution was characterized with X-ray diffractometer (XRD). The degradation rates were determined in Hank’s solution using potentiodynamic polarization corrosion method and degradation rate calculated using equation (1) based on ASTM G59.

$$DR = 3.27 \times 10^{-3} i_{corr} EW / \rho \quad (1)$$

RESULTS: Figure 1 shows the effect of texture on the degradation rate of the pure Fe specimens. Table 1 shows average grain size, calculated texture index and degradation rates of some of the cold rolled and annealed pure Fe specimens. Our results indicate that texture index of (110) and (200) increased and decreased with increase in the degree of cold work and annealing temperatures, respectively. The degradation rate of pure Fe also displayed the same trend with the texture strength, increasing with

increase and decrease in texture strength of (110) and (200), respectively.

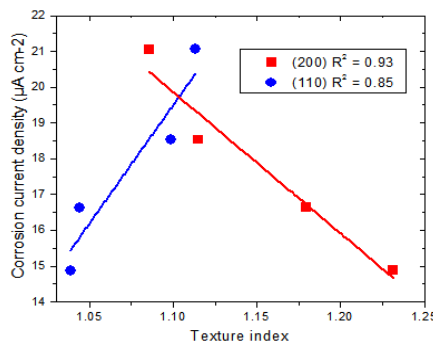


Fig. 1: Effect of texture on the degradation rate of pure Fe.

Table 1. Texture index, grain sizes and degradation rates of some of the cold-rolled and annealed pure Fe specimens.

Material code	Texture index			Preferential orientation	Average grain size (µm)	Potentiodynamic polarization test	
	(110)	(200)	(211)			Current density i_{corr} (µA cm ⁻²)	Corrosion rate (mm year ⁻¹)
As-received	1.1033	0.9239	0.8454	110	29.6	20.8±0.6	0.242 ± 0.010
UD50%CR	0.3369	6.1781	0.9798	200	-	-	-
UD75%CR	0.3662	5.0260	1.4691	200	-	-	-
UD85%CR	0.9503	2.6290	0.5379	200	-	-	-
UD85%CR-550	1.0387	1.2314	0.9829	200	14.1	14.88±0.92	0.172±0.012
UD50%CR-550	1.0445	1.1796	0.7582	200	19.8	16.63±0.58	0.192±0.011
UD75%CR-800	1.0989	1.1149	0.7391	200	28.1	18.50±0.70	0.215±0.043
UD85%CR-1000	1.1134	1.0856	0.7058	110	164.6	21.05±2.63	0.244±0.031

DISCUSSION & CONCLUSIONS: The increase in degradation rate with increase in texture index of (110) plane could be ascribed to its higher atomic density and surface energy [3, 4], which makes it more susceptible to dissolution in corrosive media [3]. It also increased with increase in grain size as earlier reported [5].

A suitable fabrication method that could tailor all these microstructural variables towards accelerated degradation of Fe-based BMS is desired as the PMS manufacturing method was originally designed for enhanced degradation resistance.

ACKNOWLEDGEMENTS: NSERC, CIHR, CFI, FRQNT, MRI Quebec, Canadian Commonwealth Scholarship Program and University of Nigeria.

Investigating the inhomogeneous degradation of biodegradable metallic stents through *in vitro* and *in silico* dynamic testing

J Frattolin^{1,2}, S Yue³, OF Bertrand,^{4,1} R Mongrain²

¹Department of Mechanical Engineering, McGill University, Montreal, Canada. ²Montreal Heart Institute, Montreal, Canada. ³Department of Mining and Materials Engineering, McGill University, Montreal, Canada. ⁴Interventional Cardiology Laboratories, Quebec Heart and Lung Institute, Laval University, Quebec City, Canada

INTRODUCTION: *In vitro* dynamic corrosion tests attempt to reproduce *in vivo* biodegradable stent behaviour. This method of testing allows the convective contribution to degradation to be taken into account. Due to complex stent geometry, however, not all stent surfaces may contribute equally to degradation or be exposed to the same convective effects, leading to inhomogeneous degradation and an under- or overestimation of the predicted corrosion rate. This investigation utilizes *in vitro* and *in silico* tests to analyze how stent geometry can influence *in vitro* degradation prediction in a dynamic environment.

METHODS: Dynamic corrosion tests were conducted utilizing a novel biodegradable stent composed of 80% iron and 20% stainless steel 316L. The fabrication method was previously described in Frattolin *et al.*¹ An *in vitro* tubing setup was utilized with Hank's Balanced Salt Solution (HBSS), under physiological conditions. A peristaltic pump provided an average flow rate of 40 mL min⁻¹. Total test duration was 7 days. To assess how stent cell geometry can affect *in vitro* degradation, scanning electron microscopy (SEM) was utilized to analyse the stent surface.

RESULTS: Microstructural analysis was conducted to characterize stent surfaces of interest: the luminal and abluminal surface, and the upstream and downstream strut surfaces (sides) within the inter-strut space. Most significantly, a substantial difference was observed between the luminal surface and the upstream/downstream strut surfaces (strut sides). The luminal surface had a proliferation of large pitted regions (Fig. 1a). The total iron loss on this surface over the test duration was 46.8%, determined by energy-dispersive x-ray spectroscopy (EDS). In contrast, the strut sides within the inter-strut space had limited degradation, and the pits observed were superficial (Fig. 1b), with limited iron loss.

DISCUSSION & CONCLUSIONS: The SEM analysis of the stent surface after degradation indicated that preferential corrosion seemed to

occur at specific locations along the stent surface as a result of flow dynamics and stent cell geometry.

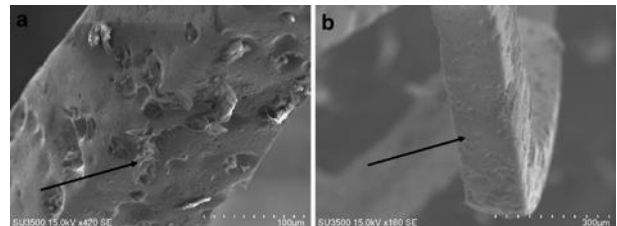


Fig. 1: (a) Stent luminal surface at $\times 420$; (b) Inter-strut surface at $\times 160$ (strut side).

To understand this phenomenon, CFD analysis was conducted in Fluent[®] (ANSYS, Inc.).² The fluid was modelled to be Newtonian, under laminar conditions, similar to the *in vitro* set-up. The variance in wall shear stress (WSS) was assessed with 3D stent geometry. It was found that large spikes of shear stress (> 7 Pa) resulted across the stent luminal surface. These spikes of shear stress led to high local shear rates, which increased ion transport. Increased degradation was observed on the luminal surface. In contrast, low WSS (< 1 Pa) was observed in the inter-strut area, with recirculation zones associated with stagnant flow. Significantly less transport would result to the inter-strut space, limiting its contribution to stent degradation, consistent with Fig. 1b.

It was determined that not all surfaces contribute equally to stent degradation, due to complex flow dynamic effects induced by the stent cell geometry. This could explain the inhomogeneous degradation of the stent during *in vitro* testing. Therefore, it appears important that the specific stent cell geometry be considered during analysis.

ACKNOWLEDGEMENTS: The authors thank the Natural Sciences and Engineering Research Council of Canada (NSERC) and the McGill Engineering Doctoral Award (MEDA).

Tailoring the degradation and biological response of a magnesium-strontium alloy for potential bone substitutes application

P Wan¹, J Han¹, L Tan¹, J Li², K Yang¹

¹ Institute of metal research, CAS, Shenyang, P.R. China. ² Shengjing Hospital of China Medical University, Shenyang, P.R. China

INTRODUCTION: Bone defects are very challenging in orthopedic practice. There are many practical and clinical shortcomings in the repair of the defect by using autografts, allografts or xenografts, which continue to motivate the search for better alternatives. The ideal bone grafts should provide mechanical support, fill osseous voids and enhance the bone healing. Biodegradable magnesium-strontium (Mg-Sr) alloys demonstrate good biocompatibility and osteoconductive properties, which are promising biomaterials for bone substitutes. The aim of this study was to evaluate and pair the degradation of Mg-Sr alloys for grafting with their clinical demands.

METHODS: In this work a range of magnesium strontium alloys in status of as-cast, as-extruded and as-cast with coating were explored to investigate the microstructure and performance of the alloys, *in vitro* degradation and biological properties including *in vitro* cytocompatibility and *in vivo* implantation.

RESULTS: The as-cast Mg-Sr alloy exhibited a rapid degradation rate compared with the as-extruded alloy due to the intergranular distribution of second phase and micro-galvanic corrosion. However, the initial degradation could be tailored by the coating protection, which was proved to be cytocompatible and also suitable for bone repair observed by *in vivo* implantation. The integrated fracture calluses were formed and bridged the fracture gap without gas bubble accumulation, meanwhile the substitutes simultaneously degraded.

Fig. 1: Post-op X-ray images after implantation of (a) 4 and (b) 8 weeks for (1) as-cast alloy, (2) as-extruded alloy and (3) as-cast alloy with coating.

DISCUSSION & CONCLUSIONS: The present study investigated the tailored degradation and biological response of different Mg-Sr alloys for use as potential bone substitute's alternative. The results of *in vitro* degradation evaluation combined with microstructure analysis showed the as-cast Mg-Sr alloy exhibited a rapid degradation rate compared with the as-extruded alloy due to the intergranular distribution of second phase and micro-galvanic corrosion. Comparatively, the MAO coating can regulate the degradation, which exhibits initially slow corrosion and then faster at the latter stage. It is beneficial for the implants without any signs of cytotoxicity and harmful effects on osteoblasts proliferation. The *in vivo* implantation test found that the integrated fracture calluses were formed and bridged the fracture gap without gas bubble accumulation for the as-cast Mg-Sr alloy with coating, meanwhile the substitutes simultaneously degraded after 8 weeks. In conclusion, the as-cast Mg-Sr alloy with coating is potential to be used for bone substitute alternative.

ACKNOWLEDGEMENTS: This work was financially supported by National High Technology Research and Development Program of China (863 Program, No.2015AA033701). Authors also thank Dr. Yifeng Pei for giving help in cell test.



Buffer-induced *in vitro* corrosion of magnesium alloys: Considerations for standardisation of *in vitro* testing

RN Wilkes^{1,2}, J Waterman¹, [MP Staiger](#)^{1,2}

¹ *Department of Mechanical Engineering, University of Canterbury, Private Bag 4800, 8140 Christchurch, New Zealand.* ² *MacDiarmid Institute for Advanced Materials and Nanotechnology, P.O. Box 600, Kelburn, Wellington 6140, New Zealand*

INTRODUCTION: Magnesium and its alloys have the potential to set a new standard for biodegradable orthopaedic implants. The unique combination of mechanical properties and biocompatibility exhibited by this family of alloys make them promising candidates as biodegradable metallic implants. A potential first step in assessing the suitability of biodegradable magnesium alloys is through the use of *in vitro* electrochemical corrosion tests. *In vitro* biodegradation tests have the potential to provide invaluable information about the degradation profile of the alloy in question as well as give insight to how the alloy may react when placed in an *in vivo* environment. However, *in vitro* tests seldom replicate the observed *in vivo* degradation behaviour largely due to the complexity of the *in vivo* environment that is difficult to artificially mimic. Additionally, standardisation of *in vitro* testing of Mg alloys is yet to be developed, making it difficult to accurately compare and contrast previously collected data. A pH of approximately 7.4 to 7.6 is constantly maintained *in vivo*, and as such pH control *via* a buffer system is an important factor in the development of *in vitro* test protocol. However, the selection of the buffer system for *in vitro* biodegradation testing has been largely overlooked in the vast majority of *in vitro* studies.

METHODS: In the present work, the effect of the buffer system on the corrosion behaviour of pure magnesium and binary alloys are examined as function of both the corrosion medium and microstructure. Alloys were subjected to varying thermomechanical processing treatments in order to produce samples with a wide variety of grain sizes. A Potentiostat (Bio-Logic VSP) was used to examine the electrochemical characteristics of the magnesium alloys immersed in SBF with varying buffer solutions. Both potentiodynamic polarisation (PDP) and electrical impedance spectroscopy (EIS) tests were carried out.

RESULTS: PDP and EIS tests showed that the buffer system and alloy grain size could play a role

in altering the degradation rate of the materials. The more biologically realistic buffering system of carbonate buffers within a partial-CO₂ atmosphere affected the corrosion rate differently than the zwitterion-based buffer system. Samples with different grain sizes also exhibited dissimilar degradation rates and passivation characteristics. Furthermore, the relationship between the buffer systems used, the grain sizes of the samples, and the degradation profiles was analyzed.

DISCUSSION & CONCLUSIONS: This systematic study provides useful background information for the development of a standardised *in vitro* corrosion testing that will assist with developing biodegradable Mg orthopaedic implant devices.

ACKNOWLEDGEMENTS: The authors would like to acknowledge the New Zealand Health Research Council for providing the funding for this research.

Interactions among Mg substrates, rapamycin and poly(lactic-co-glycolic acid) coatings on biodegradable Mg-based drug-eluting stents

YJ Shi^{1,2}, J Pei¹, K Park², GY Yuan^{*1}

¹ *School of Materials Science and Engineering, Shanghai Jiao Tong University, Shanghai, China.*

² *Weldon School of Biomedical Engineering, Purdue University, IN, USA.*

INTRODUCTION: Degradation of magnesium substrates makes the behaviour of Mg-based drug eluting stents (DESs) different from that of DESs based on non-degradable substrates. This study aims to investigate the interactions among the Mg substrate, the drug rapamycin (RAPA) and the drug carrier PLGA coating on Mg-based DESs.

METHODS: PLGA or PLGA/RAPA coatings were prepared on Mg and SS disk samples ($\phi 15 \times 3$ mm) by dip-coating. Mg and SS-based drug-eluting stents were prepared by an ultrasonic spray coating method [1]. The chemical state of RAPA in the coating was confirmed by FTIR. The in vitro drug release profiles were carried out using a UV spectrophotometer in PBS containing 0.5% Tween 20 (PBST), and factors influencing the drug release kinetics of Mg-based DESs were discussed. Electrochemical measurements and hydrogen evolution tests were applied to examine the short-term and long-term protective effect of PLGA for the Mg substrate in simulated body fluid. Meanwhile, the effect of substrate degradation on the hydrolysis of the PLGA coating was studied using GPC, monitoring the decrease of the molecular weight of the coating.

RESULTS: The Mg and SS-based DES were prepared and the FTIR spectra of PLGA/RAPA indicated RAPA distributed in the PLGA coating physically without any chemical bonds. The interactions among the substrate, the drug and PLGA coating are displayed in Fig.1. The potentiodynamic curves and H₂ evolution results (Fig.1 a-b) demonstrated that PLGA could provide short-term protection for the Mg substrate for about 3 weeks. In vitro drug release profiles (Fig.1c) confirmed that the degradation of Mg enhanced the RAPA release kinetics dramatically compared to that of SS-based DESs. The GPC results (Fig.1d) indicated that the degradation of Mg substrate slowed down the hydrolysis of the PLGA coating rather than accelerated it, as the MW of PLGA on Mg exhibited a slower decrease than that on SS samples.

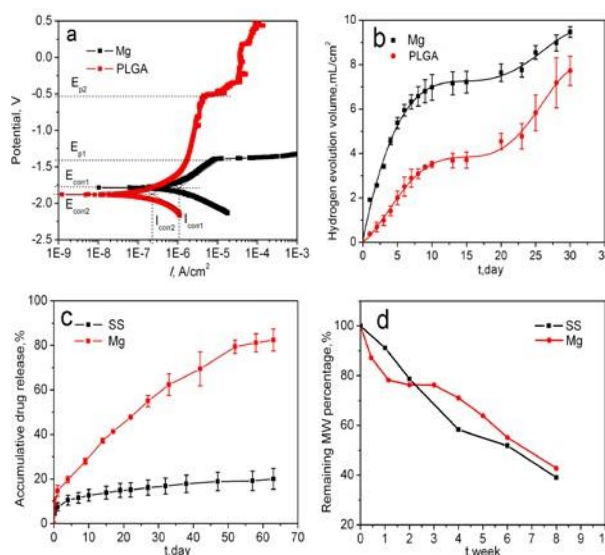


Fig. 1: (a) Potentiodynamic curves and (b) H₂ evolution of bare Mg and PLGA-coated Mg; (c) drug release kinetics from Mg and SS-based DESs; and (d) the decrease of MW of PLGA coatings on Mg and SS disks

DISCUSSION & CONCLUSIONS:

PLGA coating provided short-term protection for the Mg substrate. In the first several weeks, the coating acts as a barrier, retarding the solution penetration into the interface to attack the substrate before it started degradation at the end of the third week. The degradation of the Mg substrate increased the drug release rate significantly due to the H₂ diffusion. The diffusion and release of H₂ deteriorated the integrality of the coating which facilitated the diffusion of the drug. The degradation of Mg resulted in a pH range of 8.5 to 9.5, and in this range, the change of pH did not accelerate the degradation of PLGA because it neutralize the acidity of the degradation products, such as carboxylic acid end groups of PLGA.

ACKNOWLEDGEMENTS: This work was supported by the National Key Technology R&D Program of the Ministry of Science and Technology (2012BAI18B01).

Qualitative evaluation of magnesium implants integrity with micro-CT (computed tomography) and quantitative degradation evaluation

LG Guy¹, F Soza¹, C Lapointe-Corriveau¹, G LeClerc¹

¹ [AccelLAB Inc](#)

INTRODUCTION: Magnesium alloy implants are evaluated for dental, bone and vascular applications. Magnesium is rapidly resorbed and leave place to magnesium hydroxide first and then calcium phosphate. We have used micro-CT techniques to image magnesium implants in swine coronary arteries and used density differences to distinguish magnesium hydroxide from pure magnesium to understand the resorption profile.

METHODS: The protocol was approved by the local animal care and use committee under compliance with the Canadian Council on Animal Care. Yucatan miniswine pigs were implanted with magnesium scaffold in coronary arteries (left circumflex artery, left anterior descending artery and right coronary artery). After incubation in the animal, the stented artery were harvested and scanned with a SkyScan 1172 micro-CT system. Images were reconstructed in 3 dimensions and thresholds were applied based on density.

RESULTS: Reconstructed 3D models of the implanted scaffold showed discontinuity in the scaffold structure (Figure 1). These were more frequent with implants that were incubated longer *in vivo*.



Figure 1: 3D reconstruction of magnesium implants illustrating regions where discontinuities were observed.

It was noticed that grey intensity was variable within the magnesium structure (Figure 2). These corresponded to slightly different density materials. The structures were segmented by simple colour coded mesh models.

Volumetric evaluation of the two types of structures can then be applied.

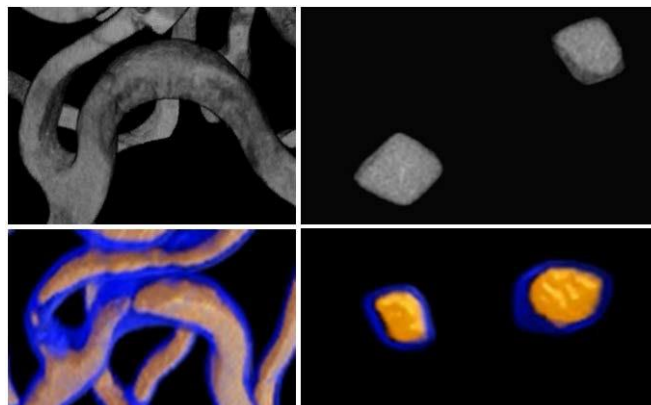


Figure 2: 3D reconstruction of magnesium implants with a grey scale (top) and using a threshold to look at lower density structures in blue and higher density material in yellow (bottom).

DISCUSSION & CONCLUSIONS: The expected strut breaks that occurred during magnesium degradation can be illustrated and quantified with micro-CT. With this type of analysis, we can establish the timeline of scaffold dismantling by strut breaks, as well as the geographical distribution of breaks (e.g. rings vs links).

It was demonstrated by Wittchow *et al.*¹ using raman and infrared spectroscopy combined with X-ray defraction analysis that the low density material was magnesium hydroxide and the high density one was intact magnesium. Volumetric evaluation of these two forms of magnesium can provide a quantitative evaluation of magnesium oxidation and resorption over time.

Bioresorbable RE-free Mg-Zn-Ca screws in a growing sheep model

J Eichler¹, SF Fischerauer¹, L Berger³, E Martinelli¹, M Cihova⁴, T Kraus²,
JF Löffler⁴, AM Weinberg¹

¹ [Dept of Orthopaedics, Medical University Graz, Graz, AT.](#) ² [Dept of Paediatric Orthopaedics, Medical University Graz, Graz, AT.](#) ³ [Institute of Building Construction and Technology, Vienna University of Technology, Vienna, AT.](#) ⁴ [Laboratory of Metal Physics and Technology, Dept of Materials, ETH Zurich, Zurich, CH.](#)

INTRODUCTION: Screw osteosynthesis represents a gold standard method for the treatment of small and middle sized bone fragment fractures. Stabilization of corresponding fragments are surgically fixated by screw osteosynthesis with stainless steel or Titanium implants. However, unwanted side effects like loosening, inflammatory reactions and discomfort may be a consequence which makes screw removal by a second surgical intervention obligatory. Biodegradable Mg screws achieve adequate mechanical properties, render a removal intervention and might additionally be able to support the healing process. In the past, a huge drawback of Mg implants was their fast degradation rate, which can be retarded by alloying additional rare-earth (RE) elements. Nevertheless, they are considered to be noxious and not suitable for the human body, especially for a growing skeleton.

A first RE-free Mg-Zn-Ca alloy with 5 wt.% Zn (ZX50) developed huge amounts of gas inside the bone and was degrading too rapid [1]. Another Mg-Zn-Ca alloy, containing less Zn (ZX10) showed promising degradation characteristic hydrogen gas evolution in [2].

The aim of this study was to evaluate degradation, gas evolution and bone-implant interface reaction on Zn-poor Mg-Zn-Ca (ZX00) screws in an *in vivo* sheep model. An additional group with surface treatment (polishing) was evaluated towards the influence of expected surface impurities caused by the manufacturing process.

METHODS: n=7 RE-free Mg screws with d=3.5 mm and l=16 mm were manufactured using the alloy ZX00 (Mg-0.3Zn-0.4Ca) and divided into two groups. N=3 screws were surface treated (polishing with ethanol and phosphoric acid) and n=4 screws were used without this treatment. Implants received cleaning, packaging and gamma sterilization treatment and were implanted into diaphyseal right tibiae of two growing sheep (n=1 with polished screws and n=1 with unpolished screws). Animal trials were accredited by the

Austrian Ministry of Science, Research and Economy, accreditation number BMWFW-66.010/0190-WF/V/3b/2014.

Screws were inserted after performing small incisions in the mid-diaphyseal region and the proximal and distal diaphysis. Tissue was mobilized carefully to avoid any harm. A monocortical drill-hole was made and a thread was cut in advance. After insertion, the wounds were closed in layers. Interventions were performed under sterile clinical conditions and general anaesthesia. Clinical CT imaging (Siemens Sensatom 64) was performed after 2 and 6 weeks. After week 6 both animals were euthanized and their tibiae were harvested and evaluated with Siemens Inveon micro CT for distinct bone incorporation and bone and tissue reactions. Implant volume, surface and gas volume was quantified with Materialise MIMICS, ver. 17.

RESULTS: All screws were well tolerated without adverse effects (redness, swelling) or osteolyses. New bone formation was found forming a tight bone-screw interface which differs in slightly lower bone contact for the polished screws. Moderate degradation and low amounts of gas were examined for polished and unpolished versions.

DISCUSSION & CONCLUSIONS: The slightly lower bone contact of polished ZX00 screws may be caused by changed surface condition or volume loss through polishing. However, further investigations are required to assess long term effects.

ACKNOWLEDGEMENTS: This work was financially supported by Laura Bassi BRIC, Austrian Promotion Agency.

***In vivo* comparison of chemically polished vs. unpolished magnesium-based screws in lamb tibiae**

L Berger¹, J Eichler², M Cihova³, E Martinelli², C Kleinhans², P Uggowitzer³, JF Löffler³, AM Weinberg²

¹ *Inst. for Building Construction and Technology, TU Wien, Vienna, AT.* ² *Dept. of Orthopaedic and Orthopaedic Surgery, Medical University of Graz, Graz, AT.* ³ *Lab. of Metal Physics and Technology, Dept. of Materials, ETH Zurich, Zurich, CH.*

INTRODUCTION: Magnesium and its alloys possess ideal characteristics in mechanical properties and biological acceptance, and thus are of great promise in surgical stabilisation of bone fractures. The relatively fast degradation ability avoids second surgeries for removal of the implant. Essential for their applicability is a sufficient load bearing capacity for a clinically relevant time frame. The purpose of this study was therefore to (1) analyse the general applicability of Mg-based screws for their use in cortical bone and (2) study whether an improved degradation and therefore biomechanical performance can be achieved by chemical surface treatment.

METHODS: Screws (diameter: 3.5 mm, length: 16 mm) were dry-machined from the Mg alloy ultrahigh-purity (XHP) ZX00 (Mg-0.3Zn-0.4Ca). The surface of 4 screws was chemically polished (mixture of ethanol and phosphoric acid), whereas the others remained untreated. Seven screws (4 chemically polished and 3 unpolished) were gamma-sterilized and inserted into two ovine right tibiae (experimental, $N=2$ animals), and six further screws were implanted in the cadaveric right tibiae (control, $N=2$) after sacrificing the animal six weeks after implantation.

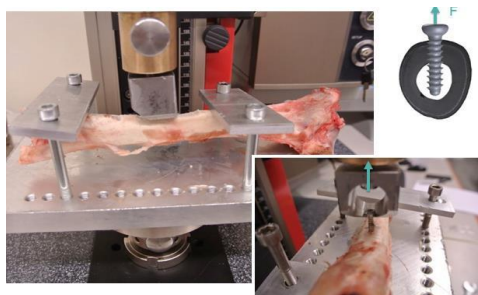


Fig. 1: Pull-out test method performed on XHP-ZX00 screws in sheep tibiae.

An axial pull-out test was performed on the screws of the *in vivo* groups, and the same method was also applied on the cadaveric control bones.

RESULTS: The pull-out tests revealed lower strength of screws that stayed in the tibia for 6

weeks in comparison to the control group (Fig. 1). Chemically polished screws exhibited lower pull-out strength than untreated samples (sample size not sufficient for statistical comparison). Analysis of bone cross section after pull-out tests revealed that the screws of both groups partly failed by shearing-off the thread flanks and partly by failure of the bone tissue.

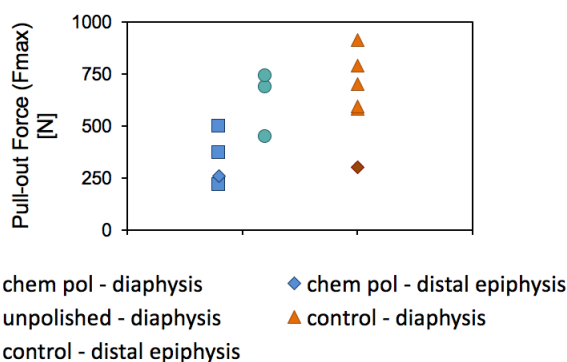


Fig. 2: Pull-out test of XHP ZX00 screws (chemically polished and untreated) inserted in ovine tibiae (diaphysis and distal epiphysis) for 6 weeks vs. ex vivo control group.

DISCUSSION & CONCLUSIONS: These first experiments show that screws made of XHP-Mg-alloy ZX00 revealed good bone integration. For all screws tested, after 6 weeks of implantation the pull-out test reveals lower load-bearing capacity in comparison to the non-degraded control. This loss in strength is associated with initial degradation of the screws and according to expectations. The lower pull-out strength of chemically polished screws may be due to volume loss resulting from the chemical surface treatment. The interface strength still appears to be sufficient for clinical applications. Obtained data is subject of high volatility. Thus, further studies need to be performed to evaluate degradation, ingrowth and tissue reactions of Mg-screws in more detail.

ACKNOWLEDGEMENTS: This work was financially supported by Laura Bassi BRIC, Austrian Promotion Agency.

Degradation progress of LAE442-cylinders in rabbit tibiae and their impact on the organism - outcome of implantation durations up to 3.5 years

N Angrisani^{1,2}, C Vogt³, F Zimmermann³, K Vano-Herrera³, A Meyer-Lindenberg⁴, J Reifenrath^{1,2}

¹ [Small Animal Clinic](#), University of Veterinary Medicine Hannover, D. ² [CrossBIT](#), Center for Biocompatibility and Implant-Immunology, Department of Orthopedic Surgery, Hannover Medical School, D. ³ [Institute of Inorganic Chemistry](#), Leibniz University of Hannover, D. ⁴ [Clinic for Small Animal Surgery and Reproduction](#), Ludwig-Maximilians-University, Munich, D.

INTRODUCTION: Magnesium based implants for the use in orthopaedic applications are the topic of numerous studies since over 15 years. Latest progress is achieved with the certification and clinical use of a magnesium based compression screw [1]. However, long term studies with implantation duration that exceed one year considerably do not exist. The present examinations show the degradation progress of LAE442 pins which have been implanted into the medullary cavity of rabbit tibiae over a period of up to 3.5 years. Evaluation included three-point-bending tests and the analysis of inner organs.

METHODS: Cylindrical implants (length 25mm, Ø 2.5mm) made of the magnesium based alloy LAE442 were implanted into the medullary cavity of rabbit tibiae (adult ♀ New Zealand White rabbits). During the follow-up, animals were monitored extensively using different techniques. After euthanasia implants were retrieved and analysed by three-point bending. Samples of organs which could be affected by the corrosion process were taken immediately under special conditions concerning the preservation of sample contamination. These organs include liver, spleen, kidneys, brain, muscles and local lymph nodes. Analysis was performed by either ICP-MS or ICP-OES and compared to baseline values (animals without implant material).

RESULTS: Clinical acceptance was without objections in all animals. No immoderate reaction of the surrounding bone could be found by either radiographic images or μ -computed tomographies. All implants of the left tibiae could be retrieved in whole part even after 3.5 years implantation duration. However, treatment with chromic acid to remove adherent organic material and corrosion products led to the disintegration of 2 pins so that only one pin remained for mechanical analysis after 3.5 years. Three-point-bending showed a percentage loss of $F(\max)$ of 41,1% for implants after 9 months implantation and 88,47% for the

implant after 3.5 years implantation (Fig. 1). Compared to animals without any implanted material, the organs of rabbits with LAE442 cylinders showed 10-20 fold increased concentrations of the alloying elements lanthanum, cerium, neodymium and praseodymium.

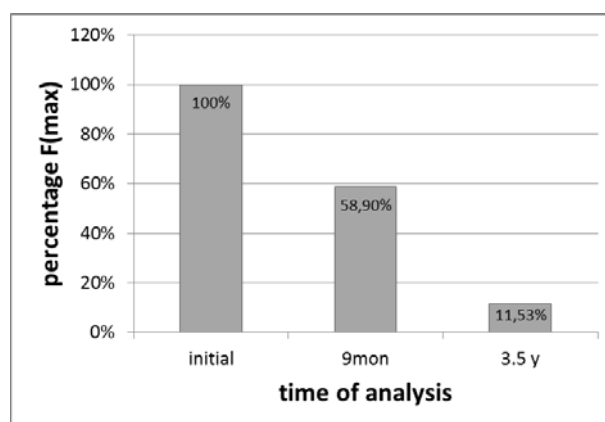


Fig. 1: Percentage loss of $F(\max)$ of intramedullary implanted LAE442 cylinders.

DISCUSSION & CONCLUSIONS: The good clinical acceptance and the minor bone reactions adjacent to the implants gave no occasion to doubt the success of clinical use of this material. While the degradation progress assessed by the percentage loss of mechanical strength was very slow, 10-20 fold elevated element concentrations could be found in the analysed organs. Since yet no NOEL or LD50 values are determined for deposited alloying elements the assessment of these results remain difficult. Further investigations are needed.

ACKNOWLEDGEMENTS: This study was funded by the DFG as part of the CRC 599.

Application of magnesium stents for the treatment of airway obstruction

J Wu¹, B Lee¹, T Yang², P Hebda², S Kathju², PN Kumta^{1,3,4}

¹ Dept. of Bioengineering. ² Dept. of Plastic surgery. ³ Dept. of Chemical and Petroleum Engineering, ⁴ Dept. of Mechanical Engineering and Materials Science, University of Pittsburgh, Pittsburgh, PA. ⁴ Center for Complex Engineered Multifunctional Materials, University of Pittsburgh, Pittsburgh, PA.

INTRODUCTION: Airway obstruction is rare, but could be extremely difficult and challenging to handle. Standard treatment is open surgery. However, these reconstructive surgical procedures are usually associated with serious complications. Stent based interventional pulmonology has raised much interest by providing immediate relief while reducing morbidity and risk. Due to the permanent nature of current non-degradable stents, no stent provides satisfactory long-term effectiveness. [1] A biodegradable stent could potentially solve this problem. In this study, we developed magnesium based absorbable stents and evaluated the biocompatibility and *in vivo* degradation in rat airway bypass model and rabbit tracheal model.

METHODS: First generation magnesium stents were made from commercial grade pure Mg, AZ31 alloys, and Mg-Y alloys with an outer diameter of 2.25mm, inner diameter of 1.25mm and length of 5mm. Donor female lewis rats were sacrificed and the tracheas were harvested to provide a bypass graft for stent evaluation. The stent was placed intra-luminally in the donor trachea, which was anastomosed to recipient rats in and end to side fashion. The animals were euthanized at 1, 8, 16, and 24 weeks for post evaluation by μ CT and standard histologic analysis. Second generation stents were machined from M-AZ31 alloy based on the *in vivo* results of first generation stents. The size of the stents was scaled up to fit the trachea size of rabbit. The stents were directly delivered inside the trachea of rabbits without a bypass. The animals were euthanized at 4 weeks for post evaluation by endoscopy and standard histologic analysis.

RESULTS: First generation stents showed the potential of Mg alloys for use as airway stents. A ciliated epithelium was maintained even after 24 weeks *in vivo*. (Fig.1 (b-g)) *In vivo* corrosion results showed that Mg-Y alloys lose configuration at 24 weeks. (Fig.1 (a)) The second generation stents, novel M-AZ31 alloys showed excellent cyto-compatibilities *in vitro* (Fig.2 (a, b)). Airway lumen was well maintained after 4 weeks of implantation as shown in the endoscopy image (Fig.2 (d)). The Mg stents were covered by

degradation product; over which healthy epithelium layers were observed. (Fig.2 (e,f)).

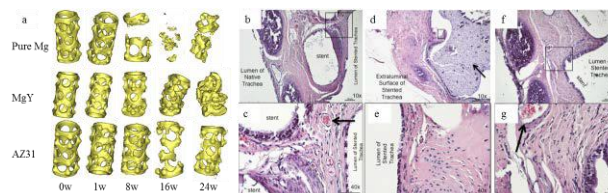


Fig. 1: (a) Micro-CT images of the first generation stents after *in vivo* implantation. Representative histology (H&E) from Pure Mg (b, c), Mg-Y (e, f) and AZ31 (g, h) stents after 24 weeks implantation.

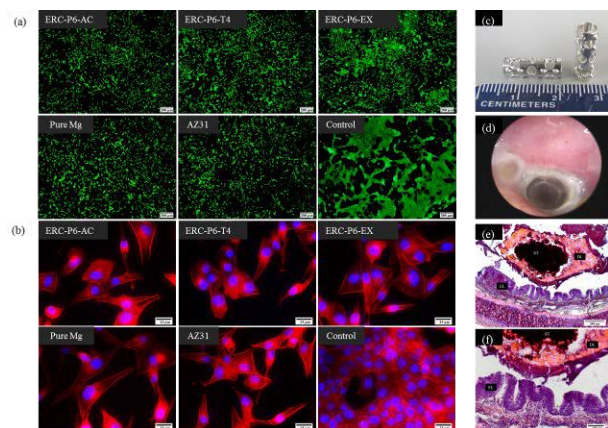


Fig. 2: (a) Live & dead, (b) DAPI & F-actin staining of tracheal epithelial cells (BEAS-2B) cultured in 50% ERC-P6 (M-AZ31) alloy extract for 3 days. (c) Second generation stents. (d) Endoscopy image of rabbit airway implanted with Mg stents. (e,f) Representative histology (H&E) after 4 weeks.

DISCUSSION & CONCLUSIONS: The two evolved stent generations proved the feasibility of using Mg stents for the treatment of airway obstruction. A better designed balloon expandable stents will be explored in the near future.

ACKNOWLEDGEMENTS: Support of NSF funded ERC-RMB via grant-EEC-0812348, and Edward R. Weidlein Chair Professorship funds is gratefully acknowledged.

Self-assembled Hybrid Alkylsilane Coating Reduces Mg Corrosion Rate *in vivo*: a pilot study.

Avinash J. Patil¹, Laura B. Fulton¹, Elia Beniash^{1,2}

¹ Department of Bioengineering, University of Pittsburgh Swanson School of Engineering;

² Department of Oral Biology, School of Dental Medicine; Center for Craniofacial Regeneration; McGowan Institute of Regenerative Medicine; University of Pittsburgh, Pittsburgh, PA 15261, USA

INTRODUCTION: Magnesium (Mg) and its alloys represent promising candidates for transient orthopedic devices. Mg is highly biocompatible, since Mg²⁺ is one of the essential ions and is present naturally in the body. It is also low weight and has mechanical properties compatible to bone. One of the obstacles for use of Mg in clinical application is its initial massive corrosion reaction leading to the formation of gas pockets around the implantable devices. To regulate the rate of corrosion we propose to use self-assembled hybrid alkylsilane (SAHAS) coatings. Here we report on our studies of anticorrosion properties of the coatings *in vivo* in a subcutaneous mouse model.

METHODS: 10 6 mm Mg disks (99.9% purity) were polished, etched with HNO₃ and passivated with NaOH. Half of the disks were dip coated with SAHAS films as follows. Amphiphilic AS decyltriethoxysilane (DTES) and tetramethoxysilane (TMOS) were co-polymerized for 24 hours and the Mg disks were dip-coated in the solution and dried at 37°C. The coated and uncoated disks were weighed prior the implantation. The coated and uncoated Mg disks were implanted subcutaneously on a dorsal side of the mouse in the midsection of the body. The disks were inserted through an incision in the mid-sagittal plane of the animals and placed ~5 mm away from the spine (**Figure 1**). The *in vivo* experiments were carried out for 6 weeks and formation of the gas pockets was monitored by visual observation and recorded using a cell phone camera. After euthanasia the disks were dissected and cleaned from the corrosion layer and biological tissues in a CrO₃ solution. The disks were weighed and the mass loss was calculated for each disk.

RESULTS: The visual observations of the mice have shown that the SAHAS coatings have effectively prevented gas pocket formation for more than 2 weeks after the surgeries, while gas pockets formed around the bare disks in the first week postop (**Figure 1**). Formation of gas pockets was observed around coated disks by the week 3

after surgery. No significant signs of inflammation were observed visually around the implants.

We observed 1/3d reduction in the corrosion rate, i.e. 15±4.5% weight loss of uncoated disks vs. 10±1.5% weight loss of SAHAS coated disks after 6 weeks of implantation. The results of t-test showed that these differences are marginally significant (p=0.07). This is attributed to a large standard deviation in the weight loss of the uncoated samples.

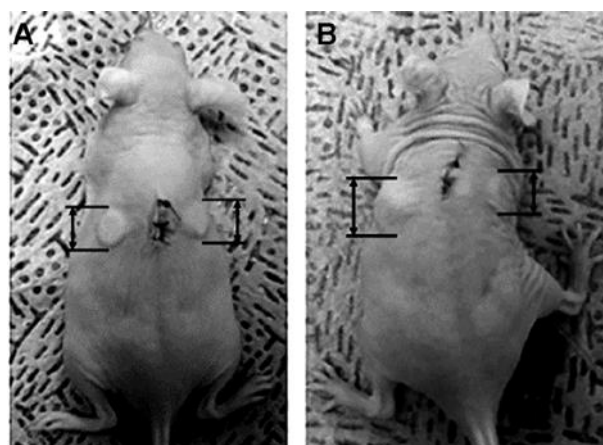


Fig. 1: Photographs of a mouse at day 0 (A) and 7 (B) after implantation. The SAHAS coated disk is in the right side of the animal and the uncoated disk is in the left.

DISCUSSION & CONCLUSIONS: Overall these results of this pilot study suggest that the SAHAS coatings are biocompatible and are able to slow down the rate of Mg corrosion. Importantly, these coatings can effectively prevent the initial burst of corrosion in the most critical first days after the implantation.

ACKNOWLEDGEMENTS: This study is supported by NSF ERC Center for Revolutionizing Metallic Biomaterials # 0812348.

Biocompatibility, degradation and rat femoral fracture healing response of ZK40 alloy

D Hong^{1,2,4}, DT Chou^{1,2,4}, S Oksuz⁵, R Schweizer⁶, A Roy^{1,2,4}, V Gorantla^{2,3}, PN Kumta^{1,2, 4*}

¹ Dept. of Bioengineering, ² McGowan Institute for Regenerative Medicine, ³ Dept. of Plastic Surgery, University of Pittsburgh, Pittsburgh, PA, US. ⁴ NSF-ERC for Revolutionizing Metallic Biomaterials. ⁵ Gulhane Military Medical Academy Haydarpaşa Training Hospital Dept. of Plastic and Reconstructive Surgery Istanbul, Turkey. ⁶ Dept. of Plastic Surgery and Hand Surgery, University Hospital Zurich, Switzerland. *pkumta@pitt.edu.

INTRODUCTION: Orthopaedic fixation devices commonly use inert metals such as Ti alloys and stainless steel. However, the risk of numerous complications arising often necessitates secondary removal surgeries. Magnesium (Mg) and Mg alloys is identified as biodegradable metals to eliminate the need for secondary surgeries and potentially replace inert metals for bone fixation. In the present study, implantation of Mg-4Zn-0.1Sr-0.5Zr (ZK40) alloys in a rat femoral fracture model helped assess the performance and toxicity.

METHODS: Machined pins of ZK40 alloy inserted into the intramedullary cavity help demonstrate biocompatibility and load-bearing functional bone response as well as repair of a full osteotomy in the midsection of rat femurs. Ti-6Al-4V rods were used as the negative control. Blood drawn provided cell counts and serum biochemical tests results prior to implantation and after sacrifice at 14 and 84 days. Femurs were explanted from the sacrificed rats and μ CT was used to observe the surrounding bone and measure the degradation rate of the Mg alloy rods. Local tissue response and bone healing was assessed by histology with Goldner's Trichrome staining. H&E staining and alloy elements evaluation by ICP-OES in the liver and kidney helped assess the potential systemic toxicity of alloying elements.

RESULTS: Blood test results exhibited no significant difference between groups or time points. Hematologic and biochemical parameters as well as electrolyte levels at 0, 14, and 84 days were within the normal range. H&E histology and ICP-OES elemental analysis of liver and kidney showed no accumulation of degradation products indicating no toxicity. Stress induced corrosion was observed at points of high stress near the fracture site suggesting the onset of stress corrosion cracking. μ CT images after 14 days exhibited 88% of the original volume with some failure in ZK40 group (see Fig. 1). Despite stress-induced fragmentation of ZK40 pins, new bone

formation with 42% of the original volume remaining after 84 days was observed. Femurs with both Ti and Mg-Zn alloy pins exhibited bone remodeling and intramembraneous bone formation in Goldner's Masson Trichrome stained images after 84 days (see Fig. 2).

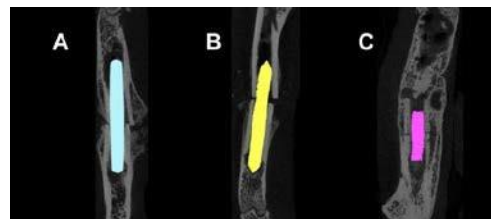


Fig. 1: X-ray images of (a) Ti-6Al-4V and (b) Mg alloy rod after 7 days implantation in rat femurs.

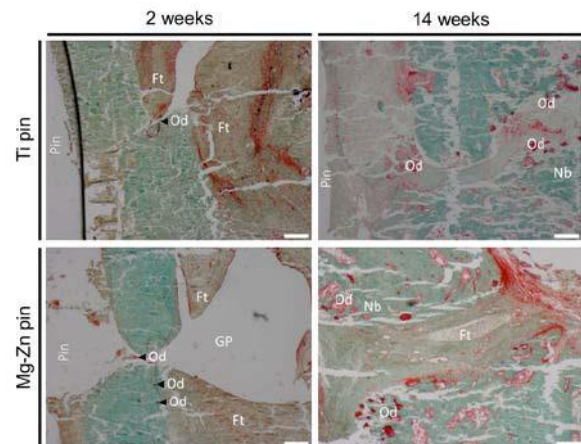


Fig. 2: Goldner's Masson Trichrome staining of rat femurs after implantation of Ti and ZK40 pins

DISCUSSION & CONCLUSIONS: A rat femoral fracture model helped demonstrate the degradation of ZK40 under load-bearing conditions. CT images confirmed fracture and corrosion of rods. However, the Mg alloy rods did not appear to cause significant toxicity, with no significant difference between groups and time points shown in blood, liver, and kidney analyses.

ACKNOWLEDGEMENTS: Authors gratefully acknowledge NSF funded ERC-Revolutionizing Metallic Biomaterials (grant-EEC-0812348) and Pennsylvania State funds for support of this research.

Biodegradable magnesium compression screws for hallux valgus surgery – a three year clinical follow up study

J Reifenrath¹, C Plaass², S Ettinger², L Sonnow³, S Könneker⁴, Y Noll², A Weizbauer¹, L Claassen², K Daniilidis², C Stukenborg-Colsmann², H Windhagen²

¹ *CrossBIT, Centre for Biocompatibility and Implant Immunology, Department of Orthopedic Surgery, Hannover Medical School, D.* ² *Department for Foot and Ankle Surgery, Department Orthopedics, Hannover Medical School, D.* ³ *Institute for Radiology, Hannover Medical School, D.* ⁴ *Department for Plastic, Hand and Reconstructive surgery, Hannover Medical School, D.*

INTRODUCTION: For hallux valgus deformities, a distal metatarsal osteotomy followed by refixation with permanent implant materials is a common surgical approach [1]. In the following clinical trial, degradable magnesium based screws were used for the first time for fixation of modified Chevron osteotomies to prevent permanent implant associated problems like stress shielding effects or foreign body reactions with subsequent necessity of implant removal.

METHODS: 26 patients were included in the study and received either a magnesium implant (n=13, MAGNEZIX® Compression Screw 3.2, Syntellix AG, Germany) or a titanium implant (n=13 cannulated compression screw 3.5, Königsee Implantate GmbH, Germany). 14 (n=8 for mg- and n=6 for ti-screws) patients were available for a final follow up after 3 years. The responsible ethics committee approved the study. Clinical examination included range of motion of the MTP1, American Foot and Ankle Society Forefoot Score (AOFAS) [2] and pain level (visual analogue scale, VAS). Additionally, a magnetic resonance tomography (MRI) was performed. (3T scanner, dedicated foot coil, Magnetom Skyra, Siemens, Germany) and the following sequences were acquired: T1w axial, T1w sagittal, TIRM (Turbo Inversion Recovery Magnitude) axial, TIRM sagittal. Two independent radiologists evaluated the MRI-scans. A semiquantitative scoring system was used to quantify implant induced alterations like edema adjacent to the screw canal, metal artifacts, soft-tissue reaction and bone resorption (Score 1-5) and bone healing (Score 1-3). MRI data were statistical analyzed using Mann-Whitney-U-Test, clinical data using student's t-test.

RESULTS: The clinical scores showed no statistical differences between magnesium and titanium group as well as median MRI scores for edema, soft-tissue reaction, bone resorption and bone healing. The median MRI score for metal

artifacts was significant (1 score-point) lower in the magnesium group. Additionally, a linear hypointensity could be seen in the magnesium group, outlining the former implant site without metal artifacts, whereas centrally, areas of intermediate signal intensity were found.

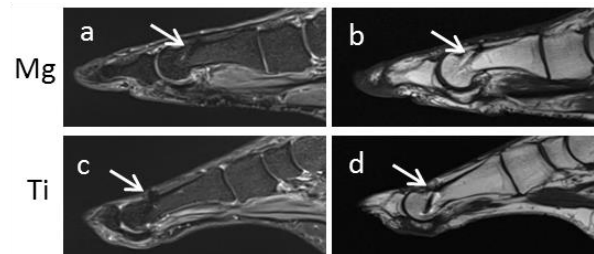


Fig. 1: MRI-images of metatarsal osteotomy and subsequent fixation with magnesium (a,b) and titanium (c,d) implants (arrows), 3 year follow up, TIRM (a,c) and T1w (b,d), sagittal.

DISCUSSION & CONCLUSIONS: For surgical treatment of hallux valgus deformities with distal metatarsal osteotomies, magnesium compression screws showed comparable clinical results to titanium screws. Although degraded and well integrated, remodelling of the magnesium implant material is not fully completed after 3 years.

ACKNOWLEDGEMENTS: H. Windhagen is member of the supervisory board of Synthellix. The authors' institution receives funding by Synthellix for research projects, this study received no direct funding.

A systematic comparison of biodegradation behaviours of absorbable metal: in standardized immersion *in vitro*, vascular bioreactor *ex vivo* and *in vivo* study

J Wang^{1,2}, L Liu¹, Y Wu³, D Kong³, J Sankar¹, Y Yun¹, N Huang²

¹ NSF Engineering Research Center for Revolutionizing Metallic Biomaterials, North Carolina A & T State University, Greensboro, USA. ² School of Materials Science and Engineering, Southwest Jiaotong University, Chengdu, China. ³ Collage of Life Sciences, Nankai University, Tianjin, China. Email: yyun@ncat.edu (Y. Yun); huangnan1956@163.com (N. Huang).

INTRODUCTION: A key step to reduce a gap *in vivo* and *in vitro* test results for absorbable metals is to identify the relevant biochemical and biophysical microenvironments in test-systems. The purpose of this study was to establish an appropriate methodology for the determinations of degradation parameters in the pre- and post-endothelialization stage after stent implantation, which plays a vital part in predicting the fate of magnesium (Mg)-based stent.

METHODS: As-drawn Mg wires of 99.9% purity with a length of 10 mm and a diameter of 250 μm (Goodfellow, USA) were used. In the standardized immersion *in vitro* test, Mg wires were immersed in DMEM solution according to the standard protocol ASTM-D1141-98 [2]. In the *ex vivo* test, the LumeGen bioreactor (TGT DynaGen® Series, USA) as a vascular bioreactor was chosen to stimulate physiological aortal conditions (Fig. 1a). Each porcine abdominal aorta with a diameter of ~ 5 mm and a length of 5 cm was mounted into a chamber with a flow rate of 100 ml/min and a pulse pressure of 80-120 mmHg (Fig. 1b). In aortal *in vivo* test, rat abdominal aortas were used for implantation. Two Mg segments were symmetrically implanted into the lumen and wall of each aorta in the *ex vivo* or *in vivo* tests (Fig. 1c). Samples were analyzed by X-ray computed tomography (CT).

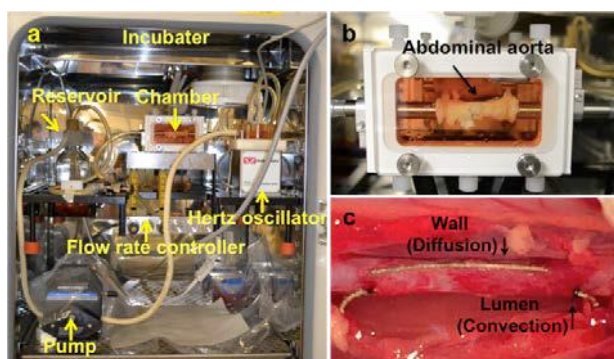


Fig. 1: (a) Physical photograph of LumeGen Bioreactor. The Mg wires were implanted into the wall and lumen of a porcine aorta in the chamber (b) and a rat aorta *in vivo* (c).

RESULTS & DISCUSSION: One of the two Mg wires exposed on the lumen and contacted the circulating medium to simulate a pre-endothelialization stage. Another one was embedded under the intima to simulate a post-endothelialization stage. The degradation product volumes, residual Mg volumes and average degradation rates were calculated utilizing the CT data. In Fig. 2, *in vivo* degradation was slower than *in vitro* and *ex vivo* degradations. The fibrous capsule absorbed on the Mg surface and Mg corrosion rate was decreased at *in vivo* conditions. In terms of *ex vivo* test, however, flow convection on the lumen surface severely accelerated bare Mg degradation due to the increase of mass transfer, fluid shear stress and pulsatile stress, compared with low Mg degradation rate in the wall. The *ex vivo* test can simulate *in vivo* corrosion products infiltration in the surrounding tissue.

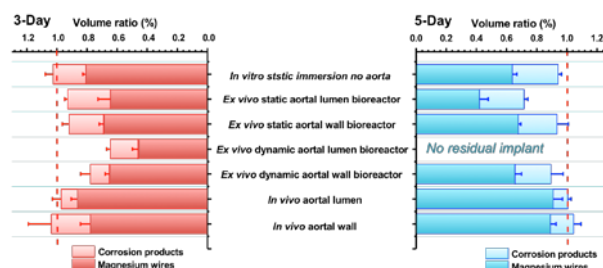


Fig. 2: Volume ratios of residual Mg alloys and corrosion products under the static *in vitro* without aorta, the static and dynamic *ex vivo* aortal lumen and wall in the bioreactors, and the aortal lumen and wall *in vivo* conditions for 3 and 5 days.

CONCLUSIONS: The *ex vivo* aortal model was first developed to study Mg biodegradation behavior using the vascular bioreactor, systematically comparing with which, *in vitro* standardized immersion and *in vivo* assessments. The established vascular bioreactor and aortal *in vivo* model are expected to provide a better understanding of degradation mechanism of absorbable metallic stents.

ACKNOWLEDGEMENTS: USA NSF-0812348, China NSF-81330031.

Performance of a magnesium plate/screws system in a miniature pig midface and mandibular fracture fixation model

B Schaller¹, M Assad², S Beck³, T Imwinkelried⁴, T Iizuka¹

¹*Bern University Hospital*, Bern, Switzerland. ²*AccelLAB*, Boisbriand, QC, Canada.

³*Synthes GmbH*, Oberdorf, Switzerland. ⁴*RMS Foundation*, Bettlach, Switzerland.

INTRODUCTION: Magnesium alloys are candidates for resorbable material in bone fixation [1,2]. However, the degradation and performance of osteosynthesis plate/screw system for midface and mandibular fracture fixation are unknown. We evaluated the outcomes of standard sized magnesium (WE-43 alloy) plate/screw systems with plasmaelectrolytic surface modifications using a miniature pig multiple fracture repair model.

METHODS: Following an IACUC-approved protocol as well as AAALAC and CCAC regulations, zygoma and orbital rim fractures were performed by osteotomy on one side of a total of five Yucatan miniature pigs. On the contralateral side, a mandibular angle fracture was performed by vertical osteotomy. In the mandible, the osteotomy was fixed with a thicker plate with bicortical screws caudally and a thinner tension plate with monocortical screws cranially. The midface fractures were fixed with monocortical screws.

A continuous monitoring using *in vivo* computed tomography (CT; Siemens Somatom Sensation 16) was conducted to follow implant degradation and fracture healing over implantation time. CTs were performed immediately post-op and also before euthanasia for the first group and at 0, 2, 4, 6 and 9 months post-surgery for the 9-month cohort.

Following necropsy, bone blocks containing the implants and surrounding tissue were harvested and reconstructed by Micro-CT (SkyScan 1172), then processed for undecalcified histology, infiltrated with PMMA, microground (Exakt 400 CS), and stained with Goldner's Trichome. A complete histopathological analysis was then performed.

RESULTS: The initial osteotomy locations in the midface showed a physiological bone healing and good fracture alignment at every time points in both groups. However, the mandibular fracture healing showed a pathological fracture healing with callus formation and no sign of consolidation at short as well as at long term. Gas formation

produced during magnesium degradation was detectable on radiological examination, but did not inhibit the fracture healing process of the midface fractures.



Fig. 1: CT-scan images of Mg implants immediately post-operation (left) and 9 months post-implantation (right).

DISCUSSION & CONCLUSIONS: The use of a magnesium plate/screw system for midface fracture fixation was successful. For mandibular fixation, the plate/screw dimensions were not sufficient to sustain the biomechanical load. Further development for the load bearing situation is required before application. This study showed promising results for further development of magnesium plate/screws for midface fracture fixation.

ACKNOWLEDGEMENTS: The authors would like to sincerely thank Dr. Cathy Tkaczyk and Mr. Yannick Trudel for their respective scientific and surgical support.

Biodegradable Mg strengthened poly-lactic acid composite through interfacial properties

MS Butt¹, J Bai¹, C Chu¹, F Xue¹

¹ *School of Materials Science and Engineering, Southeast University, Nanjing, China.*

INTRODUCTION: We developed surface modification on Mg alloy by composite coatings of PLA/AO (anodic oxidation) and PLA/MAO (micro arc oxidation) and compared with pure PLA (Fig.1). PLA coating were prepared by plastic injection molding to improve the corrosion resistance and to control the degradation rate of magnesium alloys [1] [2]. As they play an essential role in restoring and improving the replacement of load-bearing bones. However, their high corrosion rate and hydrogen release during degradation leads to a potential limitation of application in future [3] [4]. It is necessary to develop a standardized system to evaluate the mechanical properties, especially the interfacial bonding strength during degradation.

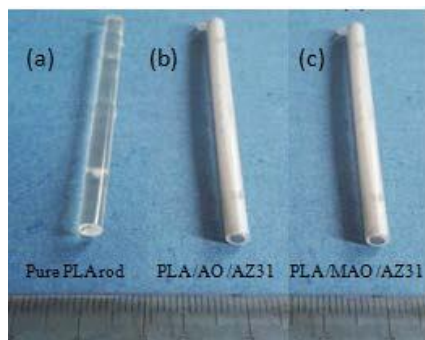


Fig. 1: The sample prepared by plastic injection molding

METHODS: The AZ31 Mg alloy rod having diameter of 2.44 mm, height 60 mm with and without surface coating were used. Two surface treatment methods AO+PLA and MAO+PLA were performed to fabricate composite by plastic injection molding (PIM). To evaluate their in vitro degradation performance, the degradation behavior of samples in SBF simulated body fluid with pH=7.4 were investigated.

RESULTS: The tensile strengths of the PLA-Mg, PLA-MAO-Mg and PLA-AO-Mg were 68.70MPa, 123.87MPa and 131.05MPa, respectively (Fig.2). The surface of Mg/MAO/PLA and Mg/AO/PLA composite coated samples presented a much more smooth morphology. Mechanical stability of the PLA-AO-Mg, PLA-MAO-Mg and PLA-Mg coated specimens in the

SBF was evaluated by measuring their tensile strength after 2, 4, 6 and 8 weeks of implantation (Table 1). During the immersion tests, the PLA-Mg shows the highest hydrogen evolution rate and the worst mechanical properties, and the PLA-AO-Mg exhibits the slowest hydrogen evolution rate and the best mechanical properties.

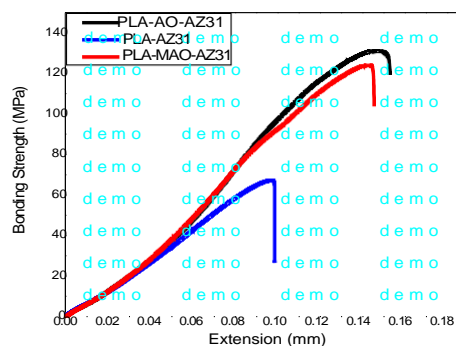


Fig. 2: Tensile test curves of the experimental samples

Table 1: Tensile strength results of different samples in SBF solution for 2-8 weeks

Samples	2-weeks (MPa)	4-weeks (MPa)	6-weeks (MPa)	8-weeks (MPa)
PLA-AZ31	64.70	52.78	44.60	37.83
PLA-MAO-AZ31	115.58	91.03	66.23	55.81
PLA-AO-AZ31	121.21	102.02	89.76	74.52

DISCUSSION & CONCLUSIONS: These composites show significant better mechanical properties than pure PLA; in addition to this the surface treatment of Mg improved its mechanical properties. Interfaces between Mg and PLA play critical roles in influencing the mechanical properties of original composites as well as during degradation. The successes here with two different composite coating would signify the use of Mg alloy in biomedical.

In vitro study of ternary Mg-2Sr-X(X=2,4,6wt.%)Zn alloys

Y Wu¹, Y Liu², N Li², Y Zheng^{1,2}

¹ Center for Biomedical Materials and Engineering, Academy of Advanced and Interdisciplinary Studies, Peking University, Beijing100871, China. ² Department of Materials Science and Engineering, College of Engineering, Peking University, Beijing 100871, China.

INTRODUCTION: Magnesium (Mg) and its alloys are widely regarded as promising temporary implants due to the proper mechanical property and good immunologic response during degradation. In Ref[1], Gu reported that the Mg-2Sr alloy exhibited the best in vitro property. However, the in vivo results released that the corrosion property need to be further improved. Alloying is an efficiency way to improve the corrosion behaviour. Taking both the biocompatibility and the corrosion property into consideration, as an essential metal element, Zinc (Zn) was selected to develop Mg-2Sr-(2,4,6)Zn (wt.%) alloys. The microstructure, phase composition, mechanical property, as well as electrochemical property were evaluated.

METHODS: Commercial pure Mg (99.95%), Sr (99.5%), Zn (99.5%) metal ingots were melted and cast under a protection atmosphere of pure argon(99.9%) using a mild graphite crucible. Followed by solution treated at 340°C for 4h, the alloys were subsequently extruded at an extrusion rate and an extrusion ratio of 2mm/s and 12:1 at the temperature of 325°C. The microstructure was observed with optical microscopy after etched with nitric acid (1%). The phase composition was detected by X-ray diffraction analysis (XRD). The tensile property was determined with an Instron-5969 universal testing machine at room temperature. Electrochemical test was applied at 37°C in Hank's solution with water bath.

RESULTS: Fig.1 is the optical micrograph of experimental alloys. The alloys with higher Zn content showed finer grain size and more second phases precipitated at the boundaries. According to the XRD detection, the second phases were MgZn and Mg₁₇Sr₂ phases. The intensity of MgZn phase increased with the increment of Zn content. As depicted in Fig.2, both the YS and UTS decreased with higher Zn contents in the experimental alloys. Mg-2Sr-2Zn alloy exhibited the highest elongation rate about 15.88%±2.74% and Mg-2Sr-6Zn alloy exhibited comparable mechanical property with Mg-2Sr-2Zn. For the electrochemical corrosion

test, Mg-2Sr-6Zn showed the lowest corrosion current density and corrosion rate about 2.43±0.34 $\mu\text{A}/\text{cm}^2$ and 0.056±0.008 mm/year, respectively.

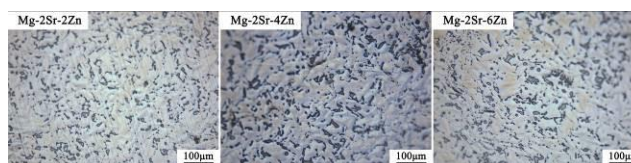


Fig. 1: Optical images of the experimental alloys.

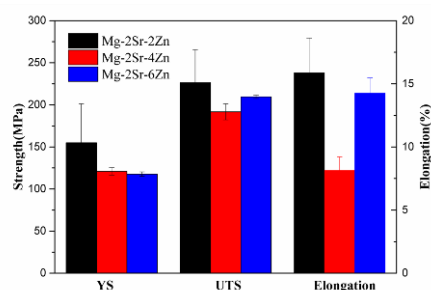


Fig. 2: Mechanical properties of experimental alloys.

DISCUSSION & CONCLUSIONS: The addition of Zn refine the grain size and results in more precipitation of second phases (MgZn and Mg₁₇Sr₂) in the alloys. Higher amount of Zn and larger second phases were detrimental to the mechanical property of the ternary alloys. For the in vitro corrosion behaviour, higher Zn contents in the alloys lead to better corrosion resistance. In the present study, Mg-2Sr-6Zn alloy would be a promising temporary implant material from the mechanical property and corrosion resistance point of view.

ACKNOWLEDGEMENTS: This work was supported by the National Basic Research Program of China (973 Program) (Grant No. 2012CB619102) and Beijing Municipal Science and Technology Project (Z141100002814008).

Development of self-healing calcium phosphate coating on biodegradable metallic implant materials

A Al Hegy¹, J Gray-Munro¹

¹ [Laurentian University](#), Sudbury, ON, Canada

INTRODUCTION: In recent years, magnesium and its alloys have received much attention as a new biomaterial in orthopedic applications due to their biodegradability, biocompatibility, and their mechanical properties that are similar to natural bone. The most common problem associated with magnesium as a biomaterial is low corrosion resistance in physiological solutions. This decreases the mechanical integrity of the implants in the early stages of healing and has a negative impact on the overall biocompatibility. Coatings can be used to control the degradation rate and provide optimum biocompatibility of these implant materials. Mesoporous silica materials have been shown to have good bioactivity and the ability to stimulate osteoblast proliferation and differentiation at implant surfaces. Furthermore, they have been shown to be non-toxic and non-inflammatory to mammalian tissues.

METHODS: The surfaces of Mg AZ31 alloys were prepared by polishing and then cleaning. Alkaline aging was used to promote the formation of hydroxyl groups on the surface. Two types of coating were used in this research: silane coating as a protective film and mesoporous silica coating. The silane coating solution was prepared by using methanol as a solvent, deionized water, ammonia, and TEOS. The mesoporous silica coating solution was synthesized by using TEOS as a silica precursor and cationic surfactant C12CAT (alkyltrimethylammonium chlorides), deionized water, methanol, and ammonia. The molar ratio of TEOS: C12CAT: deionized water, methanol, and ammonia was 1:0.4:774:1501:72. The solution was hydrolysis for 1h before coated the samples by spin coating. The samples were dried and curing for 1h after each coated step. To remove the surfactant, the coated samples were calcined at 350°C for 3h. These mesoporous silica films would be further modified through deposition of calcium phosphate to produce self-healing.

RESULTS:

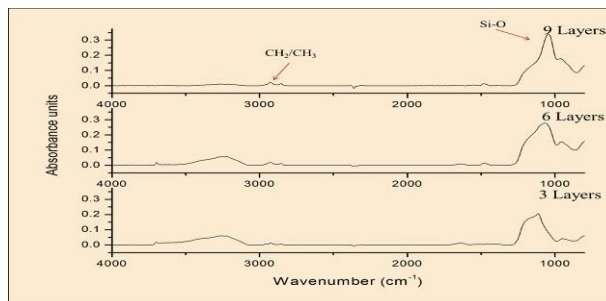


Fig. 1: IR Spectra for as Deposited Mesoporous Silica-Multilayers of spin coating

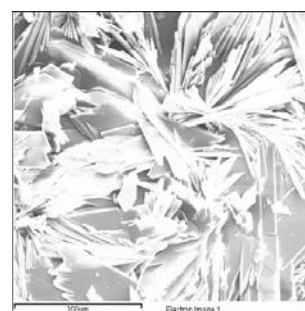


Fig. 2: SEM Image for Deposited Calcium Phosphate on Mesoporous Silica-Three Layers of Spin Coating

DISCUSSION & CONCLUSIONS: The results show that with the right conditions, it is possible to deposit mesoporous silica particles on Mg alloys. IR Spectra for as deposited mesoporous silica at different number of layers is shown in (Fig.1). The thickness of the film was increased with increase the number of layers. Moreover, the AFM images (the results are not shown) indicated the presence of the spherical particles on the film and increase the density of the film with increase the number of layers. Therefore, to get the mesoporous silica film, the surfactant was removed completely after calcination. Calcium phosphate ($\text{CaHPO}_4 \cdot 2\text{H}_2\text{O}$) is successfully deposited on the mesoporous silica film on Mg alloys (Fig. 2).

ACKNOWLEDGEMENTS: Laurentian university and Ministry of Education in Saudi Arabia.

Chemical methods for the biomimetic surface modification of magnesium alloys

JE Gray-Munro¹, J Campbell¹, X Yang¹

¹ [Department of Chemistry and Biochemistry](#), Laurentian University, Sudbury, Ontario, Canada.

INTRODUCTION: Magnesium alloys are an emerging class of biodegradable implant material. However, their biodegradation rate and biocompatibility must be optimized to maintain mechanical integrity in the early stages of healing and promote cell/surface interactions that lead to enhanced osteoconduction¹. In recent years biomimetic surfaces that mimic the structure and chemistry of biological systems have become of interest for use in a variety of applications². In particular, superhydrophobic surfaces that mimic the hierarchical structure of the lotus leaf have attracted significant attention due to their increased corrosion resistance². This paper describes a simple chemical method for producing superhydrophobic magnesium alloy surfaces that can be further modified to immobilize biomolecules for improved biocompatibility.

METHODS:

Surface Modification: 0.81 mm thick magnesium AZ31 foil was purchased from Alfa Aesar and machined into 1.27 cm diameter disks. The magnesium disks were sequentially polished, etched in a sulfuric acid solution and sonicated in 20% H₂O₂ solution. The etched samples were then immersed in a mixed organosilane-polydimethylsiloxane (MPTS/PDMS) solution, air dried and cured prior to further analysis.

Surface Characterization: The surfaces were characterized with a combination of contact angle goniometry, scanning electron microscopy (SEM), atomic force microscopy (AFM) and attenuated total reflectance fourier transform infrared spectroscopy (ATR-FTIR). The stability of the surface coatings was evaluated through immersion in aqueous solution for 24 hours.

RESULTS: The SEM image in Fig. 1a shows the micron scale topography of the chemically etched magnesium alloy surface. Fig. 2 is an AFM image showing the nanostructure of the composite coating. Fig. 1b shows the $>150^\circ$ contact angle of a water droplet on the etched and coated surface. ATR-FTIR analysis (not shown) confirmed the presence of a mixed MPTS/PDMS coating. The preliminary coating stability tests indicate that the surface modification is stable in aqueous solution.

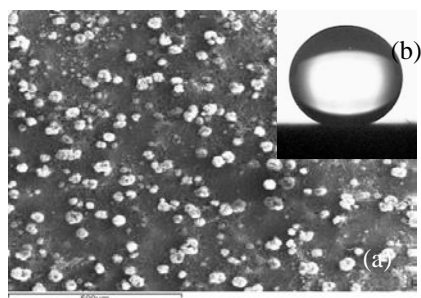


Fig. 1: Topography and water repellance of a biomimetic superhydrophobic magnesium surface. a) SEM image and b) image of a water droplet sitting on the surface.

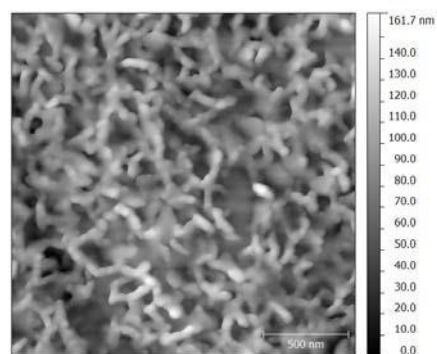


Fig. 2: Atomic force microscopy image of the mixed organosilane/polydimethylsiloxane coating on magnesium alloy AZ31.

DISCUSSION & CONCLUSIONS: This surface modification resulted in a hierarchical surface structure composed of microscale and nanoscale features similar to that of the lotus leaf resulting in superhydrophobicity². In addition, the composite coating employed contains functional groups that can be used for subsequent immobilization of biomolecules to enhance biocompatibility. Preliminary tests indicated that it is possible to covalently attach cell adhesive proteins to these surfaces.

ACKNOWLEDGEMENTS: The authors gratefully acknowledge the support of NSERC.

Synthesis and corrosion behaviour of dual-layer calcium-deficient hydroxyapatite coatings on magnesium-based bone screws

Lei Chang¹, Jun Wang¹, Yanhua Wang¹, Ligu Wang¹, Shijie Zhu¹, Shaokang Guan^{1*}

¹School of Materials Science and Engineering, Zhengzhou University, Henan, China

INTRODUCTION: Magnesium-based alloys have merged as one of the most promising resorbable orthopaedic implant materials due to the favourable mechanical properties as well as the potential osteoconductive effects¹⁻². However, detrimental corrosion occurs immediately when it is applied in physiochemical environment; and the implantation of bulk magnesium-based materials is possible to be accompanied with fast hydrogen evolution as well as localized alkalisation at the material-tissue interface, leading cell apoptosis³. Therefore, it is crucial to modify its surface with improved corrosion resistance in the body fluid during the initial implantation period. Various types of coatings have been reported⁴ but rarely applied on the implant surface. In this study, a dual-layer dense coating was first directly synthesized on magnesium-based bone screws via microarc oxidation (MAO) technique combined with dual-pulse electrodeposition technique.

METHODS: Prior to the fabrication into screw shape, MgZnCa alloys were processed by solid solution treatment followed by extrusion. MAO technique was first applied to generate a porous base layer on surface with the electrolytic solution of $\text{Na}_3\text{PO}_4 \cdot 12\text{H}_2\text{O}$, NaOH and glycerine; and subsequently, electrodeposition technique in dual-pulse mode was utilized to synthesize the top layer. As-deposited coatings were characterised by SEM, EDX, XRD, FTIR and AFM. Mechanical properties including adhesion strength, tensile strength, wear resistance and torque were also examined. The effect of coatings on *in vitro* degradation behaviours was studied via immersing specimen in simulated body fluid at 37°C. Electrochemical tests besides hydrogen evolution and weight loss measurement were performed.

RESULTS: A uniform coating was formed on the whole screw surface without obvious cracks, of which the composition was hydroxyapatite with the Ca/P ratio less than 1.67. Coatings were highly hydrophilic and the thickness was around 20µm, which was favourable for initial adhesion and spreading of osteoblast. Adhesion strength was examined over 20 MPa and the tensile strength was not be compromised by the presence of

coatings. The corrosion current density of screws with coatings decreased significantly. After immersion test in SBF solution, screws with coatings maintained the shape integrity without severe pitting corrosion and delamination of coatings, which indicated the improved corrosion resistance (as shown in Fig.1).

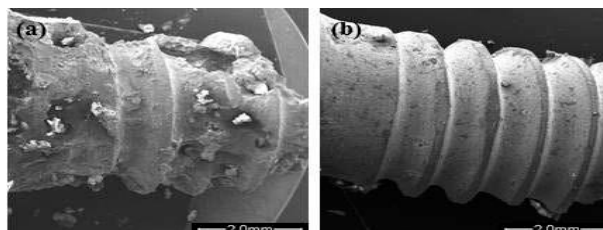


Fig. 1: Surface morphology of magnesium-based bone screws (a) without and (b) with dual-layer calcium-deficient coatings after immersed in SBF solution for six days.

DISCUSSION & CONCLUSIONS: A dense calcium-deficient hydroxyapatite coating was successfully synthesized on magnesium-based bone screws with improved *in vitro* corrosion resistance and mechanical properties. The effects of coatings on corrosion resistance will be further investigated by long-term immersion tests as well as *in vitro* cell culture study, of which the results shall shed a light in the research of magnesium-based orthopaedic implants.

ACKNOWLEDGEMENTS: Authors are grateful for the financial support of the National Key Technology R&D Program of China (No. 2015AA033603; No. 2015AA020301) and Major Science and Technology Project of Henan Province (No. 141100310900).

Cytotoxic effect of magnesium on human osteosarcoma cells (U2-OS)

L Ren¹, Y Zhang², M Li², K Yang¹

¹Institute of Metal Research, Chinese Academy of Sciences, China. ²Department of Orthopedic Surgery, Guangzhou General Hospital of Guangzhou Military Command, China.

INTRODUCTION: Cancer is one of the leading causes on human deaths from diseases. However, radiotherapy and chemotherapy are still not fully satisfied, and other alternative ways of curing cancers are still welcome by clinical doctors. It has been well recognized that degradation of Mg based metals could obviously increase the local alkalinity[1], which may suppress the survivals of cancer cells. The aim of this paper is to study on the cytotoxic effect of Mg degradation to osteosarcoma cells, the typical bone cancer cells, was preliminarily performed in order to provide an alternative way to cure bone cancers through creation of a localized alkaline environment by degradation of Mg based metals.

METHODS: The experimental materials used in this study were 99.9% pure Mg with and without a surface modification by micro arc oxidation (MAO). The extracts of different samples were prepared. U2-OS, a typical human osteosarcoma cell, was cultured in the above extracts. After 48 h co-culture, CCK-8 was conducted in order to evaluate the cytotoxic effect of different sample on U2-OS by measuring the optical density (OD) of different extract cultured with U2-OS at wavelength of 490 nm. Relative growth rate (RGR) of cells was calculated using equation: $RGR = (OD \text{ of experimental material extract} / OD \text{ of normal culture medium}) \times 100\%$. pH value and Mg^{2+} concentration were changed respectively in the culture medium, in order to independently study the cytotoxic effect on U2-OS by increasing either the alkalinity or the Mg^{2+} concentration owing to the degradation of Mg.

RESULTS: Mg samples with and without MAO coating all showed strong cytotoxicities to U2-OS, which morphology shown in Fig. 1. With the increase of pH in the culture medium, i.e., the increase of alkalinity, RGR of U2-OS cells was gradually decreased, showing strong cytotoxicity for the pH over 9.4. A variation of Mg^{2+} concentration from 1 to 50 mmol/L in the culture medium had no obvious cytotoxic effect on U2-OS cells, keeping RGR over 80%. This confirms that the cytotoxic effect on U2-OS during the Mg degradation should mainly come from the great increase of alkalinity in the surrounding

environment. However, it is expected that an increase of alkalinity during the Mg degradation will mainly kill the cancer cells and have less negative effect on the normal cells. This might be realized through a proper surface modification such as MAO in the present work, since the MAO coating has been reported to improve the cell compatibility of Mg based metals.

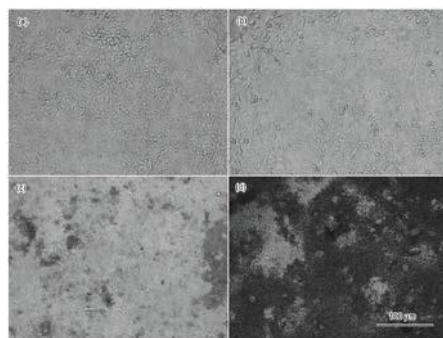


Fig. 1: Morphologies of U2-OS cells cultured with extract of different experimental sample for 24 h: (a) normal culture medium; (b) Ti extract; (c) MAO coated Mg extract; (d) uncoated Mg extract.

DISCUSSION & CONCLUSIONS: The present in vitro study indicated that the extract of Mg showed strong cytotoxic effect on osteosarcoma U2-OS cells due to a creation of high alkalinity caused by the degradation of Mg in the culture medium, and this cytotoxicity could be somewhat adjusted by a MAO coating on the surface of Mg to reduce its degradation rate. This finding may provide an alternative way to cure bone cancers through creation a high alkalinity surrounding the cancer cells.

ACKNOWLEDGEMENTS: This work was financially supported by the National Basic Research Program of China (No. 2012CB619101).

The *in vitro* biocompatibility and macrophage phagocytosis of Mg₁₇Al₁₂ phase in Mg–Al–Zn alloys

L Tan¹, C Liu¹, Y Zhang², K Yang¹

¹*Institute of Metal Research, Chinese Academy of Sciences, Shenyang, China.* ²*Hospital of Orthopedics, Guangzhou General Hospital of Guangzhou Military Command, Guangzhou, China.*

INTRODUCTION: Mg alloys are gaining interest for applications as biodegradable medical implant, including Mg–Al–Zn series alloys with good combination of mechanical properties and reasonable corrosion resistance. However, the degradation behavior of the second phase particles and whether the existence of second phase particles in the alloys exerts influence on the biocompatibility are still not clear. A deeper understanding of how the particles degrade and regulate specific biological responses is becoming a crucial requirement for their subsequent biomedical application.

METHODS: The *in vitro* biodegradation behavior of Mg₁₇Al₁₂ as a common second phase in Mg–Al–Zn alloys was investigated via electrochemical measurement and immersion test. The *in vitro* biocompatibility was investigated via hemolysis, cytotoxicity, cell proliferation, and cell adhesion tests. Moreover, osteogenic differentiation was evaluated by the extracellular matrix mineralization assay. The Mg₁₇Al₁₂ particles were also prepared to simulate the real situation of second phase in the *in vivo* environment in order to estimate the cellular response in macrophages to the Mg₁₇Al₁₂ particles.

RESULTS : The Hank's solutions with neutral and acidic pH values were adopted as electrolytes to simulate the *in vivo* environment during normal and inflammatory response process. Furthermore, the local orbital density functional theory approach was employed to study the thermodynamical stability of Mg₁₇Al₁₂ phase. All the results proved the occurrence of pitting corrosion process with crackings for Mg₁₇Al₁₂ phase in Hank's solution, but with a much lower degradation rate compared with both AZ31 alloy and pure magnesium.

The experimental results indicated that no hemolysis was found indicated in Table 1 and an excellent cytocompatibility was also proved for the Mg₁₇Al₁₂ second phase when co-cultured with L929 cells, MC3T3-E1 cells and BMSCs as shown in Fig.1. Macrophage phago-cytosis co-culture test revealed that Mg₁₇Al₁₂ particles exerted no harmful effect on RAW264.7 macrophages and

could be phagocytized by the RAW264.7 cells as shown in Fig.2. Furthermore, the possible inflammatory reaction and metabolic way for Mg₁₇Al₁₂ phase were also discussed in detail.

Table 1. Hemolysis Test Results of Mg₁₇Al₁₂ and Pure Mg

Sample	OD Value at 545 nm	Hemolysis Rate/%
Mg ₁₇ Al ₁₂	0.047±0.0012	0.57
Pure Mg	0.051±0.0015	1.72

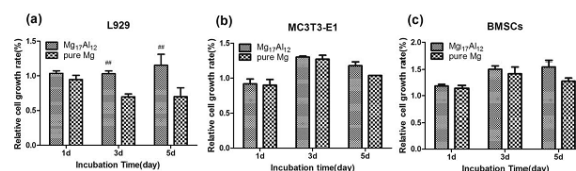


Fig. 1: Relative cell growth rates after 1, 3, and 5 days of incubation in Mg₁₇Al₁₂ and pure Mg extraction mediums: (a) L929, (b) MC3T3-E1, (c) BMSCs. **p*<0.05 compared with pure Mg.

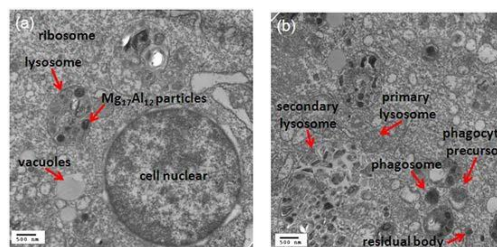


Fig. 2: Typical TEM images of murine monocyte macrophages (RAW264.7) phagocytizing Mg₁₇Al₁₂ particles after co-culture for 24 h.

DISCUSSION & CONCLUSIONS: The Mg₁₇Al₁₂ phase presents a lower degradation by pitting corrosion, no hemolysis and an excellent cytocompatibility. It can be phagocytized by the RAW264.7 cells.

In vitro study on as-cast Mg-2Al-1Ba alloy

Y Liu¹, Y Zheng¹, H Dieringa²

¹ [Department of Materials Science and Engineering, College of Engineering, Peking University, Beijing 100871, China.](#) ² [Magnesium Innovation Centre- MagIC, Institute for Materials Research, Helmholtz-Zentrum Geesthacht, Geesthacht 21502, Germany.](#)

INTRODUCTION: Barium is in the same main group as Ca and Sr. Besides, Barium was found in teeth of human children and also thought to stimulate muscle [1, 2]. Up to date, there were plenty of studies on the Mg-Ca and Mg-Sr alloys for biomedical application, yet there is no report on Ba containing Mg alloys. Microalloying of Barium to Mg is worthy for investigation.

METHODS: As-cast Mg-2Al-1Ba (wt.%) with as-cast pure Mg as control was utilized in this study. The samples of 10mm x 10mm x 2mm were cut from ingots, following with mechanically polished up to 2000 grit, ultrasonically cleaned in acetone, absolute ethanol and distilled water, and then dried in open air. The microstructure was visualized by metalloscope. The phase composition was examined by X-ray diffraction. The hardness was tested using a microhardness tester. A three electrodes cell with a platinum counter-electrode and a saturated calomel electrode (SCE) as the reference electrode was utilized for electrochemical test. The electrochemical test was carried out in Hank's solution using electrochemical working station. Immersion test was also conducted in Hank's solution at 37 °C.

RESULTS: The microstructure (Fig. 1(a)) showed that the second phase was mainly aggregated in the grain boundaries and also visualized inside the grain. Besides, the grain size was large at cast state, which may not be good for corrosion resistance. The XRD pattern (Fig. 1(b)) revealed that AB21 alloy was composed of α -Mg and Mg₁₇Ba₂. Thus Al may exist as solid solution element in α -Mg phase. The hardness test results (Fig. 1(c)) indicated a strong hardening effects after the addition of Al and Ba, with significant improvement from lower than compared to pure Mg. Fig.1(d) shows the potentiodynamic polarization curve of AB21 with pure Mg as control. The addition of Al and Ba increased the corrosion potential. However, the corrosion current density was also increased. Immersion test revealed a quick increase of pH to 11 in less than 72 hours.

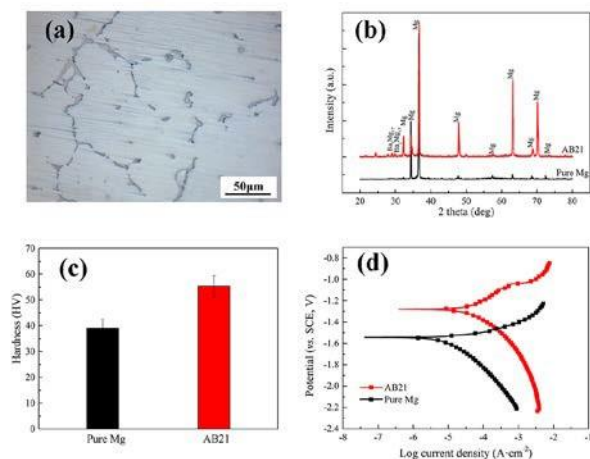


Fig. 1: Microstructure (a), XRD patterns (b), hardness (c) and potentiodynamic polarization curve (d) of AB21 alloy with pure Mg as control.

DISCUSSION & CONCLUSIONS: In this study, the microstructure, hardness and in vitro degradation property of as-cast AB21 alloy were evaluated. The hardness results revealed a significant improvement by adding Al and Ba. As for in vitro degradation performance, both the electrochemical test and the immersion test revealed a quick corrosion rate. According to the Periodic Table, Ba is more active than Ca and Sr, which resulted in a more active second phase Mg₁₇Ba₂ with Mg. As for the cast alloy, the coarse grain boundaries where the second phase aggregated may strongly react with α -Mg via galvanic corrosion. However, the effects of Al still need a further investigation in such alloy. Moreover, the effects of trace amount Ba on the osteoblast viability also need further research.

New magnesium-strontium (Mg-Sr) based alloys; corrosion and cytotoxicity

M Top¹, M Ascencio², MO Pekguleryuz³, M Tabrizian¹

¹[Faculty of Dentistry](#), McGill University, Montreal, QC. ²[Chemical Engineering](#) McGill University, Montreal, QC. ³[Mining & Materials Engineering](#), McGill University, Montreal, QC.

INTRODUCTION: Magnesium has become increasingly popular during the last decade for the researchers who work on biodegradable metallic implants. It is a promising material due to its superior bio-compatibility, low density, and good mechanical properties. This study aimed at investigating the corrosion rate and electrochemical behavior of novel magnesium - strontium - calcium - zinc (Mg-Sr-Ca-Zn) based alloys and evaluate their biocompatibility via cytotoxicity testing.

METHODS: Three different alloys (Alloy A; Mg-Sr-Ca, Alloy B; Mg-Sr-Ca-Zn, Alloy C; Mg-Sr-Ca-Zn) were cast and scanning electron microscopy (SEM) was used for general observation of the surface morphology and for the microstructural characterization of the alloy samples. WE43-a corrosion resistant Mg alloy-was utilized as control. Immersion tests were conducted on the samples using simulated body fluid (SBF)¹ to elucidate their corrosion resistance. Corrosion rate was calculated by measuring hydrogen release and amount of magnesium dissolved in the SBF that was determined via inductively coupled plasma atomic emission spectroscopy (ICP-AES). Two parameters; the corrosion potential (E_{corr}) and the corrosion current density (i_{corr}) was used to evaluate the corrosion behavior. The *in vitro* cytotoxicity of the alloys was examined using human umbilical vein endothelial cells (HUVEC) and rat osteoblast precursor cells (MC 3T3).

RESULTS: SEM observation showed that for the cast alloys exhibited a fine uniform grain structure (Fig. 1). The results of electrochemical measurements and immersion tests showed that the presence of the zinc in the alloy seems to increase the corrosion potential in simulated body fluid (SBF) and reduce the degradation rate. An indirect cytotoxicity test using MTT and Alamar Blue (AB) assays revealed that for both HUVEC and MC 3T3 cells all three alloy compositions exhibited results similar to those obtained with WE43 ($p < 0.05$). There were no statistically significant differences observed between Alloy B and Alloy C, which has different amounts of zinc

($p > 0.05$). These findings suggested that the alloys were highly biocompatible with HUVEC's and MC 3T3 cell *in vitro*, yielding results similar to WE43 and pure Mg.

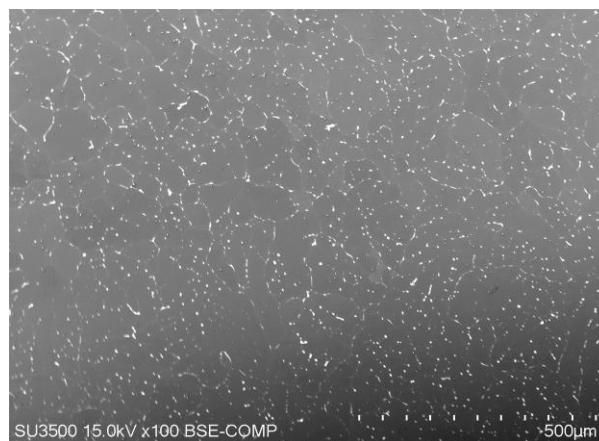


Fig. 1: SEM image of Alloy C. in the image.

DISCUSSION & CONCLUSIONS: The cytotoxicity and corrosion results for the alloys suggested that they have good biocompatibility. In order to investigate their potential for different implant applications, mechanical properties i.e. tensile strength and elongation, needs to be further investigated and *in vivo* studies were planned.

ACKNOWLEDGEMENTS: This study was conducted under an NSERC (Natural sciences and Engineering Research Council) of Canada Strategic Grant with Baylis Medical Inc.

Differential regulation of vascular genes and proteins expression by bioabsorbable metal ions Mg and Zn

D Zhu¹, M Jun¹, D Conklin², J Waterman²

¹Bioengineering, North Carolina A&T State University, Greensboro, North Carolina, USA. ²Animal Science, North Carolina A&T State University, Greensboro, North Carolina, USA.

INTRODUCTION: Magnesium (Mg) and zinc (Zn) are promising next generation of cardiovascular stent materials. These tailored alloys have the potential to eliminate or minimize the long-term complications of current permanent stent implants. However, the fundamental cellular and molecular alterations on vascular cells induced by Mg and Zn ions from implant degradation remains unclear despite the success of pre-clinical and clinical testing. Therefore, we examined the differential effects of these biometal ions on human primary vascular endothelial cells (EC) and smooth muscle cells (SMC).

METHODS: Cells are exposed to typical low and high concentrations of Mg or Zn for 1 h according to our previous study [1-3]. Then cell lysate and supernatant are collected. Vascular cell gene array is used in RT-PCR for gene expression analysis. ELISA and Western-blot are used to examine the related protein expression.

RESULTS: Both Mg and Zn ions treatment on EC or SMC induced differential regulation of gene and protein expression. The mostly affected genes and associated proteins were in the functional group of inflammation, vessel tone, cell mobility, and angiogenesis.

DISCUSSION & CONCLUSIONS: Vascular cells were treated with Mg and Zn ion at concentrations of no adverse effect on cell viability and proliferation as demonstrated before [1-3]. The mostly affected cellular functions appeared to be related to inflammation, vessel tone, cell mobility and angiogenesis. These findings on cell genes and proteins regulation by Mg or Zn ion help explain the notion that relatively low concentrations of Mg or Zn are beneficial to vascular cell functions, including viability, proliferation, adhesion, migration, and inflammatory responses at the molecular level. Information obtained from this study provides some guidance for controlling the pace of implant degradation to maintain a low concentration of such metal ions in the local environment of vascular tissues.

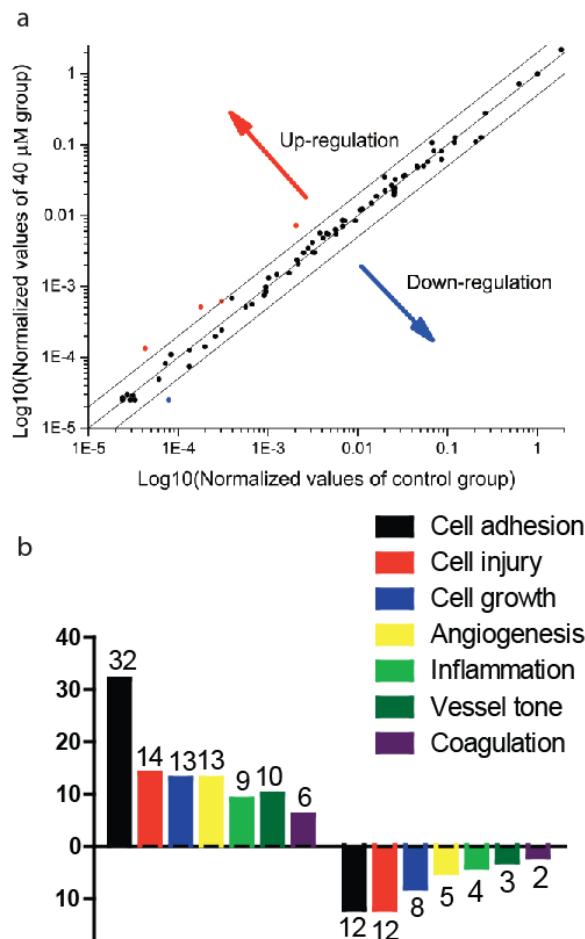


Fig. 1: Effects of Zn ion on SMCs gene expression profiles. a. The scatter plot of gene expression profiles of SMCs treated with 40 μM Zn; b. Number of functional genes regulated at 40 μM Zn.

ACKNOWLEDGEMENTS: Research reported in this publication was supported by the National Institute of General Medical Sciences of the National Institutes of Health under Award Number SC3GM113762. The content is solely the responsibility of the authors and does not necessarily represent the official views of the National Institutes of Health.

Effect of anodization on platelet adhesion on polymer coated MZC

E Mirtaheeri¹, S Amruthaluri¹, V Musaramthota¹, N Munroe¹

¹ [*Department of Mechanical and Materials Engineering*](#), Florida International University, Miami, USA.

INTRODUCTION: Recently, researchers have shown great interest in the usage of magnesium alloys as a biodegradable implant material. Magnesium is biocompatible and is metabolized by the body, thereby negating the need for additional surgeries, which lowers medical costs and reduces patient morbidity. A major concern with magnesium alloys is the high rate of corrosion during the initial period of implantation, which results in hydrogen evolution and localized elevated metal ion concentration at adjacent cells. These conditions are undesirable for cell viability and proliferation. Thus, there have been major efforts to reduce the rate of degradation of these alloys.

METHODS: Two surface treatments were adopted in this study to reduce the rate of corrosion of magnesium-zinc-calcium (MZC) alloys: a) Anodization which produces a passivating oxide; and b) coating which provides an impermeable barrier to protect the underlying metal. Anodized MZC was dip-coated with the copolymer polyglycolic-co-caprolactone (PGCL) (90/10). The effect of anodization and polymer coating on the rate of corrosion of MZC were compared, as was their effect on platelet adhesion which was assessed using a flow chamber through which porcine blood was circulated.

RESULTS: It was observed that the polymer-coated surface on of an anodized surface rendered the surface more hydrophobic and therefore less wettable. The degree of wettability was changed with changing the anodization parameters. Platelet adhesion test was conducted on different anodized and polymer coated samples and a relationship was established between wettability and platelet adhesion.

DISCUSSION & CONCLUSIONS: The wettability of MZC and polymer coated MZC were compared with respect to platelet adhesion. Anti-thrombogenic behavior was observed on polymer coated MZC when anodization parameters were optimized.

Biodegradation of AZ31 alloy in calota of rabbits for bone repair applications

MC Garcia-Alonso¹, OG Bodelon¹, C Clemente², MA Alobera³, I Diaz¹, M Monica³, ML Escudero¹

¹ National Centre for Metallurgical Research (CENIM), CSIC, Madrid, 28040, Spain.

² School of Medicine, University of Alcalá, Alcalá de Henares, Madrid, Spain.

³ Hospital Universitario La Paz, Madrid, 28046, Spain.

INTRODUCTION: One of the main problems occurred in bone repair surgery is the invasion of fibrotic tissue in the cavity before the new neoformed bone appears. A solution proposed to avoid this invasion is the implantation of a barrier biomaterial that impedes the intrusion of fibrotic tissue. This physical barrier is usually made of non-biodegradable materials, so it needs to be removed once the damage has been repaired. In this work, the use of AZ31 alloy as barrier biomaterial is proposed in osseosynthesis applications as a way to impede the colonization of fibrotic tissue until the bone repair is achieved, taking advance of its biodegradable properties and avoiding the second surgery.

METHODS: The chemical composition of the AZ31 alloy was determined by WDXRF: 3.37 ± 0.09 wt.% Al, 0.78 ± 0.04 wt.% Zn, 0.22 ± 0.01 wt.% Mn (balance Mg). To reduce the biodegradation rate of AZ31 implants, half of the samples were subjected to a chemical conversion treatment in 48 wt.% HF solution in order to produce MgF₂ on the surface [1]. AZ31 was machined as a cover of 2 mm height and 7 mm diameter (Fig.1).

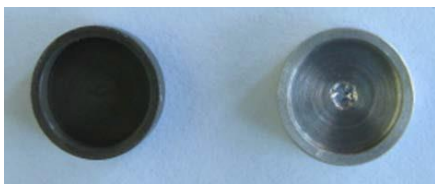


Fig. 1: Images of implant AZ31 coated and uncoated.

The *in vivo* study was carried out in 16 New Zealand male rabbits of 5 kg. AZ31 alloy with and without Mg-fluoride coating were inserted in the calota of rabbits and removed after 1, 3, 4 and 6 months. The study was followed by means of histological and histomorphometric analysis.

RESULTS: As an example, Fig. 2 shows the reabsorption of the coated AZ31 occurred in the edges, the presence of biodegradation products around which fibrotic tissue and islands of new formed bone under the biomaterial are observed.

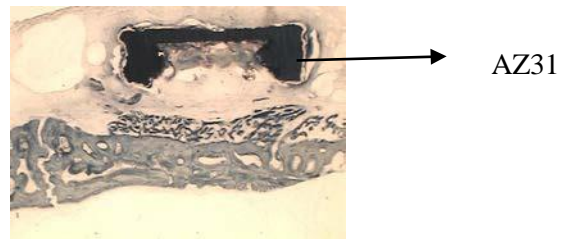


Fig. 2: Histological section of coated AZ31.

Fig. 3 shows that there is not statistically significant differences in the resorption process between coated and uncoated AZ31 implants inserted in calota after 3 months.

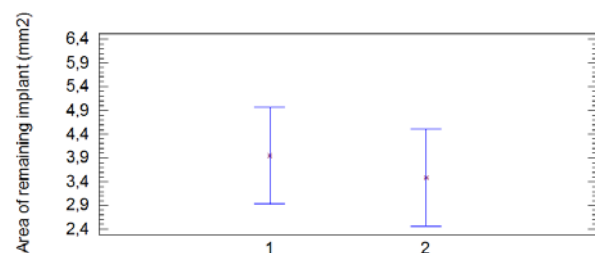


Fig. 3: Area of remaining implant. 1) coated AZ31; 2) uncoated AZ31.

DISCUSSION & CONCLUSIONS: No histological and biodegradation differences are seen between the reactions that take place on MgF₂ coated and uncoated surfaces.

ACKNOWLEDGEMENTS: Thanks for financial support of projects MAT 2008-06719-C03-01-03 and MAT 2011-29152-C02-01.

UNCOATED MG-LI ALLOY RODS DEGRADATION BEHAVIOR *IN VITRO*

Mark Paquin¹, Louis-Georges Guy², Sandra Iacampo², Fabian Soza², Guy LeClerc² & David Broecker¹

¹Zorion Medical Inc.; ²AccellAB Inc.

Background: Currently, magnesium (Mg) alloys are being investigated as an alternative to other biodegradable materials in the development of implantable medical devices. However, due to the magnesium's poor corrosion characteristics — which can lead to rapid degradation — implantable devices made from Mg can compromise a device's integrity.¹ We sought to evaluate the degradation behavior of our patented, uncoated magnesium-lithium (Mg-Li) alloy *in-vitro* and compare our degradation results to those published in literature.

Methods: Five (5) uncoated Mg-Li alloy rods of equal length (250 mm) and diameter (0.175 mm) were weighed and placed into vials containing physiological saline solution. The vials containing the rods were then immersed into a static water bath held constant at 37°C. A sixth (6th) Mg-Li alloy rod of the same dimensions was used as a reference. At pre-determined time-points, the rods were removed from their containers, rinsed with distilled water, and allowed to dry. Weights were retaken and rods were sent for Micro-Computed Tomography (μCT) for evaluation.

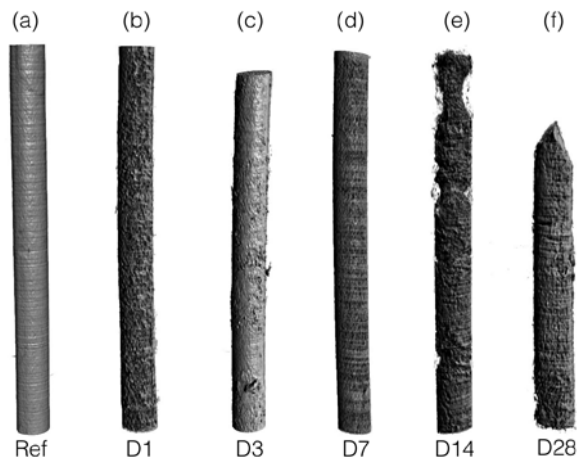


Figure 2. μCT images of Mg-Li alloy

Results: Mg-Li alloy rod weights following *in-vitro* corrosion testing through 28 days are presented in **Figure 1**. The mean baseline weight for all rods measured was 1.0 mg +/- 0.01. μCT images are presented **Figures 2(a)-2(f)**. Volume-loss appeared to be both time-dependent and inhomogeneous for the uncoated alloy. Pitting corrosion was observed as early as Day-1 (D1).

Conclusions: μCT assessment of our uncoated alloy revealed inhomogeneous volume-loss and corrosive pitting as early as D1. The results observed in this study are similar to those observed by *Seitz et al.*¹ of uncoated Mg alloys evaluated in a study comparing the behavior of coated and uncoated Mg alloys in an *in-vitro* corrosion environment.



Figure 1. Mg-Li alloy weight loss following *in vitro* static testing